UNDERSTANDING THE PHYSIOLOGICAL CONSEQUENCES OF *VITREOSCILLA* HEMOGLOBIN (VHb) EXPRESSION IN *ESCHERICHIA COLI*

Thesis by

Philip S. Tsai

In Partial Fulfillment of the Requirements

for the Degree of

Doctor of Philosophy

Department of Chemical Engineering

California Institute of Technology

Pasadena, California

1995

(Submitted April 10, 1995)

ACKNOWLEDGMENTS

I would like to thank my advisor Jay Bailey for his research guidance and support over the years. The numerous discussions with him have taught me to think critically and to be scientifically precise. I appreciated his faith in me and patience throughout my research, especially during my "proton pumping" days.

This thesis is possible largely because of the help from the Bailey group, and without them the graduate life would not be as fun. During my early Caltech period, I am indebted to many people who were always there when I needed them. In particular, I would like to extend my gratitude toward Girish, Neilay, Pauli and Wilfred. Their warm friendship made me feel at home when I first joined Jay's group. Thank you for introducing me around the labs and giving me the "bag of tricks" for doing experiments. I will remember the "Bulls vs. Lakers" rivalry that went on all year round on the blackboard in 312. Many thanks also to the Swiss Bailey group during my Schwiitz Doktorand days. It has been a pleasure to work in such a dynamic group that generates stimulating and, quite frequently, theatrical atmosphere: Miguel, Uwe, Wolfgang^3, Claire, Ellen, Roberto, Christian, Pablo, Adriana, and the supporting cast. I am especially grateful to Pauli for being patient with me when teaching me molecular biology and being a good partner on our VHb projects. Thanks also to Wilfred for sharing the fun excursions to Paris, Stuttgart and Münich with us; to Wolfgang & Sigi for their wonderful friendship, toy train, handicrafts, and the upcoming Asia adventure; Vassily for his scientific feedback and camaraderie Monday and Wednesday nights in the dark, foggy, cold Zürich winter on Tram 11 through the empty Bahnhofstrasse to the Deutsche Kurs and back; Alex the Internet Czar for showing me the access to the "Top Ten" lists through the network; and

Kelvin for tying the Bailey group together and making it an exciting place to be. I am also grateful to Susy for taking care of the toughest part of our bioreactor cultivations, the late-night sampling hours, during my last months of research. Finally, I thank Conny, an enthusiastic help and a great friend in and out of the lab, for leaving me with a positive impression of Switzerland.

I am blessed with a loving wife, Becky, for she always believes in me and gives me constant encouragement through the years. Her understanding and patience, often tested through my overnight fermentations and weekend experiments, are greatly appreciated. I thank her also for creating a warm and loving home for me to come to every evening. The addition of Kyle has been a real joy for the family and me. I am also immeasurably indebted to both of our parents for their support and steadfast confidence in me.

As I glance back, there were times of failure and frustration and times of triumph. I thank God for carrying me through those darkest periods and for giving me courage and perseverance. Every bit of joy and agony has been a maturing experience and seems all worthwhile now.

ABSTRACT

Physiological effects of *Vitreoscilla* hemoglobin (VHb) expression in recombinant *Escherichia coli* were investigated to expand the understanding of the means by which VHb enhances oxygen–limited cell growth and recombinant protein production. The proton pumping efficiency (protons extruded per oxygen reduced) of VHb–synthesizing *E. coli* (VHb^+) grown under microaerobic conditions (dissolved oxygen concentration less than 2% air saturation) was 1.5 times the respective value of a control strain not expressing VHb (VHb^-). Deconvolution of VHb, cytochrome *o* and *d* bands from absorption spectra revealed a 5–fold increase in cytochrome *o* content and a 1.5–fold increase in cytochrome *d* content of the VHb^+ strain relative to the VHb^- parent. Substrate–utilization kinetic measurements of *E. coli* mutants lacking one of the two terminal oxidases disclosed enhancement by VHb of the specific activity of cytochrome *o* but not that of cytochrome *d*. These results are consistent with a proposed model of VHb action in *E. coli* hypothesizing that VHb increases the effective dissolved oxygen concentration, resulting in an increase of cytochrome *o* activity and energy synthesis efficiency.

On–line NAD(P)H fluorescence measurement of VHb^+ and VHb^- cultures subjected to several high/low oxygen transients showed that microaerobic *E. coli* expressing VHb maintained a more oxidized state by affording a 2.4–fold smaller NAD(P)H utilization rate under decreasing oxygen tensions and a steady NAD(P)H level of 1.8–fold less under non–aeration than those of the isogenic controls. A rudimentary simulation of oxygen oscillations typical of large–scale bioreactors showed dampened fluorescence response by VHb–containing *E. coli* to sudden changes of oxygen tension. The oxygen uptake rate, estimated from culture redox

potential of cells under submicromolar oxygen tension, was 25% higher for VHb^+ cells relative to the VHb^- controls.

The possible involvement of the *E. coli* global oxygen–sensing regulators, Fnr and the Arc system, in modulating the activity of the *vhb* promoter, P_{vhb}, were explored using *E. coli fnr* and *arc* mutants. Expression of VHb and the activity of P_{vhb} were activated by Fnr but relatively unaffected by the Arc system. The presence of VHb increased the activity of ß-galactosidase from a cytochrome *d* promoter-*lacZ* fusion by 1.5-fold relative to the wild–type control.

VHb expression was modulated over a broad range to study the response of *E. coli* physiology to VHb dosage. Final cell density increased stepwise with increasing VHb concentration until saturation of cell density at a 2.7–fold increase over the cell density of the VHb^- culture was observed. The presence of VHb reduced CO_2 evolution, by–product excretions, and enhanced growth rate, growth yield and respiration rate. Metabolic flux distribution analysis revealed increased and decreased carbon fluxes to the pentose phosphate pathway and tricarboxylic acid cycle, respectively, of VHb^+ *E. coli* under oxygen–limited conditions. This analysis also predicted higher overall NAD^+ and ATP fluxes for the VHb^+ cells.

TABLE OF CONTENT

CHAPTER 1:

Introduction

1.1 VHb Technology in Oxygen–Limited Bioprocesses

Limitation of growth, and consequently productivity, by oxygen in aerobic bioprocesses involving high–density microbial cultivations is a primary concern for pharmaceutical and biotechnology industries. Oxygen limitation occurs when cellular oxygen demand exceeds supply capacity. Inadequate oxygenation not only impedes an efficient oxidative energy generation pathway but also results in excretion of undesirable by–products. By-product formation, an alternative energy synthesis pathway in the absence of oxygen, provides some additional energy and equilibrates internal redox balance. Hence, cell growth and product yield diminish with increasing oxygen starvation.

Two types of approaches have been applied to address oxygen limitation in bioprocesses. One approach focuses on manipulation of environmental parameters to improve oxygen transfer property. Implementing agitation devices with improved hydrodynamics for higher oxygen transfer to the cells (Nienow et al., 1994) is one such example. Mathematical modeling of microbial behavior under hypoxic environments (Kalina, 1993) can also benefit oxygen–limited productivity by guiding programmed aeration and refined nutrient feeding strategy. In recent years, with increasing sophistication in on–line instrumentation and feedback controls, cell activity and production pattern can be studied *in situ*, and an optimal oxygen feeding program can be implemented to minimize oxygen starvation or to maximize productivity under low oxygen tensions (Liden et al., 1994; Franzen et al., 1994).

The other approach, which centers on the principle of metabolic engineering (Bailey, 1991) in achieving desirable enzymatic rates or cellular functions through

genetic manipulation, has attracted increasing attention with the progression of recombinant DNA technology. Consideration of oxygen–limitation in metabolic engineering includes identification and modification of key oxygen–affected enzymes (or pathways) either through alteration of existing enzymes or integration of new functions from heterologous hosts. The initial demonstration of the second approach for alleviating oxygen limitation was the introduction of a bacterial hemoglobin from the aerobic microorganism *Vitreoscilla* in engineered *Escherichia coli* (Khosla and Bailey, 1988a).

The gram–negative bacterium, *Vitreoscilla*, which is usually found in poorly aerated environments such as decaying vegetable matter and stagnant ponds (Pringsheim, 1951), synthesizes a large quantity of a homodimeric, oxygen–binding hemoprotein (VHb) in response to oxygen starvation (Wakabayashi et al., 1986). Although there is no data to indicate a functional role of VHb in its natural host, sequence and predicted structure similarities between VHb and other globins (Webster, 1988) have lead to a presumed participation of VHb's oxygen–binding activity in supporting hypoxic cell survival. Prompted by the supposition that VHb may exert its beneficial effect in other industrial organisms, the gene encoding VHb, *vhb*, was transferred to *E. coli* in which its protein was functionally expressed in its native form (Khosla and Bailey, 1988b). Transcription of *vhb* in *E. coli* is activated when culture dissolved oxygen becomes low but not anoxia, and is maximally induced under microaerobic conditions (dissolved oxygen less than 2% of air-saturation; [Khosla and Bailey, 1989]). When grown under microaerobic conditions in bioreactors, VHb–expressing *E. coli* attains higher cell density and recombinant protein production relative to VHb–negative control (Khosla and Bailey, 1988a; Khosla et al. 1990; Khosravi et al., 1990).

1.2 Motivation for This Work

The example of VHb in *E. coli* has sparked cloning of VHb in other industrially important organisms. Such efforts resulted in increased antibiotic production from *Streptomyces coelicolor* and *Acremonium chrysogenum* (Magnolo et al., 1991; DeModena et al., 1993), and enhanced titer and yield on glucose of L–lysine from *Corynebacterium glutamicum* (Sander et al., 1993). Cloning of VHb in recombinant Chinese hamster ovary cells expressing human tissue plasminogen activator (tPA) also increases the specific production of tPA by 40–100% (Pendse and Bailey, 1994). In *Saccharomyces cerevisiae*, VHb expression alters the respiration–specific ethanol synthesis pathway (Chen et al., 1994). Furthermore, the oxygen–regulated promoter of *vhb*, because of its strength, inducibility, and economy of use, finds a different class of applications. Induced upon cessation of aeration or low oxygenation, the *vhb* promoter has been employed to direct high level expression of recombinant proteins in two–stage fed–batch fermentations (Khosla et al., 1990). The success of cloned VHb in heterologous hosts has substantiated the genetic approach to overcome process limitations.

Although the goal of this metabolic engineered example has been achieved, challenge remains ahead in further advancements of the VHb technology. While the presence of VHb elicits metabolic changes in several organisms, there is no data to support a mechanistic role of VHb nor data on the possible interactions between VHb and host cellular components that might contribute to the altered physiology. Furthermore, little is known about the trans–acting regulatory molecules that determine the activity of the *vhb* promoter in various host organisms. Clearly,

understand these mechanisms is important in providing guidance for further expansion and optimization of VHb applications to aerobic bioprocesses. Knowledge of the consequence of VHb expression on central (carbon and energy) metabolism and flux distributions may assist further rational design of pathways leading to formation of products of interest. Identification of possible regulators of *vhb* may allow additional controlled expression of VHb and increase the effectiveness of VHb in bioprocesses. It has been well established that the introduction of VHb in several organisms enhances microaerobic cell growth and product synthesis. However, further improvements on these qualities is limited by our current knowledge on the mechanism of VHb action. Without information on VHb–altered physiology, refinements on the VHb protein and the optimization of interactions between VHb and its effectors will not be possible, and the applicability of VHb technology to other bioprocesses cannot be extended beyond the present random cloning.

1.3 Scope of Thesis

Advancing knowledge of intracellular and extracellular perturbations caused by the presence of VHb in *E. coli* is the aim of this research. As a first step toward the goal, the consequence of VHb expression on the energetic efficiency of the microaerobic electron transport chain is assessed by measuring the number of protons extruded across the cytoplasmic membrane in response to oxygen consumption. Details of the experiment are summarized in Chapter 2. Chapter 2 also presents a proposed hypothesis of VHb mechanism of action based on the available biophysical data of VHb (Tyree and Webster, 1978), its previously reported physiological effects

(Khosla et al., 1990), and the observed modifications of respiratory efficiency by VHb.

The hypothesized function of VHb anticipates enhanced activity for the aerobic terminal oxidase, cytochrome *o*, in VHb–expressing *E. coli* under microaerobic conditions. Therefore, Chapter 3 examines the effects of VHb on the amount and specific activity of cytochrome *o* and cytochrome *d* of *E. coli*. Mathematical deconvolution analyses are employed to estimate concentrations of VHb, cytochrome *o* and *d* from their absorbance spectra. An *E. coli* strain lacking both functional cytochromes is also used to study the possibility of VHb acting as an additional terminal oxidase.

Results from the previous chapters suggest possible involvement of VHb in influencing the oxidation–reduction state of cells under hypoxic conditions. By monitoring culture fluorescence, the response of NAD(P)H utilization to diminishing oxygen transients of *E. coli* synthesizing VHb is investigated and presented in Chapter 4. The oxygen uptake rate of cells respiring under submicromolar oxygen tensions is also estimated from the culture redox potential profiles. In addition, behavior of VHb–expressing *E. coli* subjected to oxygen fluctuations that are typical of large–scale bioreactors is reported.

Chapter 5 examines the possibility of the global oxygen–sensing transcriptional regulators of *E. coli*, Fnr and Arc system, modulating *vhb* promoter activity. Effects of VHb and the *vhb* promoter on transcriptional activity of other cellular genes are also investigated. Chapter 6 summarizes a study on VHb dosage–physiological response of microaerobic *E. coli* synthesizing different amounts of VHb. Several growth parameters (specific growth rate, glucose consumption rate,

oxygen uptake rate, and carbon dioxide production rate) and by–product excretions are measured. A stoichiometric balancing method based on the observed metabolism is applied to model intracellular carbon and energy flux distribution of VHb–producing *E. coli*.

The conjectured role of VHb (Chapter 2) in binding and releasing additional oxygen molecules to terminal oxidases raises the question whether the consequent oxygen–limited growth improvement is a unique attribute of VHb or is generic and can be achieved using other oxygen–binding hemoproteins. Appendix A describes the cloning and expression of horse heart myoglobin and yeast flavohemoglobin in *E. coli*, as well as mutagenesis to obtain single amino acid–substituted VHb. Effects of these globins and VHb mutants on microaerobic cell growth are investigated.

1.4 References

Bailey, J. E. Toward a science of metabolic engineering. *Science* **1991**, *252,* 1668-1675.

Chen, W.; Hughes, D. E.; Bailey, J. E. Intracellular expression of *Vitreoscilla* hemoglobin alters the aerobic metabolism of *Saccharomyces cerevisiae*. *Biotechnol. Prog.* **1994**, *10*, 308-313.

DeModena, J. A.; Gutierrez, S.; Velasco, J.; Fernandez, F. J.; Fachini, R. A.; Galazzo, J. L.; Hughes, D. E.; Martin, J. F. The production of cephalosporin C by *Acremonium chrysogenum* is improved by the intracellular expression of a bacterial hemoglobin. *Bio/Technol.* **1993**, *11*, 926-929.

Franzen, C. J.; Liden, G.; Niklasson, C. A new method for studying microaerobic fermentations. II. An experimental investigation of xylose fermentation. *Biotechnol. Bioeng.* **1994**, *44*, 429-435.

Kalina, V. Dynamics of microbial growth and metabolic activity and their control by aeration. *A. van Leeuwenhoek* **1993**, *63*, 353–373.

Khosla, C.; Bailey, J. E. Heterologous expression of a bacterial haemoglobin improves the growth properties of recombinant *Escherichia coli*. *Nature* **1988a**, *331*, 633-635.

Khosla, C.; Bailey, J. E. The *Vitreoscilla* hemoglobin gene: Molecular cloning, nucleotide sequence and genetic expression in *Escherichia coli*. *Mol. Gen. Genet.* **1988b**, *214*, 158-161.

Khosla, C.; Bailey, J. E. Characterization of the oxygen-dependent promoter of the *Vitreoscilla* hemoglobin gene in *Escherichia coli*. *J. Bacteriol.* **1989**, *171*, 5995-6004.

Khosla, C.; Curtis, J. E.; DeModena, J.; Rinas, U.; Bailey, J. E. Expression of intracellular hemoglobin improves protein synthesis in oxygen-limited *Escherichia coli*. *Bio/Technol.* **1990**, *8*, 849-853.

Khosravi, M.; Webster, D. A.; Stark, B. C. Presence of bacterial hemoglobin gene improves α-amylase production of a recombinant *Escherichia coli* strain. *Plasmid* **1990**, *24*, 190-194.

Liden, G.; Franzen, C. J.; Niklasson, C. A new method for studying microaerobic fermentations. I. A theoretical analysis of oxygen programmed fermentation. *Biotechnol. Bioeng.* **1994**, *44*, 429-435.

Magnolo, S. K.; Leenutaphong, D. L.; DeModena, J. A.; Curtis, J. E.; Bailey, J. E.; Galazzo, J. L.; Hughes, D. E. Actinorhodin production by *Streptomyces coelicolor* and growth of *Streptomyces lividans* are improved by the expression of a bacterial hemoglobin. *Bio/Technol.* **1991**, *9*, 473-476.

Nienow, A. W.; Hunt, G.; Buckland, B. C. A fluid dynamic study of the retrofitting of large agitated bioreactors. *Biotechnol. Bioeng.* **1994**, *44*, 1177-1185.

Pendse, G. J.; Bailey, J. E. Effect of *Vitreoscilla* hemoglobin expression on growth and specific tissue plasminogen activator productivity in recombinant Chinese Hamster Ovary cells. *Biotechnol. Bioeng.* **1994**, *44*, 1367-1370.

Pringsheim, E. C. The *Vitreoscillaceae*: a family of colorless, gliding, filamentous organism. *J. Gen. Microbiol.* **1951**, *5*, 124-149.

Sander, F. C.; Fachini, R. A.; Hughes, D. E.; Galazzo, J. L.; Bailey, J. E. Expression of *Vitreoscilla* hemoglobin in *Corynebacterium glutamicum* increases final concentration and yield of L-lysine. *ECB6: Proceedings of the 6th European Congress on Biotechnology* **1993**, pp. 607-610.

Tyree, B.; Webster, D. A. Electron-accepting properties of cytochrome *o* purified from *Vitreoscilla. J. Biol. Chem.* **1978**, *253*, 6988-6991.

Wakabayashi, S.; Matsubara, H.; Webster, D. A. Primary sequence of a dimeric bacterial haemoglobin from *Vitreoscilla. Nature* **1986**, *322*, 481-483.

Webster, D. A. Structure and function of bacterial hemoglobin and related proteins. In *Advances in inorganic biochemistry* **1988**, vol. 7, pp. 245-265.

CHAPTER 2:

Enhanced Energetic Efficiency by *Vitreoscilla* Hemoglobin (VHb) and A Proposed Functional Role of VHb

Source: *Partially from* Kallio, P. T.; Kim, D. J.; Tsai, P. S.; Bailey, J. E. Intracellular expression of *Vitreoscilla* hemoglobin alters *Escherichia coli* energy metabolism under oxygen-limited conditions. *Eur. J. Biochem.* **1994**, *219*, 201-208.

2.1 Abstract

An earlier stoichiometric analysis of oxygen-limited metabolism of *Escherichia coli* expressing cloned *Vitreoscilla* hemoglobin (VHb) suggested improved efficiency of ATP production relative to wild–type controls [Khosla et al., (1990) Bio/Technol. **8**: 849-853]. This hypothesis has been further examined by comparing the respiratory efficiency (protons extruded per oxygen reduced) of a VHb–expressing *E. coli* (VHb^+) relative to a control not expressing VHb (VHb^-). The H^+/O ratio of the VHb^+ cells grown under microaerobic conditions was 1.5 times the respective value of the VHb^- controls. Data from this experiment and other energetic parameter measurements of VHb–expressing cells are consistent with a model of VHb action that hypothesizes enhancement by VHb of the activity of the lower oxygen-affinity, higher proton-pumping–efficiency terminal oxidase cytochrome *o* under oxygen–limited growth conditions.

2.2 Introduction

Proteins which bind heme, exhibit Soret bands characteristic of hemoglobins, and which exhibit substantial primary sequence homology to leghemoglobins have been isolated from *Rhizobium meliloti* (David et al., 1988; Gilles-Gonzales et al., 1991), *Vitreoscilla* (Khosla and Bailey, 1988b), *Escherichia coli* (Vasudevan et al., 1991), and *Saccharomyces cerevisiae* (Iwaasa et al., 1992; Zhu & Riggs, 1992). However, the physiological significance of these microbial globins is unknown. The most thoroughly studied one, *Vitreoscilla* hemoglobin (VHb), is expressed at elevated levels in *Vitreoscilla* under oxygen-limited cultivation conditions. While this pattern of regulation and the oxygen-binding properties of the molecule portend physiological function, there is no data to suggest a metabolic role for VHb in *Vitreoscilla*. However, cloning and expression of the gene (*vhb*) for VHb has enabled demonstration of a significant metabolic effect of VHb in several heterologous organisms (DeModena et al., 1992; Dikshit & Webster, 1988; Khosla & Bailey, 1988a; Khosravi et al., 1990; Magnolo et al., 1991).

When introduced in *E. coli* the promoter of the *vhb* gene is transcribed, the expression of *vhb*-specific mRNA is elevated, and dimeric protein (the MW of the aposubunit is 15,775) containing heme and exhibiting Soret bands is produced during growth at low oxygen concentrations (Khosla & Bailey, 1988a; Dikshit et al., 1989). The maximal VHb expression level is achieved when the dissolved oxygen concentration decreases below 2% of air saturation in the culture medium (Khosla & Bailey, 1988b; Dikshit et al., 1990). Under oxygen-limited growth conditions, cells producing VHb protein grow to higher cell densities and synthesized more protein (Khosla & Bailey, 1988b; Khosla et al., 1990). Although the presence of VHb causes

significant metabolic changes during aerobic growth in *E. coli*, the mechanism of VHb action is still unknown. Measurements of net synthesis of total cellular protein, uptake of glucose and ammonia, and production of acid in fed-batch grown *E. coli*, analyzed using a stoichiometric model of oxygen-limited growth, suggest that the introduction of VHb into *E. coli* improves the efficiency rather than the rate of respiration under microaerobic conditions (Khosla et al., 1990). The simplified stoichiometric representation of the major oxygen-limited metabolic functions formulated in that work suggests that VHb may either enhance production of ATP or decrease maintenance energy consumption (Khosla et al., 1990).

The branched respiratory pathway of *E. coli* contains two different terminal oxidases, cytochrome *o* and cytochrome *d* [reviewed in (Anraku, 1988; Anraku & Gennis, 1987; Babcock & Wikström, 1992)]. The expression of these two terminal oxidases depends differently on the availability of oxygen, with cytochrome *o* being dominant under high oxygen tension and cytochrome *d* maximally expressed under microaerobic conditions. The biochemical properties of VHb [reviewed in (Webster, 1987)] combined with present knowledge of the respiratory pathways of *E. coli* led Khosla et al. (1990) to propose a hypothesis for the mechanism of VHb action which proposes that the presence of VHb increases the activity of one or both terminal oxidases.

This hypothesis and its inferred effect of VHb on energy metabolism prompted a collaboration with Dr. P. T. Kallio and Dr. D. J. Kim to investigate the influence of VHb on energetic parameters and growth of terminal oxidase mutants. This chapter describes the result of a proton pumping experiment from such effort (Kallio et al., 1994) which also includes a ^{31}P NMR spectroscopic measurement and bioreactor experiments using *E. coli* cytochrome mutants. Results from the ^{31}P NMR

study indicated that the transmembrane ΔpH and ATP content of VHb^+ constructs are 1.6 and 2 times, respectively, the corresponding values of VHb^- constructs. Bioreactor cultivation of terminal oxidase mutants showed significant growth enhancement by VHb only in the strain having functional cytochrome *o* lacking cytochrome *d*.. A plausible model for the function of VHb in *E. coli* based on enzyme kinetics of *E. coli* terminal oxidases and VHb was proposed and discussed.

2.3 Materials and Methods

2.3.1 Strains and Cultivation Conditions

E. coli MC4100 [F^- *araD139* Δ(*argF-lac*), *U169, rpsL150, relA1, flb-5301, deoC1, ptsF25 ,rbsR*] (a generous gift of Dr. R. P. Gunsalus of UCLA) was used to study the effect of valinomycin and KSCN concentrations on respiratory stoichiometry measurement. *E. coli* JM101 [F', *traD36, lacI^q, Δ(lacZ)M15, proAB/supE, thi, Δ(lac-proAB)*] harboring either pRED2 or pUC9 was used to study the effect of VHb on proton translocation efficiency. Construction of the VHb-expressing plasmid, pRED2, and its *vhb*$^-$ parent, pUC9, have been described elsewhere (Khosla and Bailey, 1988a; Yanisch-Perron et al., 1985) Seed culture was grown overnight in phosphate buffered LB medium (10g/L Bacto-tryptone, 5 g/L Bacto-yeast extract, 10 g/L NaCl, 3 g/L K_2HPO_4, 1 g/L KH_2PO_4, adjusted to pH 7) in a New Brunswick Scientific InnOva 4000 shaker at 37°C, 275 rpm. 50 mL of the starter culture was used to inoculate a Bioflo III fermentor containing 2.5 L LB medium. The bioreactor conditions were controlled at 37°C, 300 rpm, and 0.16 vvm of air flow. The pH of the culture was maintained at 7 ± 0.1 by adding either 4M

NaOH or 4M HCl. Ampicillin (100 mg/l) was added to JM101:pRED2 culture for selection.

2.3.2 Western Blotting

15% SDS-PAGE was performed according to the method of Laemmli (1970) and the production of VHb protein was assayed using the standard Western protocol (Winston et al., 1987). The rabbit anti-VHb antiserum was obtained from Cocalico Biologicals and horseradish peroxidase-conjugated sheep IgG fraction to rabbit IgG from Cappel™.

2.3.3 Respiratory Stoichiometric Measurement

Samples for respiratory stoichiometry assay were taken during the late exponential phase of batch cultivations. Cells were cooled on ice immediately and harvested by centrifugation using a Beckman J2-21 centrifuge at 4°C, 7,000 x g for 7 minutes. Cell pellets were washed 3 times with ice cold phosphate buffer saline (PBS; 8 g/L NaCl, 0.2 g/L KCl, 1.44 g/L Na_2HPO_4, 0.24 g/L KH_2PO_4, at pH 7.3) then resuspended to a final concentration of 7 g wet weight/L in a testing buffer which consisted of 50 mM K_2SO_4, 10 mM $MgSO_4$, 0.25 mM 3-[N-morpholino]-propanesulfonic acid (MOPS), 75 mM KSCN, and 0.50 µg/mL valinomycin. 40 mL of the cell suspension was transferred to a double-wall glass dewar where the temperature was maintained at 30°C with a circulating water bath. Cell suspension was agitated with a magnetic stirrer and the dissolved oxygen tension was measured by a microelectrode (Microelectrodes Inc., MI-730). The extracellular pH was monitored with a Fisher pH electrode (Fisher Co., 13-620-293) and a Fisher Accumet 925 Microcoprocessor pH meter with sensitivity of 0.001 pH unit, and recorded by a

Kipp & Zonen BD 401 recorder. The cell suspension was purged with nitrogen gas to establish anaerobic background conditions. After oxygen depletion, the head space of the vessel was continuously flushed with nitrogen gas for the duration of the assay. After the pH of the cell suspension stabilized, pulses ranging from 50 µl to 150 µl of 30°C, air-saturated 100 mM KCl solution were injected into the nitrogen-saturated cell suspension and acidification (ΔpH) of the suspension medium as the result of proton expulsion from cells was recorded. Pulses of nitrogen-saturated 100 mM KCl solution at 30°C were then added as control. At the end of the assay, a pulse of nitrogen-saturated 25 mM NaOH in 100 mM KCl was injected to the suspension for calibration. Decay curves were extrapolated to zero time for accurate calculation of H^+/O ratios (Kawahare et al., 1988). The H^+/O ratio was obtained by evaluating the slope of the ΔpH vs. O atom added data.

2.4 Results

2.4.1 Factors Influencing Respiratory Stoichiometry Measurement

Respiratory stoichiometry assay measures the extracellular pH change as a consequence of small oxygen additions to an anaerobic cell suspension (Kawahara et al., 1988; Meyer and Jones, 1973; Mitchell, 1961; Mitchell and Moyle, 1967). Based on multiple measurements of this type, one can estimate the number of protons expelled outside the cell per oxygen atom consumed. To ensure that the observed pH difference was a direct consequence of respiration and not activities from membrane movements such as ion transport and/or proton leakage, ionophores and membrane permeant ions were added to cell suspension to equilibrate ions across the membrane. However, ionophores and membrane permeant ions, such as valinomycin and KSCN

used in this study, are detrimental to the cell as they abolish membrane potential. Therefore, the concentration of these molecules was optimized and the time of which cells were subjected to assay conditions was minimized.

An overnight culture of *E. coli* MC4100 was used to study the effect of KSCN and valinomycin concentrations on respiratory stoichiometry (H^+/O). Sample preparation and assay conditions are described in Materials and Methods. Result indicated that H^+/O ratios did not vary significantly with the different valinomycin concentrations tested (0.75 μg/mL to 20 μg/mL; data not shown). The concentration of KSCN, however, affected the observed proton translocation efficiency (Fig. 1). Among the KSCN concentrations tested, cells achieved the highest H^+/O ratio of 2.8 at 75 mM KSCN. Based on these results, the subsequent respiratory stoichiometry experiment was performed with 0.5 μg/mL valinomycin and 75 mM KSCN.

2.4.2 Effect of VHb on Microaerobic *E coli* Proton Translocation Efficiency

The effect of VHb on the respiratory efficiency was examined using cells cultivated in a bioreactor under microaerobic conditions. Dissolved oxygen tension of both JM101:pRED2 and JM101:pUC9 cultures dropped below 20% of air saturation within the first two hours of fermentation. JM101:pRED2 culture had a higher specific growth rate than the control JM101:pUC9 and attained a higher cell density at the end of cultivation (Fig. 2). During the exponential growth phase the specific growth rate was 1.3 h^{-1} for JM101:pRED2 and 0.8 h^{-1} for JM101:pUC9. The final A_{600} obtained after 9 hr of cultivations were 2.7 and 1.4 for JM101:pRED2 and JM101:pUC9, respectively. Production of VHb in JM101:pRED2 was verified by Western blotting as described in Materials and Methods (data not shown).

Two samples for respiratory stoichiometry measurement were taken toward the end of exponential growth phase where dissolved oxygen tension was less than 2% of air saturation. Samples were prepared as described in Materials and Methods: small pulses of air-saturated solution were injected into the cell suspension, and acidification (= ΔpH) of the suspension medium as the result of proton expulsion from cells were measured. The number of protons translocated outside the cell per oxygen atom consumed (H^+/O) was 3.0 ± 0.1 for the VHb-expressing strain and 2.0 ± 0.1 for the control (Fig. 3). Results indicated that the presence of VHb improves the proton translocation efficiency of microaerobic *E. coli*. Similar values of H^+/O from duplicate samples confirmed the reproducibility of this measurement (Fig. 3).

2.5 Discussion

Khosla and co-workers (1990) proposed, based on a stoichiometric metabolic model and extracellular measurements, that expression of VHb in *E. coli* increases the efficiency of ATP production in oxygen-limited growth. We outline next a biochemical hypothesis for such an effect, followed by examination of this hypothesis based on the data obtained from this study.

The respiratory chain of aerobically grown *E. coli* contains two terminal oxidases, cytochrome *o* and cytochrome *d* complexes, which catalyze oxidation of quinol and reduction of molecular oxygen to water. Biosynthesis of cytochrome *o* is maximal under well-aerated conditions and is repressed at low dissolved oxygen levels. Under the latter conditions, cytochrome *d*, which has a much higher affinity towards oxygen, is induced (Kita et al., 1984). Cultures in the present experiments undergo a transition from well aerated to oxygen–limited growth, and therefore the

presence of both terminal oxidases late in such cultivations is expected. This has been confirmed in recent experiments showing both cytochrome *d* and cytochrome *o* signatures in absorption spectra (P.S. Tsai and M. Naegeli, unpublished results). A study of the *E. coli* respiratory chain in membrane vesicles showed that twice as many protons are extruded through the cytoplasmic membrane when it contains cytochrome *o* instead of cytochrome *d* as its sole terminal oxidase (Puustinen et al., 1991).

Based on previous studies on the effect of VHb on overall oxygen–limited metabolism (Khosla et al., 1990) and the data reported here, we hypothesize that *Vitreoscilla* hemoglobin increases the intracellular effective dissolved oxygen concentration under microaerobic condition and thereby shifts the relative activities of the terminal oxidases. As elaborated below, such an effect would cause an increase in proton pumping efficiency and, as a result, an increase in the efficiency of ATP production. Protein studies have shown that *Vitreoscilla* hemoglobin is a dimeric hemoprotein which exists intracellularly and in cell extracts primarily in a stable reversibly oxygenated form, similar to that of oxymyoglobin and oxyhemoglobin (Dikshit et al., 1989). A simple relationship can be written for the reversible binding of oxygen with VHb:

$$VHb + O_2 \xleftrightarrow[K_D=0.25\mu M]{} VHb \cdot O_2 \qquad (K_D \text{ from Khosla \& Bailey, 1989}) \qquad (1)$$

The concentration of the oxygenated hemoglobin can be calculated if the concentrations of intracellular oxygen and cytoplasmic hemoglobin are known:

$$[VHb]_{cytoplasm} = [VHb] + [VHb \cdot O_2] \qquad (2)$$

$$[VHb \cdot O_2] = [VHb]_{cytoplasm}[O_2]/(K_D + [O_2]) \qquad (3)$$

We hypothesize that the oxygenated VHb may act as an additional oxygen source for the terminal oxidases. Accordingly, we define an effective dissolved oxygen in the presence of VHb as the sum of dissolved oxygen (DO) and the oxygenated hemoglobin concentrations:

$$DO_{eff} = DO + [VHb \cdot O_2] \tag{4}$$

The effect of VHb on DO_{eff} can be clearly seen from the plot of DO_{eff}/DO vs. DO (Fig. 4). Under a typical oxygen-limited condition (say, 1 μM dissolved oxygen concentration), with 20 μM of cytoplasmic VHb (the estimated cytoplasmic concentration in a single copy VHb-expressing construct; Khosla & Bailey, 1989), the effective dissolved oxygen is 17 μM, a 17-fold increase.

We conjecture that the increase in the intracellular dissolved oxygen tension raises the activities of both cytochrome *o* and cytochrome *d* but to different extents. If we assume Michaelis-Menten kinetics for the two terminal oxidases of *E. coli,* we can see that at 1 μM DO the specific activity of cytochrome *d* is much higher than that of cytochrome *o* at low oxygen concentrations (Fig. 5; these rate functions are based on presumed hyperbolic kinetics and the measured oxygen K_m values of 2.9 μM and 0.38 μM for purified cytochrome *o* and *d* complexes, respectively (Kita et al., 1984). If the dissolved oxygen concentration increased, the specific activity of cytochrome *o* would increase more rapidly than that of cytochrome *d*. Thus, if VHb increases the effective dissolved oxygen concentration as hypothesized, it would shift the distribution of electron flow toward cytochrome *o* and thereby increase the overall proton translocation efficiency since cytochrome *o* possesses a higher H^+/e^- than cytochrome *d* does (Puustinen et al., 1991).

The respiration stoichiometric assay is a direct measurement of the cell's energetic efficiency. Although this technique does not account for proton leakages and slips in oxidative phosphorylation, and although questions still exist about the exact mechanism of the electron transport chain of *E. coli*, we are mainly interested in the comparative values of overall proton translocation efficiency between the control strain and the VHb-producing strain. In this study we have demonstrated that *E. coli* JM101 carrying the VHb-expression plasmid pRED2 extrudes one extra proton per oxygen atom consumed ($H^+/O = 3$) compared to the control strain JM101:pUC9 ($H^+/O = 2$) harvested at the end of the exponential growth phase under microaerobic conditions. This finding is consistent with the hypothesis presented above that VHb production increases the overall proton translocation efficiency in *E. coli* under microaerobic growth conditions. Also, as one major function of proton extrusion under these conditions is to generate ATP when protons reenter the cytoplasm via ATPase, the higher ATP levels observed by NMR in VHb-expressing wild type *E. coli* cells are also consistent with the above hypothesis. Finally, the effect of a higher intracellular effective DO in the context of extreme microaerobic conditions is expected to have a much greater relative effect on the specific growth rate of a strain which uses only cytochrome *o* than on a strain using only cytochrome *d*. This was the observed result in bioreactor studies with the cytochrome mutants. A more detailed study which further solidified the model described above on the effect of VHb on terminal oxidases is described in the following chapter.

There are several reasons why our interpretation of these studies did not consider a possible role of the hemoglobin-like domain (HMP) associated with ferrisiderophore reductase activity in *E. coli* (Andrews et al., 1992). To date, there is no report of any physiological effect due to globin activity of this protein similar to

those observed when VHb is expressed in *E. coli*. It is unlikely that the HMP interferes with our measurements since no measurable endogenous globin was detected relative to VHb in absorption spectra of control and VHb-expressing *E. coli* strains. Furthermore, in each set of measurements reported here, a control experiment without VHb was conducted for comparison. Presumably, any physiological effect of the endogenous HMP is similar in the VHb-free and the VHb-containing constructs.

2.6 Acknowledgments

This work was supported by the Advanced Industrial Concepts Division of the U.S. Department of Energy. We are grateful to Dr. C. Khosla for helpful advice. We also thank Dr. J. Galazzo for technical advice on proton pumping measurements.

2.7 References

Andrew, S. C., Shipley, D., Keen, J. N., Findlay, J. B. C., Harrison, P. M. & Guest, J. R. (1992) The haemoglobin-like protein (HMP) of *Escherichia coli* has ferrisiderophore reductase activity and its C-terminal domain shares homology with ferredoxin $NADP^+$ reductases. *FEBS Lett. 302*, 247-252.

Anraku, Y. (1988) Bacterial electron transport chain, *Ann. Rev. Biochem. 57*, 101-132.

Anraku, Y. & Gennis, R. B. 1987. The aerobic respiratory chain of *Escherichia coli, Trends Biochem. Sci. 12*, 262-266.

Babcock, T. G. & Wikström, M. (1992) Oxygen activation and the conservation of energy in cell respiration, *Nature 356*, 301-357.

David, M., Daveran, M.-L., Batut, J., Dedieu, A., Domerque, O., Ghai, J., Hertig, C., Boistard, P. & Kahn, D. (1988) Cascade regulation of *nif* gene expression in *Rhizobium melilotti*, *Cell 54*, 671-683.

DeModena, J. A., Gutierrez, S., Velasco, J., Fernandez, F. J., Fachini, R. A., Galazzo, J. L., Hughes, D. E. & Martin, J. F. (1993) The production of Cephalosporin C by *Acremonium chrysogenum* is improved by the intracellular expression of a bacterial hemoglobin. *Bio/Technol., 11*, 926-929.

Dikshit, K. L., Dikshit, R. P. & Webster, D. A. (1990) Study of *Vitreoscilla* globin (*vhb*) gene expression and promoter activity in *E. coli* through transcriptional fusion, *Nucleic Acids Res. 18*, 4149-4155.

Dikshit, K. L., Spaulding, D., Braun, A. & Webster, D. A. (1989) Oxygen inhibition of globin gene transcription and bacterial haemoglobin synthesis in *Vitreoscilla*, *J. Gen. Microbiol. 135*, 2601-2609.

Dikshit, K. L. & Webster, D. A. (1988) Cloning, characterization and expression of the bacterial globin gene from *Vitreoscilla* in *Escherichia coli, Gene 70,* 377-386.

Gilles-Gonzalez, M. A., Ditta, G. S. & Helinski, D. R. (1991) A haemoprotein with kinase activity encoded by the oxygen sensor of *Rhizobium melilotti, Nature 350*, 170-172.

Iwaasa, H., Takagi, T. & Shikama, K. 1992. Amino acid sequence of yeast hemoglobin: a two-domain structure, *J. Mol. Biol. 227*, 948-954.

Kallio, P. T., Kim, D. J., Tsai, P. S. & Bailey, J. E. (1994) Intracellular expression of *Vitreoscilla* hemoglobin alters *Escherichia coli* energy metabolism under oxygen-limited conditions. *Eur. J. Biochem., 219*, 201-208.

Kawahare, Y., Tanaka, T., Ikeda, S. & Sone, N. (1988) Coupling sites of the respiratory chain of *Brevibacterium lactofermentum, Agric. Biol. Chem. 52*, 1979-1983.

Khosla, C. & Bailey, J. E. (1988a) Heterologous expression of a bacterial haemoglobin improves the growth properties of recombinant *Escherichia coli, Nature 331*, 633-635.

Khosla, C. & Bailey, J. E. (1988b) The *Vitreoscilla* hemoglobin gene: molecular cloning, nucleotide sequence and genetic expression in *Escherichia coli, Mol. Gen. Genet. 214*, 158-161.

Khosla, C. & Bailey, J. E. (1989) Evidence of partial export of *Vitreoscilla* hemoglobin into the periplasmic space in *Escherichia coli*. Implication for protein function, *J. Mol. Biol. 210*, 79-89.

Khosla, C., Curtis, J. E., DeModena, J., Rinas, U. & Bailey, J. E. (1990) Expression of intracellular hemoglobin improves protein synthesis in oxygen-limited *Escherichia coli*, *Bio/Technol. 8*, 849-853.

Khosravi, M., Webster, D. A. & Stark, B. C. (1990) Presence of the bacterial hemoglobin gene improves α-amylase production of a recombinant *Escherichia coli* strain, *Plasmid 24*, 190-194.

Kita, K., Konishi, K. & Ankaru, Y. (1984) Terminal oxidases of *Escherichia coli* aerobic respiratory chain, *J. Biol. Chem. 259*, 3375-3381.

Laemmli, U. K. (1970) Cleavage of structural proteins during the assembly of the head of bacteriophage T4, *Nature 227*, 680-685.

Magnolo, S. K., Leenutaphong, D. L., DeModena, J. A., Curtis, J. E., Bailey, J. E., Galazzo, J. L. & Hughes, D. E. (1991) Actinorhodin production by *Streptomyces coelicolor* and growth of *Streptomyces lividans* are improved by the expression of a bacterial hemoglobin, *Bio/Technology 9*, 473-476.

Meyer, D. J. & Jones, C. W. (1973) Oxidative phosphorylation in bacteria which contain different cytochrome oxidases. *Eur. J. Biochem.*, *36*, 144-151.

Mitchell, P. (1961) Coupling of phosphorylation to electron and hydrogen transfer by a chemi-osmotic type of mechanism, *Nature 191*, 144-148.

Mitchell, P. & Moyle, J. (1967) Acid-base titration across the membrane system of rat-liver mitochondria, *Biochem. J. 104*, 588-600.

Puustinen, A., Finel, M., Haltia, T., Gennis, R. B. & Wikström, M. (1991) Properties of the two terminal oxidases of *Escherichia coli, Biochemistry 30*, 3936-3942.

Vasudevan, S. G., Armarego, W. L. F., Shaw, D. C., Lilley, P. E., Dixon, N. E. & Poole, R. K. (1991) Isolation and nucleotide sequence of the *hmp* gene that encodes a haemoglobin-like protein in *Escherichia coli* K-12, *Mol. Gen. Genet. 226*, 49-58.

Webster, D. (1987) Structure and function of bacterial hemoglobin and related proteins, in *Advances in Inorganic Biochemistry* (Eichhorn, G. C. & Marzilli, L. G., eds) vol. 7, pp. 245-265, Elsevier, New York.

Winston, S. E., Fuller, S. A. & Hurrell, J. G. R. (1987) Western blotting, in *Current protocols in molecular biology* (Ausubel, F. M., Brent, R., Kingston, R. E., Moore, D. D., Seidman, J. G., Smith, J. A. & Struhl, K., eds.) pp. 10.8.1-10.8.6., John Wiley & Sons, Inc., New York.

Yanisch-Perron, C., Vieira, J. & Messing, J. (1985) Improved M13 phage cloning vectors and host strains: nucleotide sequence of the M13mp18 and pUC19 vectors, *Gene 33*, 103-119.

Zhu, H. & Riggs, A. F. (1992) Yeast flavohemoglobin is an ancient protein related to globins and a reductase family, *Proc. Natl. Acad. Sci. USA. 89*, 5015-5019.

2.8 Figures

Figure 1 Effect of KSCN concentration on H^+/O ratio. Shake flask culture of *E. coli* MC4100 was grown overnight in LB medium. After harvest, cells were resuspended in a testing buffer which consisted of 50 mM K_2SO_4, 10 mM $MgSO_4$, 0.25 mM MOPS, 0.50 μg/mL valinomycin, and indicated concentration of KSCN. Respiratory stoichiometry measurement was performed as described in Materials and Methods.

Figure 2 Batch cultures of *E. coli* JM101 carrying either the VHb-expression vector, pRED2 (●), or the parental vector, pUC9 (O). Dissolved oxygen profiles of JM101:pRED2 (– – –) and JM101:pUC9 (——) are also shown. Culture density is reported as the absorbance at 600 nm (A_{600}). Time points at which samples were taken for H^+/O measurement are indicated by arrows.

Figure 3 Proton extrusion (ΔpH) vs. oxygen pulse plots of JM101:pRED2 at the 3.5^{th} hr (O) and the 4.5^{th} hr (●), and JM101:pUC9 at the 3^{rd} hr (□) and the 4^{th} hr (X) of bioreactor cultivations. The slopes (H^+/O) of these plots are 3.0 and 3.1 for JM101:pRED2 at the 3.5^{th} hr and the 4.5^{th} hr, respectively, and 2.0 and 2.1 for JM101:pUC9 at the 3^{rd} hr and the 4^{th} hr, respectively.

Figure 4 Hypothetical effects of *Vitreoscilla* hemoglobin protein on the dissolved oxygen concentration in *E. coli*. The effect has been calculated according to equations (2) and (3) as described in the Discussion. DO_{eff} as defined in Equation (4) is the hypothesized effective dissolved oxygen concentration

equal to the sum of dissolved oxygen concentration and the concentration of oxygenated VHb ($DO_{eff} = DO + [VHb \cdot O_2]$).

Figure 5 Michaelis-Menten kinetics of the two terminal oxidases at various oxygen concentrations.

Figure 1

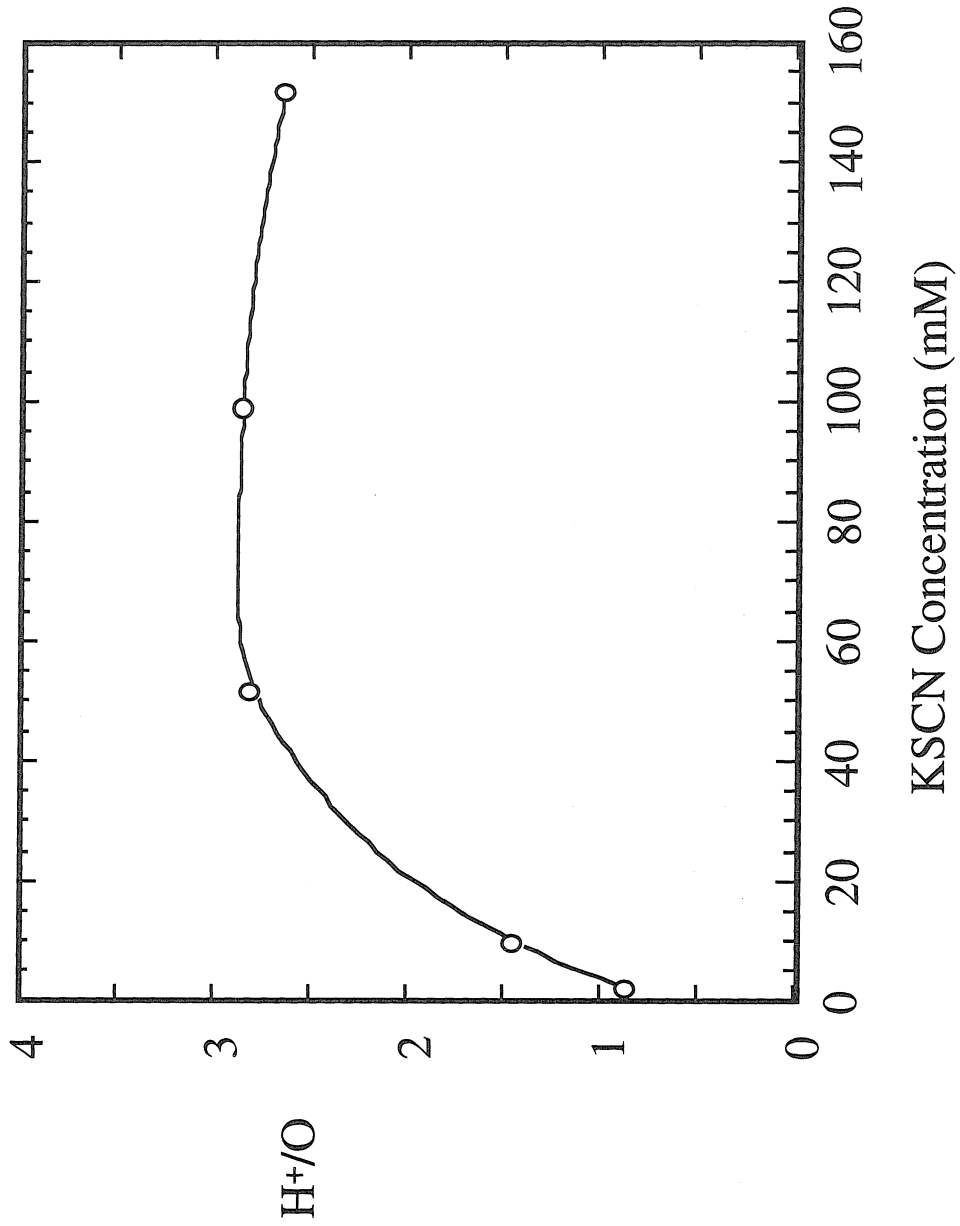

Figure 2

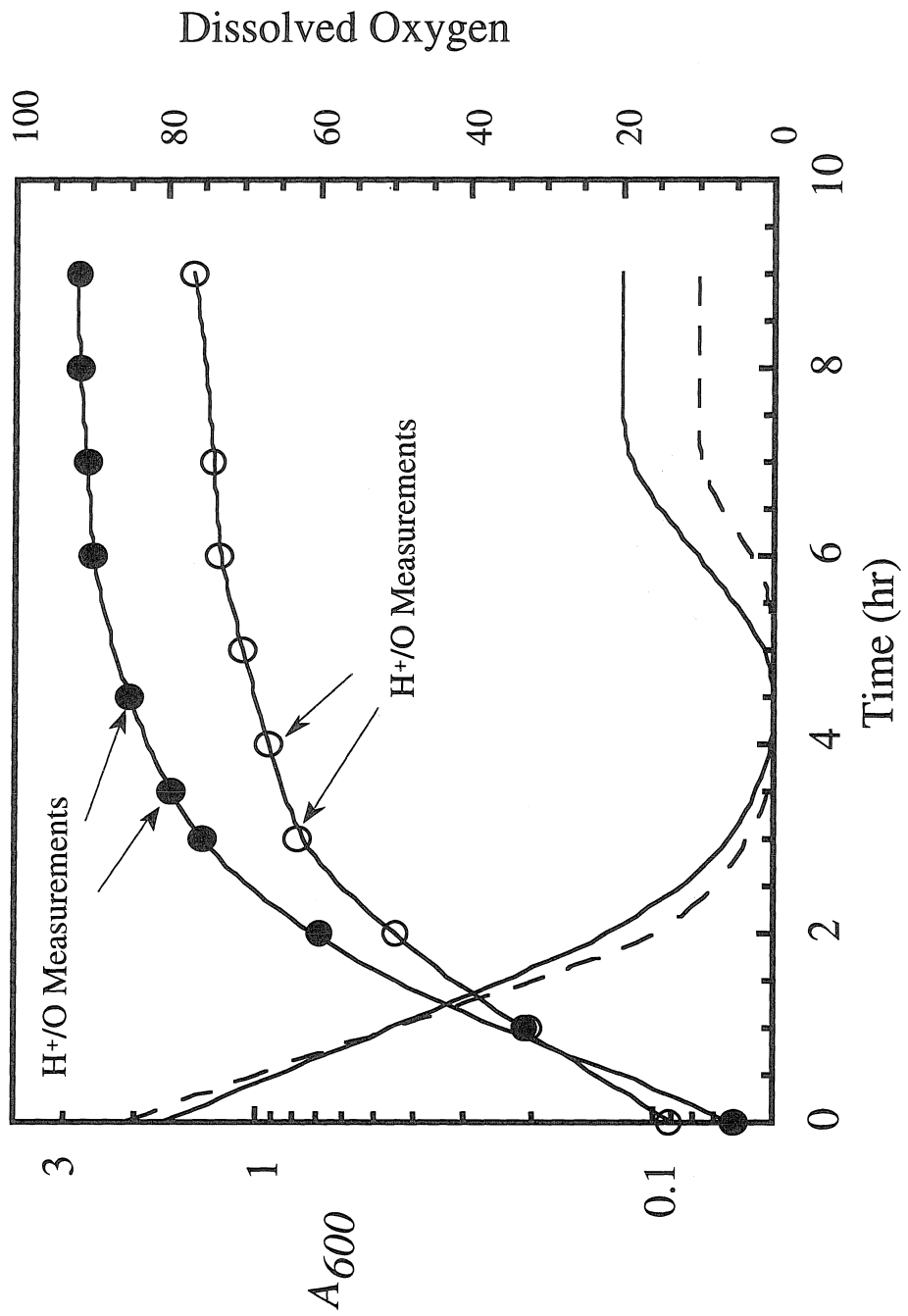
Dissolved Oxygen
100
80
60
40
20
0
10
8
6
4
2
0
Time (hr)
H+/O Measurements
H+/O Measurements
3
1
0.1
A600

Figure 3

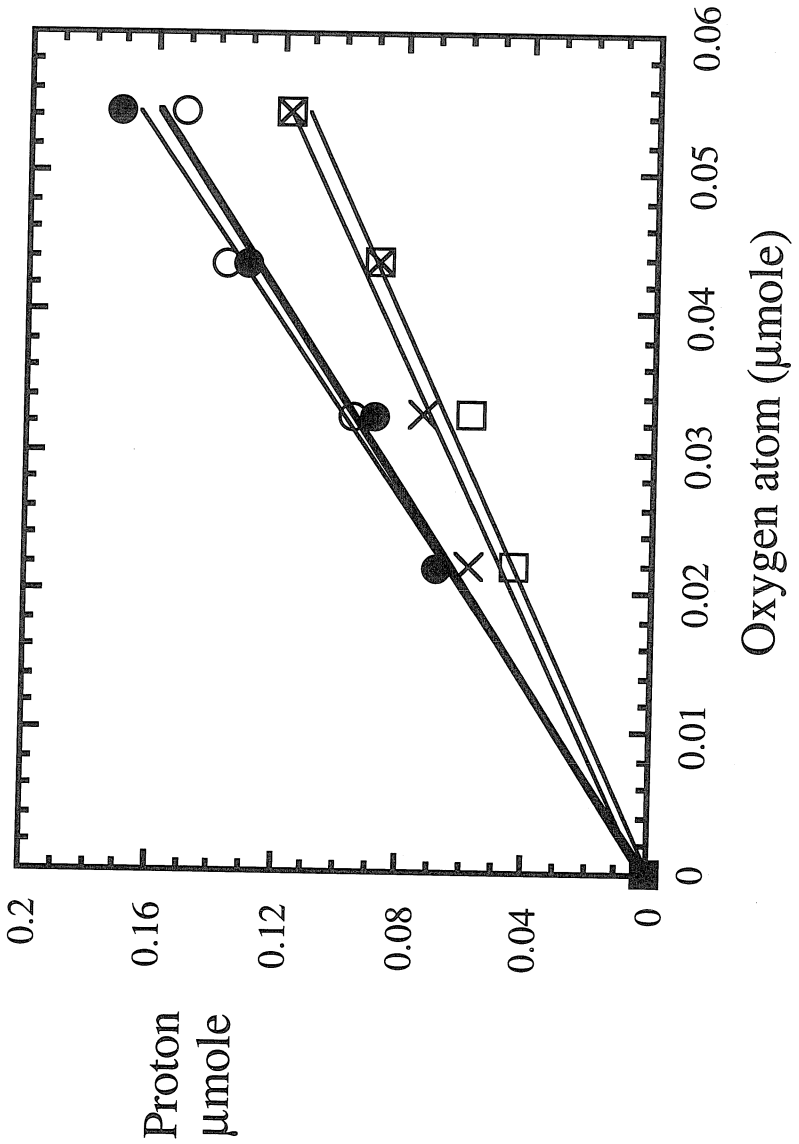
Proton µmole
0.2
0.16
0.12
0.08
0.04
0
0
0.01
0.02
0.03
0.04
0.05
0.06
Oxygen atom (µmole)

Figure 4

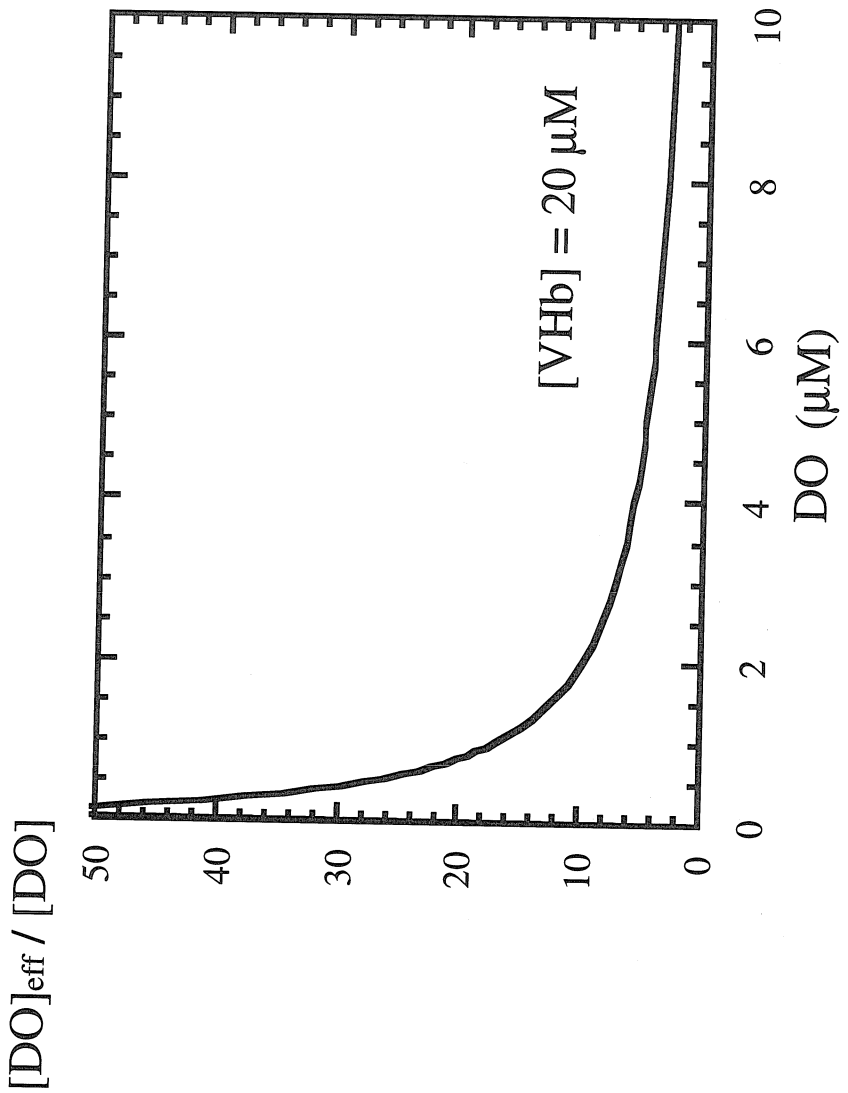

Figure 5

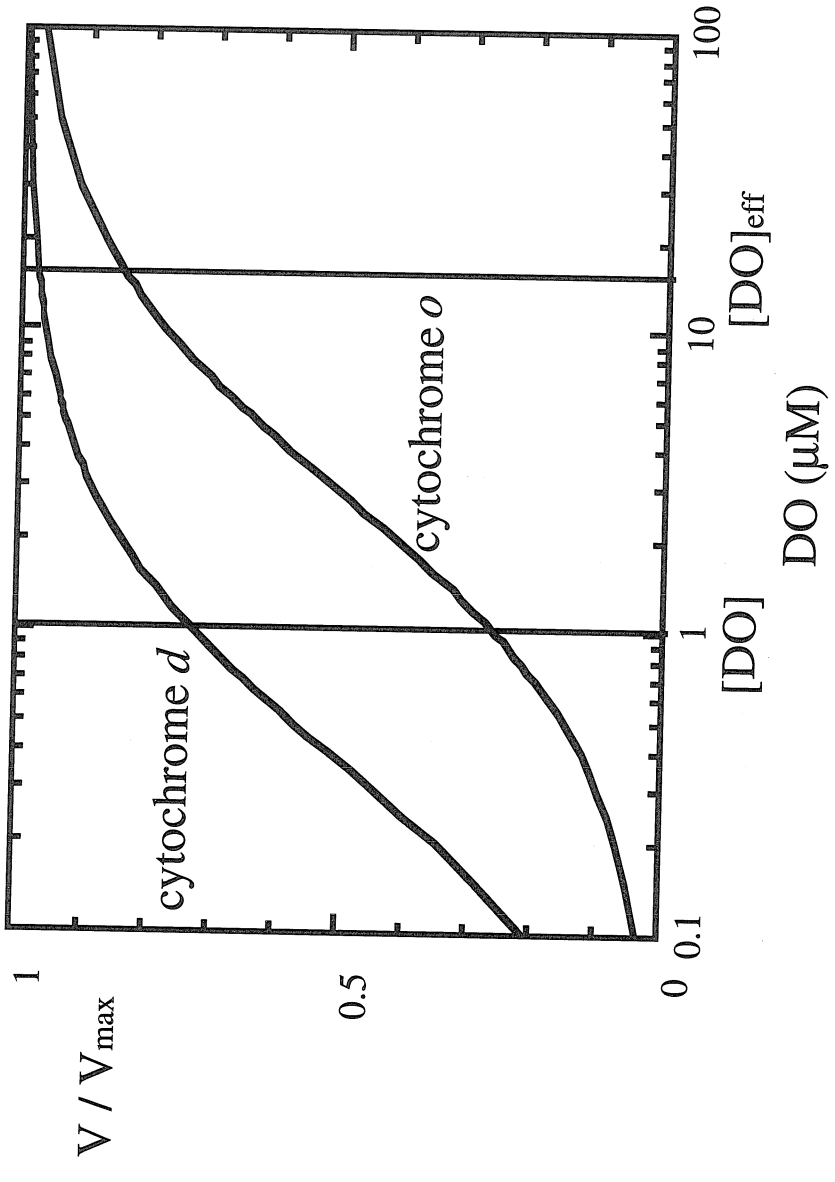
1
0.5
0
V / Vmax
cytochrome d
cytochrome o
0.1
1
10
100
[DO]
[DO]eff
DO (μM)

CHAPTER 3:

Elevated Concentration and Specific Activity of *Escherichia coli* Cytochrome *o* by *Vitreoscilla* Hemoglobin

Source: Tsai, P. S.; Naegeli, M.; Bailey, J. E. Intracellular expression of *Vitreoscilla* hemoglobin modifies microaerobic *Escherichia coli* metabolism through elevated concentration and specific activity of cytochrome *o*. 1995. Submitted to *Biotechnology and Bioengineering*.

3.1 Summary

The function of the reversible oxygen-binding hemoprotein from *Vitreoscilla* (VHb), which enhances oxygen-limited cell growth and recombinant protein production when functionally expressed in *Escherichia coli* (*E. coli*), was investigated in wild-type *E. coli* and in *E. coli* mutants lacking one of the two terminal oxidases, cytochrome *o* complex (aerobic terminal oxidase) or cytochrome *d* complex (microaerobic terminal oxidase). Deconvolution of VHb, cytochrome *o*, and cytochrome *d* bands from *in vivo* absorption spectra revealed a 5-fold enhancement in cytochrome *o* content and a 1.5-fold increment in cytochrome *d* by VHb under microaerobic environments (dissolved oxygen less than 2% air-saturation). Based upon oxygen-uptake kinetics measurements of these mutants, the apparent oxygen affinity of the cytochrome *o*–only *E. coli* was increased in the presence of VHb but no difference in the apparent K_m was observed for the cytochrome *d*–only strain. Results suggest that the expression of VHb in *E. coli* increases the level and activity of terminal oxidases and thereby improves the efficiency of microaerobic respiration and growth.

Key words: Cytochrome *o*, Globin function, *Vitreoscilla* hemoglobin, Oxygen starvation.

3.2 Introduction

In contrast to vertebrate hemoglobins and myoglobins, non-vertebrate globins exhibit great diversity, not only in primary sequences but also in functions in their respective hosts (48, 49). Leghemoglobin from symbiosis-independent, legume plants such as soybean root has been suggested to function as an electron donor (6) and as an oxygen sensor to switch on and off the oxidative and fermentative pathways of root energy metabolism (5). A hemoglobin from protobranch bivalve molluscs' bacterial symbionts which binds and releases sulfide to the bacterial symbiont and oxygen to the gill was thought to act as a terminal oxidase (53). While hemoglobin in non-vertebrates has been the subject of studies for many years, relatively few bacterial and lower eucaryotic hemoglobins are isolated and characterized, and their functions are still unknown.

The most well known bacterial hemoglobin, *Vitreoscilla* hemoglobin (VHb), accumulates to high level in *Vitreoscilla* under hypoxic conditions (50). When VHb was functionally expressed in *Escherichia coli* (22, 25, 26), *Streptomyces coelicolor*, and *Streptomyces lividans* (30), significant growth, recombinant protein and antibiotic production enhancements were observed. Although no detailed biochemical and biophysical data are available, several possible roles of VHb action have been suggested from physiological observations. Wittenberg and Wittenberg (52) have proposed the possibility that VHb acts as a terminal oxidase which actively mediates electron transfer and oxygen reduction in *Vitreoscilla*. Recently, another function of VHb has been postulated (21): VHb may provide additional available oxygen to the electron transport chain of *E. coli*, thereby modulating the terminal oxidase activity and changing the oxidative phosphorylation efficiency. The *E. coli* -VHb system has

now been developed to be perhaps the most well-characterized and well-defined framework for study of the functions of invertebrate globins. In this work we investigate the influence of VHb on the aerobic electron transport chain, especially the terminal oxidases, of *E. coli*.

The electron transport chain of aerobically grown *E. coli* contains two different quinol oxidases, cytochrome *bo* and cytochrome *bd*, that reduce oxygen to water (3, 4, 17). Cytochrome *bo* (cytochrome *o* complex), which consists of *b*-type and oxygen-binding *o*-type heme groups, is the predominant terminal oxidase during fully aerobic conditions (43). Cytochrome *bd* (cytochrome *d* complex), which consists of two *b*-type heme groups and an oxygen-binding heme *d* group, has a higher oxygen affinity (cytochrome *d* K_m = 0.38 μM) (28) than does cytochrome *o* complex (cytochrome *o* K_m = 2.9 μM) (27) and is synthesized under low-oxygen conditions. During aerobiosis a proton gradient which drives ATP synthesis by ATPase is generated by concomitant coupling of proton translocation to the outside of the cytoplasmic membrane with electron transfer from dehydrogenases via quinones to the terminal oxidases. When electrons are channeled through the proton-pumping cytochrome *o* complex, an H^+/e^- ratio of 2 is achieved (41, 42). However, when the electron pathway goes through cytochrome *d* complex, which is not a proton pump but scalarly separates protons and electrons, a lower H^+/e^- ratio of 1 is obtained (33, 41).

The reduced heme *o* in the cytochrome *o* complex of *E. coli*, when bound to CO, exhibits a characteristic absorption peak at 416 nm and a trough at 430 nm (27). The absorption spectrum of heme *d* of the *E. coli* cytochrome *d* complex depends on pH, has a maximum around 628 nm and a minimum around 650 nm in a reduced minus oxidized difference spectrum, and has a maximum at 637 nm in CO-reduced

minus reduced spectrum (32). The reduced cytochrome *d* complex is also known to absorb light and gives troughs and shoulders in the Soret region under a CO atmosphere (12, 28).

Vitreoscilla hemoglobin contains protoheme IX, binds oxygen reversibly, and has an oxygen affinity similar to those of cytochrome *o* and *d* of *E. coli* (VHb K_D = 0.25 μM) (39, 46). The CO-bound, reduced protoheme of VHb absorbs similarly to cytochrome *o* in the Soret region except the peak occurs at 419 nm and the trough at 437 nm (51). Expression in *E. coli* of VHb from its associated promoter is maximally induced under microaerobic conditions (dissolved oxygen level below 2% of air-saturation), but transcription does not occur under anaerobic conditions (23). In contrast to cytochrome *o* and *d* complexes which are transmembrane proteins (10, 36), VHb is a soluble protein and is located on both sides of the cytoplasmic membrane in both *E. coli* and *Vitreoscilla* (24).

In this study, we investigated the possibilities of VHb as an effective dissolved oxygen enhancer that affects the energetics of terminal oxidases and as an additional terminal oxidase in microaerobic *E. coli*. To focus on the role of VHb in influencing the terminal oxidases of *E. coli*, we determined the effects of VHb on the levels and activities of terminal oxidases in *E. coli* mutants lacking either functional cytochrome *o* or cytochrome *d* complexes. The amount of VHb, cytochrome *o* and *d* were determined from intact-cell absorbance spectra at room temperature. Due to overlapping absorption of VHb, cytochrome *o*, and cytochrome *d* complex in the Soret region, deconvolution analyses were employed to decouple these spectra into their respective components. An *E. coli* strain lacking both terminal oxidases but synthesizing VHb enabled investigations on the possibility that VHb functions as a

terminal oxidase. The oxygen reactivity and proton translocation capability of this strain were assessed.

3.3 Materials and Methods

3.3.1 Strains and Plasmids

E. coli strains and plasmids used in this study are listed in Table 1. ECL strains (a generous gift of Dr. E. C. C. Lin) are derivatives of ECL525 (F^-, Δ*frd*-101, *ara*D139Δ(*arg*F-*lac*)U169, *rps*L150, *rel*A1, *deo*C1, *flb*-5301, *pts*F25). Strains ECL933, ECL936, and ECL937 were transformed with the control plasmid pMS421, the *vhb* expression plasmid pMSV1, and pMSC1 which carries the *Vitreoscilla* hemoglobin promoter P_{vhb}–*cat* gene fusion. Plasmid pMSC1 was constructed by inserting the 1 kb *Hin*d III-*Bam*H I fragment containing P_{vhb}-*cat* from pOX2 (23) into the corresponding sites in pMS421. Construction of pMSV1 was described elsewhere (21). *E. coli* strain GK100, which contains deletions in both *cyo* and *cyd*, is not able to synthesize functional cytochrome *o* and *d* complexes. GK100 cells were transformed with either the control plasmid pBR322 or the *vhb* expression plasmid pINT2 (24).

3.3.2 Media and Bioreactor Cultivations

Cultures were grown in buffered LB medium consisting of 10 g/L Bacto-tryptone, 5 g/L Bacto-yeast extract, 10 g/L NaCl, 3 g/L K_2HPO_4, 1 g/L KH_2PO_4 and adjusted to pH 7. Ampicillin (100 mg/L), spectinomycin (40 mg/L), and kanamycin (25 mg/L) were added to all ECL strains harboring either plasmids pMS421 or pMSV1 for plasmid maintenance except ECL933 to which only ampicillin and

spectinomycin were added. *E. coli* strains GK100 carrying either plasmid pINT2 or pBR322 were supplemented with 0.5% glucose, kanamycin (25 mg/L), and ampicillin (100 mg/L).

For growth comparison and preliminary cytochrome measurement ECL 933, ECL936, ECL937 containing either pMS421 or pMSV1 were grown in a 2.5 L MBR bioreactor MCS11 with a 1.8 L working volume. 18 ml of an overnight seeding culture was used to inoculate each fermentation. Process parameters of batch cultivation (37°C, pH 7, 400 rpm, and 0.2 L/min air input) were maintained constant for the duration of each 9-h cultivation. A 350 ml sample was taken for the whole-cell spectroscopic assay when cells reached A_{600} 0.7. To study the effect of VHb on the terminal oxidase time-trajectory, ECL933:pMS421, ECL933:pMSV1, and ECL933:pMSC1 were cultivated in an LH bioreactor 210 (Inceltech, Inc.) with 4 L working volume. 50 ml of overnight–grown inoculum was used to initiate the 8-h batch cultivation during which the process parameters were kept constant at 37°C, pH 7, 300 rpm, and 1 L/min of air flow. Four 300 ml samples were withdrawn from the bioreactor during the course of cultivation for whole-cell spectroscopic assay.

E. coli strains GK100:pINT2 and GK100:pBR322 were cultivated in a Six-fors bioreactor (Infors AG) with working volume of 350 ml. A 10% of total volume seeding culture was used to inoculate the batch cultivation, and the reactor was maintained at 37°C, pH 7, 300 rpm, and zero air-input. Nitrogen gas was temporarily bubbled in the reactor 6.5 h after inoculation at the rate of 0.5 L/min to reduce the dissolved oxygen concentration to 5% air saturation and was then stopped. A 50 ml sample was taken 9 hours after inoculation for the respiratory stoichiometry measurement.

3.3.3 Protein Determination and CAT Assay

Samples for protein assay were prepared by resuspending cells 1:1 in a sonication buffer (100 mM Tris, 50 mM NaCl, 1 mM EDTA) and sonicated on ice at 35 watts in 30 s intervals 5 times using a Sonifier B12 (Branson Co.). Cell debris was removed by centrifuging at 4°C, 15,000 rpm for 15 minutes. Protein content of the sample was determined using a Bio-Rad protein assay kit (Bio-Rad Laboratories, Inc.) which is based on the method of Bradford (7).

CAT contents in ECL933:pMSC1 samples were determined from a CAT ELISA kit (5 Prime—>3 prime, Inc.). CAT activity was normalized with protein content of each sample and is reported in ng CAT per mg total soluble protein.

3.3.4 Respiratory Stoichiometry Assay

The respiratory stoichiometry assay, which measures the acidification of a cell suspension as a consequence of oxygen consumption by the cells, determines the ratio of protons extruded outside the cell per oxygen atom consumed (H^+/O) (34, 35). The H^+/O ratio was calculated by evaluating the slope of data from several experiments on pH change vs. amount of oxygen consumed, and is reported as mol proton per mol oxygen atom. A detailed description of this experimental method was provided elsewhere (21).

3.3.5 Respiration and Oxidase Activity Measurements

Oxygen consumption rates of ECL strains were monitored in a closed, stirred chamber of 0.6 ml with an Instech Model 125/05 platinum/silver microelectrode (Instech Laboratories, PA) and a YSI Oxygen Monitor 5300 Micro System (Yellow Springs Instrument, Co.) at 37°C. Cells were cultivated in 250 ml non-baffled shake

flasks containing 50 ml LB at 250 rpm for the first three hours and 100 rpm for an additional three hours before harvest. At harvest, 1 ml of culture sample was pelleted at 14,000 rpm and resuspended in 15 μL of phosphate buffer saline (PBS) (8 g/L NaCl, 0.2 g/L KCl, 1.44 g/L Na_2HPO_4, 0.24 g/L KH_2PO_4, adjusted to pH 7) at 37°C and was immediately injected to the reaction chamber containing 0.6 ml air-saturated PBS at 37°C to initiate the respiration measurement.

The kinetics of oxygen consumption as a function of oxygen concentration were measured using a procedure similar to the method described by Rice and Hempfling (44). Measurements were performed in a 45 ml glass vessel fitted with a water jacket for constant temperature maintenance. Cells for kinetics measurement were harvested from a 6-h old shake flask culture grown in 500 ml LB medium with 10% inoculum at 37°C and 250 rpm. After washing once with PBS, roughly 0.4 mg (dry weight) of cells was resuspended in 1 ml of succinate-phosphate buffer (20 mM succinate-sodium salt, 12.5 mM potassium phosphate, adjusted to pH 7.0) and added to the reaction vessel containing 44 ml of succinate-phosphate buffer. The system was stirred by a magnetic stirrer and maintained at 25°C by a circulating water bath. The cell suspension was rendered anaerobic by flushing with nitrogen gas and by respiration. The dissolved oxygen concentration time trajectory of the system was monitored with an Instech model 125/05 platinum/silver microelectrode (Instech Laboratories, PA) fitted with a 0.001–inch thick polyethylene membrane for rapid oxygen diffusion, and the output signals were recorded by a chart recorder. Once a stable anaerobic baseline was established, portions of 25°C air-saturated water were injected to the suspension through a port on top of the vessel to give an initial oxygen concentration inside the vessel of from 0.25 μM to 6 μM O_2. The velocity of oxygen uptake following each injection was calculated by drawing a tangent line through the

oxygen time-profile. K_m and V_{max} of the cells were determined from Hofstee plots (16). V_{max}, which equals to K_{cat}*[Enzyme]$_{total}$, was normalized by the total cytochrome *o* or *d* contents in the cells and reported as K_{cat}. Cytochrome *o* and *d* concentrations were determined from the membrane fraction (prepared from 400 ml of the remaining cultures) using difference spectrophotometry. Methods of membrane fraction preparation and spectroscopic determination of cytochrome *o* and *d* are described in the following sections. K_m and K_{cat} of the cells are reported in μM and sec^{-1}, respectively.

3.3.6 *E. coli* Cell Membrane Preparation

Cell membrane fraction was prepared as previously described (37) with a few modifications (Ma and Gennis, personal communication). After two passages through a French press (SLM-Aminco), samples were centrifuged at 10,000 x *g* for 20 min at 4°C to remove unbroken cells. The supernatant was then centrifuged at 12,000 x *g* at 4°C for 30 min to remove outer membrane. Membrane fraction was obtained by further centrifugation of the supernatant at 200,000 x *g* for 1 h at 4°C. The membrane fraction pellet was homogenized in 30% ethylene glycol for spectroscopic measurements.

3.3.7 Spectrophotometry

Room-temperature difference absorbance spectra were recorded using the split-beam mode of a Hitachi-Perkin Elmer 557 dual-wavelength scanning spectrophotometer at 300 nm/min with 2 nm slit width and 2 mm pathlength cuvettes. Samples were harvested and washed once with ice cold PBS and then resuspended to a final concentration of 100 mg (wet weight)/ml in 30% ethylene glycol. Cell suspensions were reduced by addition of a few grains of sodium dithionite (Sigma

Chemical Co.) and oxidized, if necessary, by addition of a few grains of ammonium persulfate (Bio-Rad) and incubated for 5 min at room temperature. CO binding to samples was achieved by bubbling CO through the suspension (one bubble per sec) until maximal spectroscopic effect was obtained (~ 2 min). CO-reduced minus reduced or reduced minus oxidized spectral data were collected by a PC via an A/D converter at the rate of 18.2 values per second.

3.3.8 Spectra Deconvolution

Contributions from absorption of VHb, cytochrome *o*, and cytochrome *d* complex in the Soret region give rise to a broad peak and a trough in the CO-reduced difference spectrum. In order to estimate the concentration of each component in the sample, multiple regression analysis (1) and a recursive least square FORTRAN program based on the Kalman Filter (15, 40) were used to resolve overlapping bands in the Soret region. Deconvolution standards of CO-reduced minus reduced spectra of cytochrome *o* and *d* complexes were prepared from one liter of either ECL937 (lacking cytochrome *d* complex) or ECL936 (lacking cytochrome *o* complex) shake flask cultures grown in LB medium to early stationary phase. At harvest, a portion of sample was used for intact-cell spectroscopic assay and the remainder was used for membrane fraction preparation. By using reported molar extinction coefficients for the purified cytochromes, $\varepsilon_{416\text{-}430}$ of 135 $mM^{-1}\cdot cm^{-1}$ for the reduced, CO-bound cytochrome *o* (Ma and Gennis, personal communication) and $\varepsilon_{628\text{-}607}$ of 7.4 $mM^{-1}\cdot cm^{-1}$ for the reduced cytochrome *d* (29), cytochrome *o* and *d* contents in the membrane fraction samples were estimated. The estimated cytochrome contents in the membrane fraction samples were the basis for calculation of cytochrome contents in the whole-cell samples, and thus for generating molar extinction coefficients of cytochrome *o* and *d* complexes for the whole-cell difference spectra. The VHb

deconvolution standard was generated in similar fashion from *E. coli* GK100 (*cyo*$^-$, *cyd*$^-$) carrying the *vhb* expression vector pINT2. The soluble fraction of cell extract obtained from double passage of sample through a French Press was used for VHb quantification. VHb concentration in the cell extract was estimated by using the reported VHb extinction coefficient, $\varepsilon_{419\text{-}437}$ of 106.7 $mM^{-1}\cdot cm^{-1}$ for the reduced CO-bound VHb (14). A control spectrum of an intact-cell sample of GK100 harboring the parental plasmid pMS421 was prepared in parallel to confirm the phenotype (lacking both cytochrome *o* and *d* complexes) of the strain. The then-calculated whole-cell ε's for each component between 405 and 450 nm (163 values) were used as deconvolution standards in deconvolution analysis which is based on Beer's law, $A=\varepsilon_{vhb} * l * c_{vhb} + \varepsilon_{cyo} * l * c_{cyo} + \varepsilon_{cyd} * l * c_{cyd}$. Cytochrome *d* concentration of a whole-cell sample was determined independently of cytochrome *o* and VHb from its absorbance characteristics in 600-650 nm. VHb and cytochrome *o* concentrations were then determined from the 400-450 nm region of the sample spectrum using deconvolution analysis.

3.4 Results

3.4.1 Spectra Deconvolution

Both multiple regression analysis (1) and a method based on the Kalman filter principle (15, 40) were employed to decouple and compare the concentrations of VHb, cytochrome *o* and cytochrome *d* from intact-cell spectra. A typical deconvolution analysis of a CO-reduced minus reduced absorbance spectrum of the VHb-synthesizing control strain (ECL933:pMSV1) is shown in Fig. 1. Cytochrome *d* is the only species that absorbs in the region of 650-600 nm (Fig. 1B), and thus its

concentration can be determined independently of both cytochrome *o* and VHb concentrations. Contribution of absorptions from VHb, cytochrome *o*, and cytochrome *d* complex in the Soret region (400-450 nm) resulted in a broad peak and a trough at 417 and 437 nm, respectively (Fig. 1A). The differences in concentrations deconvoluted by the two methods considered were less than 1% in all spectra analyzed. The degree of fit (R) of the composite spectrum to the sample spectrum was greater than 0.96 according to the index of determination (31), with R=1 being a perfect fit. To examine the accuracy of these methods, spectra taken from various mixtures of known concentrations of ECL936 (cyo^-) which synthesizes only cytochrome *d* complex, ECL937 (cyd^-) which synthesizes only cytochrome *o* complex, and ECL933:pMSV1 cell crude extract containing VHb were deconvoluted. Analyses correctly recovered the concentrations of different species from various mixtures with a 5% error. Furthermore, our deconvolution methods were sensitive in all concentration ranges reported in this study. Since both Kalman filter and multiple regression analysis gave very similar results, only concentrations deconvoluted by multiple regression analysis are reported.

3.4.2 Effect of VHb on Terminal Oxidase Accumulation

A previous report (21) has shown that significant microaerobic growth enhancement by VHb expression is observed in an *E. coli* mutant having functional cytochrome *o* lacking cytochrome *d* but not in a mutant synthesizing cytochrome *d* lacking cytochrome *o*. To examine whether the growth advantage for the cytochrome *d* mutant is a result of VHb influence on cytochrome levels, we cultivated ECL933, ECL936, and ECL937 (Table 1) carrying either the control plasmid pMS421 or the VHb expression plasmid pMSV1 under microaerobic conditions in a controlled bioreactor environment and assayed their cytochrome contents. In order to minimize

artifacts which might arise from sampling cells at different physiological states, cytochrome levels were deconvoluted from sample spectra taken when cultures reached the same A_{600} of 0.7. Results showed a seven-fold increase in cytochrome *o* content of the Cyo^+, Cyd^+ ECL933:pMSV1 (0.14 nmol/mg protein) when VHb was synthesized compared with the control (ECL933:pMS421, 0.02 nmol cytochrome *o*/mg protein). No significant difference in cytochrome *d* level was detected in these same strains (0.19 and 0.20 nmol/mg protein for ECL933:pMSV1 and ECL933:pMS421, respectively). The level of cytochrome *d* in ECL936:pMS421 (Cyd^+), 0.17 nmol/mg protein, was similar to that in parental construct (ECL936:pMSV1, 0.18 nmol cytochrome *d*/mg protein). The cytochrome *o* content in ECL937:pMS421 (Cyo^+) (0.07 nmol/mg protein) was 3.5 times larger than that in ECL933:pMS421. VHb production increased the cytochrome *o* level in ECL937:pMSV1 further to 0.16 nmol/mg protein, a concentration similar to that of cytochrome *o* in ECL933:pMSV1.

The finding of preferential enhancement in cytochrome *o* level in the mutants by VHb prompted us to study in detail the effect of VHb on the time course of cytochrome *o* and *d* accumulations in wild-type microaerobic cultures. The concentration time-trajectories of VHb and the two terminal oxidases in ECL933 harboring either pMS421 or pMSV1 were monitored during a batch bioreactor cultivation (see Materials and Methods). These batch cultures entered microaerobiosis 2 h after initiation of cultivation and remained microaerobic until the end of cultivation. Concentrations of the oxidases and VHb at different times of cultivation were normalized with total cellular protein and are shown in Fig. 2. VHb level increased from 0.35 nmol/mg protein at the 4^{th} h to 0.64 nmol/mg protein at the 7^{th} h post inoculation (Fig. 2A). Cytochrome *o* amount from ECL933:pMSV1 was on the

average 5-fold larger than that from ECL933:pMS421 at all time points (0.1 and 0.02 nmol/mg protein, respectively) (Fig. 2A). Cytochrome *d* amounts in ECL933:pMS421 and in ECL933:pMSV1 were similar at the 4^{th} and the 5^{th} h of the cultivations (Fig. 3B). The effect of VHb on cytochrome *d* level was significant only toward the end of cultivation where a two-fold increase in cytochrome *d* was observed in VHb-producing ECL933 (0.15 and 0.29 nmol cytochrome *d*/mg protein for ECL933:pMS421 and ECL933:pMSV1, respectively, at the 7^{th} h).

It is quite feasible that the *vhb* promoter could bind trans-acting transcriptional regulators involved in an oxygen-sensing system, and this perturbation in the wild-type distribution of such transcription factors could contribute to the observed terminal oxidase responses. We therefore examined the cytochrome levels in ECL933 carrying a P_{vhb}-*cat* fusion plasmid pMSC1. Results showed the presence of P_{vhb} did not significantly alter the level of cytochrome *o* compared with the same strain harboring the parental plasmid pMS421 (Fig. 2A). The cytochrome *d* time-trajectory of ECL933:pMSC1 gave values on the average 20% less than those observed for ECL933:pMS421. This could possibly be attributed to the competition between the *vhb* and *cyd* promoters for transcriptional activation by Fnr and the Arc system of *E. coli*, resulting in low transcriptional activities (45). Nevertheless, findings from this study indicate that the presence of VHb, and not the presence of P_{vhb}, enhances the level of cytochrome *o* much more than cytochrome *d* in microaerobic *E. coli*.

3.4.3 Effects of VHb on Cell Respiration and Terminal Oxidase Activity

It is not yet known how the location of VHb (24) influences the effect of VHb on *E. coli* microaerobic metabolism (22). In order to preserve the compartmentalization and spatial arrangement of VHb and cellular components with

which VHb may interact, the influence of VHb on the oxygen reactivities of cytochrome *o* and *d* was assayed in intact cells of ECL strains lacking one of these terminal oxidases.

We asked first how VHb would affect the oxygen uptake rate (OUR) of cells if only one terminal oxidase is active. The OUR was measured for each sample by adding concentrated cell suspension to air-saturated PBS at 37°C in a respirometer without addition of exogenous substrates and by monitoring the oxygen time-profile. OUR of the wild-type control was increased in the presence of VHb (4.5 and 6.8 μM $O_2 \cdot min^{-1} \cdot A_{600}^{-1}$ for ECL933:pMS421 and ECL933:pMSV1, respectively) (Table 2). In mutants lacking one of the terminal oxidases, VHb has a larger effect on the cytochrome *o*–only mutant. The OUR of ECL936:pMS421 (*cyo*⁻), 6.8 μM $O_2 \cdot min^{-1} \cdot A_{600}^{-1}$, was similar to that of ECL936:pMSV1, 6.7 μM $O_2 \cdot min^{-1} \cdot A_{600}^{-1}$, but the OUR of ECL937:pMS421 (*cyd*⁻), 4.2 μM $O_2 \cdot min^{-1} \cdot A_{600}^{-1}$, was higher when VHb is present (ECL937:pMSV1, 6.2 μM $O_2 \cdot min^{-1} \cdot A_{600}^{-1}$). This respiration measurement has an error margin of 5% and therefore the difference in the observed OURs was significant.

It is possible that the increase in the OUR of the cytochrome *d* mutant by VHb was a result of combined effects from an increase in the cytochrome *o* amount and an increase in the specific activity of cytochrome *o*. To differentiate between these two qualities we examined the oxygen uptake kinetics and measured the apparent K_m and V_{max} of the mutants, the latter normalized by the oxidase contents. The Hofstee plots of ECL936 (*cyo*⁻) and ECL937 (*cyd*⁻) for K_m and V_{max} determination yielded straight lines with 0.95 or higher correlation coefficients (Table 2), consistent with the characteristic of single-enzyme kinetics. The apparent K_m of cytochrome *o* for oxygen, which is independent of the oxidase concentration, was decreased in the

presence of VHb from 4.1 to 2.6 μM O_2 (Table 2). The apparent K_m of cytochrome *d*, however, was not significantly affected by the presence of VHb; the apparent cytochrome *d* K_ms were 0.19 and 0.21 μM O_2 for ECL936:pMS421 and ECL936:pMSV1, respectively. These K_m values were reproducible as similar results were obtained from duplicate experiments. Consistent with our earlier observation, cytochrome *d* content in the ECL936:pMS421 (*cyo*⁻) sample for oxidase activity measurement was similar to that of the ECL936:pMSV1 sample (0.25 nmol/mg protein), and cytochrome *o* content in ECL937:pMS421 (*cyd*⁻) was higher than that in ECL937:pMSV1 (0.10 and 0.06 nmol/mg protein, respectively). After normalizing the activity of each sample by its respective oxidase content, the K_{cat} (calculated by dividing V_{max} by the total cytochrome content) was similar with or without VHb in each genetic background: 4.6 sec^{-1} and 5.0 sec^{-1} for ECL936:pMS421 and ECL936:pMSV1, respectively, and 33 sec^{-1} and 28 sec^{-1} for ECL937:pMS421 and ECL937:pMSV1, respectively (Table 2). Based on the findings that the apparent K_m of cytochrome *o*, but not that of cytochrome *d*, was decreased by VHb, and that the apparent K_{cat} of the oxidases was not significantly affected by VHb, we conclude that the presence of VHb enhances the specific activity of cytochrome *o* under microaerobic conditions in addition to increasing the oxidase concentration.

3.4.4 VHb as a Terminal Oxidase

Hemoglobins such as yeast hemoglobin and VHb which contain protoheme IX and which are present at low intracellular concentration (less than 100 μM) have been suggested to possess terminal oxidase activities (52). Ycas (54) demonstrated that yeast synthesizes a hemoglobin and is able to grow aerobically without cytochrome oxidases. Recently, VHb was also shown to support aerobic growth of *E. coli* lacking both terminal oxidases (11). To further explore the possibility that VHb functions as a

terminal oxidase and to estimate the importance of this function in *E. coli* microaerobic growth, we examined the respiratory stoichiometry (H^+/O ratio) and the rate of H^+ gradient generation in response to oxygen addition in the *cyo*$^-$, *cyd*$^-$ mutant GK100. GK100, which was also used by Dikshit and co-workers (11) in their report, was transformed with either the control plasmid (pBR322) or the VHb expression plasmid (pINT2). Plasmids pMS421 and pMSV1 were not chosen for this study because GK100 already contains the spectinomycin-resistant gene harbored by pMS421 and pMSV1 (Table 1).

Samples for H^+/O measurement were obtained from bioreactor cultivations supplemented with 0.5% glucose as described in Materials and Methods. To simulate cultivation conditions under which the physiological effects of VHb were the most significant in wild-type *E. coli*, the dissolved oxygen tension (DO) was kept microaerobic by addition of nitrogen gas. As expected from a cytochrome *o* and *d* mutant, samples of GK100:pBR322 analyzed for H^+/O ratio did not respond to oxygen addition; no extracellular pH change was recorded upon oxygen injection. For the samples containing GK100:pINT2, very small changes in extracellular pH were detected when oxygen was injected to the testing medium, indicating a weak respiratory activity. However, in contrast to the H^+/O measurement performed previously on *E. coli* JM101 (21), the size of pH change (ΔpH) in response to oxygen addition for GK100:pINT2 was small and was not linearly proportional to the size of oxygen pulse, which made the estimation of H^+/O ratio difficult. The response time of GK100:pINT2 to oxygen inputs (measured by monitoring the time duration of a ΔpH transient after each oxygen pulse) was eight times longer than those recorded with ECL936 and ECL937 with either pMS421 and pMSV1 (results not shown), indicating the respiration rate of these cells was an order of magnitude lower than

those of ECL strains. More than 40 s were needed to complete a ΔpH transient after each oxygen addition to GK100:pINT2 suspension. The long time required for a ΔpH change to cease allows backflow of H^+ across the cytoplasmic membrane and would result in an underestimation of H^+/O ratio (35).

During the course of this study, mutants of GK100 were observed in bioreactor cultures. Samples of GK100:pBR322 and GK100:pINT2 from bioreactor cultures were able to grow slowly on LB-agar plates without glucose. Intact-cell spectra of the GK100 samples taken after H^+/O measurements showed CO-binding absorption characteristics (a peak at 417 nm and a trough at 432 nm) resembling those of cytochrome *o* and VHb in the 400-450 region, but did not match either VHb or cytochrome *o* spectra exactly (data not shown). The average intensity of absorption from GK100:pBR322, $\Delta A_{417\text{-}432}$ of 0.08, was small compared with that of an ECL strain (Fig. 1). Although difference spectra showed a faint CO-binding activity for GK100:pBR322 samples tested, no ΔpH was observed when oxygen was injected during H^+/O measurement.

Compared with the control (GK100:pBR322), it is most reasonable to assign the proton pumping activity of GK100:pINT2 to VHb. However, it is also possible that the cytochrome *o*-like compound, or the combination of the cytochrome *o*-like compound and VHb, contributed to the observed properties of GK100:pINT2. Nevertheless, the oxygen reactivity of GK100:pINT2 was not significant compared with those of strains expressing either cytochrome *o* or *d*.

3.5 Discussion

The possibility of VHb accepting electrons and reducing oxygen to water has previously been proposed (11, 52). Our study on the *E. coli* strain deficient in both cytochrome complexes showed that the strain with VHb slowly generated a very small proton gradient in response to oxygen while the control did not. This result suggests that VHb is capable of mediating oxygen reduction and proton translocation. Dikshit *et al.* (11) have also shown that the same *E. coli* strain was able to grow aerobically with a non-fermentable substrate when VHb was synthesized. However, VHb acting as a terminal oxidase alone cannot explain why the presence of VHb did not affect the growth (21) nor the oxygen utilization kinetics of the cytochrome *o* mutant (Cyd^+), yet significant increases in those qualities were observed in both the control strain (Cyo^+, Cyd^+) and the cytochrome *d* mutant (Cyo^+) producing VHb. Whatever oxidase activity VHb exhibits is small compared to that of the native cytochromes, so that VHb terminal oxidase activity can be significant only when there are no native cytochromes available.

A physiological study has shown that VHb-producing *E. coli* generate a larger intra- to extracellular pH difference and a larger H^+/O compared with the isogenic control (21). While a higher H^+/O suggests a higher energetic efficiency, cells with a low oxygen affinity, high energetic efficiency terminal oxidase (such as cytochrome *o*) may not generate as much proton gradient under hypoxic conditions as cells with a lower H^+/O ratio but a higher oxygen affinity terminal oxidase (such as cytochrome *d*). However, cells capable of coupling a higher H^+/O ratio with a higher oxygen affinity, such as *E. coli* expressing VHb, may produce a larger membrane potential under hypoxic conditions. Previously we have proposed a plausible functional role of

VHb to explain the physiological perturbations caused by VHb expression (21). The present study demonstrated that VHb improves *E. coli* microaerobic oxygen uptake rate through an elevated cytochrome *o* activity. In the following section, by applying the conjectured ability of VHb to bind and transfer oxygen to terminal oxidases in an enzymatic kinetic analysis, we approximate the observed effect of VHb in raising oxygen affinity, or decreasing K_m, of cells reported in this study.

Assuming oxygen utilization of cells follows simple Michaelis–Menten kinetics, the rate of oxygen uptake can be expressed as:

$$V = \frac{V_{\max}[O_2]_{eff}}{K_m + [O_2]_{eff}} \qquad [1]$$

where $[O_2]_{eff}$ refers to the effective DO which is given by Kallio et al. (21)

$$[O_2]_{eff} = [O_2] + \frac{[VHb]_{total}[O_2]}{K_D + [O_2]} \qquad [2]$$

Substitution and rearrangement of Equations [1] and [2] yield another Michaelis–Menten expression with a VHb–affected K_m, K_m^*, in terms of the original K_m, the dissociation constant of VHb, K_D (0.25 μM) (46, 39), the total VHb concentration, $[VHb]_{total}$, and the DO, $[O_2]_{eff}$:

$$V = \frac{V_{\max}[O_2]}{K_m^* + [O_2]} \qquad [3]$$

$$\text{where } K_m^* = \frac{K_m(K_D + [O_2])}{K_D + [O_2] + [VHb]_{total}} \qquad [4]$$

Under microaerobic conditions (say, DO in the range of 2 and 5 μM) with an apparent K_m of 4.1 μM and a VHb concentration of 2 μM for the cytochrome *o*–only *E. coli* (2 μmol VHb/g DCW for the *cyd*$^-$ mutants estimated from the soluble fraction of the

cell extracts with 1 g DCW/L cell density), the K_m^* calculated from Equation [4] is between 2.2 and 2.9 μM for the VHb-synthesizing, cytochrome *o*-only mutant. A similar calculation gives a VHb–influenced apparent K_m^* of between 0.12 and 0.16 μM for the cytochrome *d*-only mutant with 0.2 μM K_m and 1.5 μM VHb concentration (1.5 μmol VHb/g DCW and 1 g DCW/L cell density). These values deviate from the experimental data for the *cyd*$^-$ and *cyo*$^-$ mutants by about 15% and 30%, respectively (Table 2).

Using the measured apparent K_m, V_{max}, and the reported H^+/O values (41) for cytochrome *o* and *d*, we constructed a theoretical model of the proton translocation rate of *E. coli* when electrons are channeled through either cytochrome *o* or *d* (Fig. 3). We incorporated into the calculation our experimentally determined oxidase concentrations for *E. coli cyo*$^-$ or *cyd*$^-$ mutants grown under microaerobic conditions (below 5 μM): 38.5 nmol/g cells for cytochrome *o* and 93.5 nmol/g cells for cytochrome *d*. The importance of the two terminal oxidases in different oxygen concentrations can clearly be seen from this figure. Below 4 μM DO, a larger proton gradient is generated when cells utilize cytochrome *d* rather than cytochrome *o*. However, the rate of proton translocation by cytochrome *o* surpasses that of cytochrome *d* when the oxygen tension is greater than 4 μM. We have shown that, under microaerobic conditions, accumulation of VHb enhanced the specific activity of cytochrome *o* but not cytochrome *d*. Thus, VHb will increase the rate of proton translocation due to a more active cytochrome *o*, resulting in higher ATP generation rate (9) and faster cell growth (22). Conversely, VHb will not have a notable effect on the physiology of a cytochrome *o* mutant, since an increase in the effective dissolved oxygen does not influence the activity of cytochrome *d* significantly.

We have also shown a five-fold increase in cytochrome *o* level and a 1.5-fold increase in cytochrome *d* level by VHb (Fig. 2). How may VHb affect the net synthesis of the terminal oxidases under microaerobic conditions? It is well documented that the expression of many oxygen-regulated genes is subject to the control of the two pleiotropic modulons, Fnr and the Arc system, which sense the changing dissolved oxygen level and activate or repress their effectors (13). In this study we observed a substantial increase in the cytochrome *o* levels in constructs expressing VHb. Working with the same proposed VHb function in raising effective dissolved oxygen concentration, perhaps Fnr and the Arc system sense a higher dissolved oxygen in the presence of VHb and derepress the expression of the cytochrome *o* genes (19). It is possible that the presence of VHb might affect expression of other oxygen-regulated genes. However, previous two-dimensional protein gel electrophoresis analysis of VHb-expressing *E. coli* and a VHb-free control showed changes in intensity of only 7 polypeptides detected on those gels (25).

Recently it was demonstrated that aerobic *E. coli* partitions substantially its electron flux to the proton motive force coupled NDH-1 NADH dehydrogenase and, to a lesser extent, to the uncoupled NDH-2 NADH dehydrogenase (8). In a mutant lacking NDH-2, the requirement for oxygen per g biomass synthesis decreases and the bioenergetic efficiency increases because all electrons are channeled through the energy yielding NDH-1 (8). We cannot exclude the possibility of VHb shifting the electron flux distribution through NDH-1/NDH-2 toward NDH-1, although we cannot discern any plausible genetic or biochemical basis for such an effect based on current knowledge of this dehydrogenase system. Furthermore, our cytochrome mutant studies showed preferential effects of VHb on the cytochrome *d* mutant. If VHb perturbs the electron flux ratio of NDH-1/NDH-2, we would expect enhancements in

energetic parameters from both *cyo*⁻ and *cyd*⁻ mutants, unless VHb shifts the NDH-1/NDH-2 electron flux only in the wild-type and in *cyd*⁻ mutant backgrounds.

Ioannidis et al. (18) have reported the spectroscopic properties of hemoglobin-like flavohemoprotein (HMP) in *E. coli* to be similar to those of VHb. This raises the question whether the presence of HMP interferes with our spectroscopic deconvolution and interpretation thereafter. We believe this not to be the case under our experimental conditions. There are no reports to date on the spectroscopic detection of wild-type level HMP in *E. coli*; all reported absorbencies are from amplified expression and subsequent concentration of HMP (2, 18, 47). Second and more importantly, our whole-cell spectra of cytochrome *o* and *d* mutants, as well as cytochrome *o*, *d* double mutant, did not show any sign of endogenous HMP activity (spectra not shown). Therefore, our quantification method for cytochromes and VHb is valid and unlikely affected by HMP interference. Whether the presence of VHb affects the synthesis of HMP is beyond the scope of this study.

3.6 Acknowledgments

This research was supported by the Swiss Priority Program in Biotechnology. We wish to thank Dr. E. C. C. Lin for generously supplying *E. coli* strains ECL933, ECL936, and ECL937, and Dr. R. B. Gennis for the gift of *E. coli* strain GK100. We would like to thank Dr. W. Chen and V. Hatzimanikatis for assistance in spectra deconvolution. We are also grateful to J. Ma of the University of Illinois for assistance in membrane preparation.

3.7 References

1. Anderson, T. W. 1985. In: Introduction to multivariate statistical analysis, Wiley, New York.

2. Andrew, S. C., Shipley, D., Keen, J. N., Findlay, J. B. C., Harrison, P. M., Guest, J. R. 1992. The haemoglobin-like protein (HMP) of *Escherichia coli* has ferrisiderophore reductase activity and its C-terminal domain shares homology with ferredoxin $NADP^+$ reductases. FEBS Lett. **302**: 247-252.

3. Anraku, Y., Gennis, R. B. 1987. The aerobic respiratory chain of *Escherichia coli*. Trends Biochem. Sci. **12**: 262-266.

4. Anraku, Y. 1988. Bacterial electron transport chain. Ann. Rev. Biochem. **57**: 101-132.

5. Appleby, C. A., Bogusz, D., Dennis, E. S., Peacock, W. J. 1988. A role for hemoglobin in all plant roots? Plant, Cell & Environment. **11**: 359-367.

6. Bakan, D. A., Saltman, P., Theriault, Y., Wright, P. E. 1991. Kinetics and mechanisms of reduction of Cu(II) and Fe(II) complexes by soybean leghemoglobin. Biochim. Biophys. Acta **1079**: 182-196.

7. Bradford, M. M. 1976. A rapid and sensitive method for the quantitation of microgram quantities of protein utilizing the principle of protein-dye binding. Anal. Biochem. **72**: 248-254.

8. Calhoun, M. W., Oden, K., Gennis, R. B., de Mattos, M. J. T., Neijssel, O. M. 1993. Energetic efficiency of *Escherichia coli*: Effects of mutants in components of the aerobic respiratory chain. J. Bacteriol. **175**: 3020-3025.

9. Chen, R., Bailey, J. E. 1994. Energetic effect of *Vitreoscilla* hemoglobin expression in *Escherichia coli*: An on-line ^{31}P NMR and saturation transfer study. Biotechnol. Prog. **10**: 360-364.

10. Chepuri, V., Gennis, R. B. 1990. The use of gene fusions to determine the topology of all of the subunits of the cytochrome *o* terminal oxidase complex of *Escherichia coli*. J. Biol. Chem. **265**: 12978-12986.

11. Dikshit, R. P., Dikshit, K. L., Liu, Y., Webster, D. A. 1992. The bacterial hemoglobin from *Vitreoscilla* can support the aerobic growth of *Escherichia coli* lacking terminal oxidases. Arch. Biochem. Biophys. **293**: 241-245.

12. Green, G. N., Gennis, R. B. 1983. Isolation and characterization of an *Escherichia coli* mutant lacking cytochrome *d* terminal oxidase. J. Bacteriol. **154**: 1269-1275.

13. Guest, J. R. 1992. Oxygen-regulated gene expression in *Escherichia coli*. J. Gen. Microbiol. **138**: 2253-2263.

14. Hart, R. A., Bailey, J. E. 1991. Purification and aqueous 2-phase partitioning properties of recombinant *Vitreoscilla* hemoglobin. Enz. Microb. Technol. **13**: 788-795.

15. Hartwell, S. 1988. Multicomponent analysis of UV-VIS spectra using the Kalman filter. International Laboratory **March**: 42-50.

16. Hofstee, B. H. J. 1959. Non-inverted versus inverted plots in enzyme kinetics. Nature **184**: 1296-1298.

17. Ingledew, W. J., Poole, R. K. 1984. The respiratory chain of *Escherichia coli.* Microbiol. Rev. **48**: 222-271.

18. Ioannidis, N., Copper, C. E., Poole, R. K. 1992. Spectroscopic studies on an oxygen-binding haemoglobin-like flavohaemoprotein from *Escherichia coli.* Biochem. J. **288**: 649-655.

19. Iuchi, S., Lin, E. C. C. 1991. Adaptation of *Escherichia coli* to respiratory conditions: Regulation of gene expression. Cell **66**: 5-7.

20. Iuchi, S., Chepuri, V., Fu, H.-A., Gennis, R. B., Lin, E. C. C. 1990. Requirement for terminal cytochromes in generation of the aerobic signal for the *arc* regulatory system in *Escherichia coli*: Study utilizing deletions and *lac* fusions of *cyo* and *cyd*. J. Bacteriol. **172**: 6020-6025.

21. Kallio, P. T., Kim, D. J., Tsai, P. S., Bailey, J. E. 1994. Intracellular expression of *Vitreoscilla* hemoglobin alters *Escherichia coli* energy metabolism under oxygen-limited conditions. Eur. J. Biochem. **219**: 201-208.

22. Khosla, C., Bailey, J. E. 1988. Heterologous expression of a bacterial haemoglobin improves the growth properties of recombinant *Escherichia coli.* Nature **331**: 633-635.

23. Khosla, C., Bailey, J. E. 1989a. Characterization of the oxygen-dependent promoter of the *Vitreoscilla* hemoglobin gene in *Escherichia coli.* J. Bacteriol. **171**: 5995-6004.

24. Khosla, C., Bailey, J. E. 1989b. Evidence for partial export of *Vitreoscilla* hemoglobin into the periplasmic space in *Escherichia coli.* J. Mol. Biol. **210**: 79-90.

25. Khosla, C., Curtis, J. E., DeModena, J., Rinas, U., Bailey, J. E. 1990. Expression of intracellular hemoglobin improves protein synthesis in oxygen limited *Escherichia coli.* Bio/Technol. **8**: 849-853.

26. Khosravi, M., Webster, D. A., Stark, B. C. 1990. Presence of bacterial hemoglobin gene improves α-amylase production of a recombinant *Escherichia coli* strain. Plasmid **24**: 190-194.

27. Kita, K., Konishi, K., Anraku, Y. 1984a. Terminal oxidases of *Escherichia coli* aerobic respiratory chain, I. J. Biol. Chem. **259**: 3368-3374.

28. Kita, K., Konishi, K., Anraku, Y. 1984b. Terminal oxidases of *Escherichia coli* aerobic respiratory chain, II. J. Biol. Chem. **259**: 3375-3381.

29. Lorence, R. M., Koland, J. G., Gennis, R. B. 1986. Coulometric and spectroscopic analysis of the purified cytochrome *d* complex of *Escherichia coli*: Evidence for the identification of cytochrome *A1* as cytochrome *B595*. Biochem. **25**: 2314-2321.

30. Magnolo, S. K., Leenutaphong, D. L., DeModena, J. A., Curtis, J. E., Bailey, J. E., Galazzo, J. L., Hughes, D. E. 1991. Actinorhodin production by *Streptomyces coelicolor* and growth of *Streptomyces lividans* are improved by the expression of a bacterial hemoglobin. Bio/Technol. **9**: 473-476.

31. Maron, M. J. 1987. In: Numerical Analysis, A Practical Approach. 2nd edition, Macmillan publishing company, New York.

32. Miller, M. J., Gennis, R. B. 1983. The purification and characterization of the cytochrome *d* terminal oxidase complex of the *Escherichia coli* aerobic respiratory chain. J . Biol. Chem. **258**: 9159-9165.

33. Miller, M. J., Gennis, R. B. 1985. The cytochrome *d* complex is a coupling site in the aerobic respiratory chain of *Escherichia coli.* J. Biol. Chem. **260**: 14003-14008.

34. Mitchell, P., Moyle, J. 1967a. Acid-base titration across the membrane system of rat-liver mitochondria. Biochem. J. **104**: 588-600.

35. Mitchell, P., Moyle, J. 1967b. Respiration-driven proton translocation in Rat liver mitochondria. Biochem. J. **105**: 1147-1162.

36. Newton, G., Gennis, R. B. 1991. In vivo assembly of the cytochrome *d* terminal oxidase complex of *Escherichia coli* from genes encoding the two subunits expressed on separate plasmids. Biochim. Biophys. Acta **1089**: 8-12.

37. Oden, K. L., Gennis, R. B. 1991. Isolation and characterization of a new class of cytochrome *d* terminal oxidase mutants of *Escherichia coli.* J. Bacteriol. **173**: 6174-6183.

38. Oden, K. L., Deveaux, L. C., Vibat, C. R. T., Cronan, J. E., Jr., Gennis, R. B. 1990. Genomic replacement in *Escherichia coli* K-12 using covalently closed circular plasmid DNA. Gene **96**: 29-36.

39. Orii, Y., Webster, D. A. 1986. Photodissociation of oxygenated cytochrome *o*(s) (*Vitreoscilla*) and kinetic studies of reassociation. J. Biol. Chem. **261**: 3544-3547.

40. Poulisse, H. N. J. 1979. Multicomponent-analysis computations based on Kalman filtering. Anal. Chim. Acta **112**: 361-374.

41. Puustinen, A., Finel, M., Haltia, T., Gennis, R. B., Wikström, M. 1991. Properties of the two terminal oxidases of *Escherichia coli*. Biochem. **30**: 3936-3942.

42. Puustinen, A., Finel, M., Virkki, M., Wikström, M. 1989. Cytochrome *o* (*bo*) is a proton pump in *Paracoccus denitrificans* and *Escherichia coli*. FEBS Lett. **249**: 163-167.

43. Puustinen, A., Morgan, J. E., Verkhovsky, M., Thomas, J. W., Gennis, R. B., Wikström, M. 1992. The low-spin heme site of cytochrome *o* from *Escherichia coli* is promiscuous with respect to heme type. Biochem. **31**: 10363-10369.

44. Rice, C. W., Hempfling, W. P. 1978. Oxygen-limited continuous culture and respiratory energy conservation in *Escherichia coli*. J. Bacteriol. **134**: 115-124.

45. Tsai, P. S., Kallio, P. T., Bailey, J. E. 1995. Fnr, the global transcriptional regulator of *Escherichia coli*, activates the *Vitreoscilla* hemoglobin (VHb) promoter and intracellular VHb expression increases cytochrome *d* promoter activity. Biotechnol. Prog. In press.

46. Tyree, B., Webster, D. A. 1978. Electron-accepting properties of cytochrome *o* purified from *Vitreoscilla.* J. Biol. Chem. **253**: 6988-6991.

47. Vasudevan, S. G., Armarego, W. L. F., Shaw, D. C., Lilley, P. E., Dixon, N. E., Poole, R. K. 1991. Isolation and nucleotide sequence of the *hmp* gene that encodes a haemoglobin-like protein in *Escherichia coli* K-12. Mol. Gen. Genet. **226**: 49-58.

48. Vinogradov, S. N., Walz, D. A., Pohajdak, B. 1992. Organization of non-vertebrate globin genes. Comp. Biochem. Physiol. **103B**: 759-773.

49. Vinogradov, S. N., Walz, D. A., Pohajdak, B., Moens, L., Kapp, O. H., Suzuki, T., Trotman, C. N. A. 1993. Adventitious variability? The amino acid sequences of nonvertebrate globins. Comp. Biochem. Physiol. **106B**: 1-26.

50. Wakabayashi, S., Matsubara, H., Webster, D. A. 1986. Primary sequence of a dimeric bacterial hemoglobin from *Vitreoscilla.* Nature **322**: 481-483.

51. Webster, D. A., Liu, C. Y. 1974. Reduced nicotinamide adenine dinucleotide cytochrome *o* reductase associated with cytochrome *o* purified from *Vitreoscilla.* J. Biol. Chem. **249**: 4257-4260.

52. Wittenberg, J. B., Wittenberg, B. A. 1990. Mechanisms of cytoplasmic hemoglobin and myoglobin function. Ann. Rev. Biophys. Chem. **19**: 217-241.

53. Wittenberg, J. B. 1991. Functions of cytoplasmic hemoglobins. In: Mangum, C. P. (ed.), Advances in comparative and environmental physiology: Oxygen carriers in blood and tissues. Springer, New York.

54. Ycas, M. 1956. Formation of hemoglobin and cytochromes by yeast in the presence of antimycin A. Exp. Cell. Res. 11: 1-6.

3.8 Tables

Table 1. ***Escherichia coli*** **strains and plasmids used in this work**

Strain and plasmid	Phenotype	Genotype	Reference or source
Bacteria			
ECL933	Cyo^+, Cyd^+	$\Phi(P_{cyo}\text{-}lac)$ bla^+, cyo^+, cyd^+, Amp^r	20
ECL936	Cyo^-, Cyd^+	$\Phi(P_{cyo}\text{-}lac)$ bla^+, cyd^+, $\Delta cyo::kan$, Amp^r	20
ECL937	Cyo^+, Cyd^-	$\Phi(P_{cyo}\text{-}lac)$ bla^+, cyo^+, $\Delta cyd::kan$, Amp^r	20
GK100	Cyo^-, Cyd^-	F^-, *thi*, *rps*L, *gal*, $\Delta cyo::kan$, $\Delta cyd::cam$, Spc^r	38
Plasmids			
pMS421		pSC101 Spc^r $lacI^{q+}$	Cold Spring Harbor Laboratory
pMSV1		pSC101 Spc^r $lacI^{q+}$ vhb^+	21
pMSC1		pSC101 Spc^r $lacI^{q+}$ $\Phi(P_{vhb}\text{-}cat)$	P. T. Kallio
pINT2		pBR322 Amp^r vhb^+	21

Table 2. Respiration kinetics of cytochrome mutants and the effect of VHb

Strain (Phenotype[a])	OUR[b] $\frac{\mu M}{\min \cdot A_{600}}$	K_m[c] μM	K_{cat}[c] sec^{-1}	R[d]
ECL933:pMS421 (Cyo^+, Cyd^+)	4.5			
ECL933:pMSV1 (Cyo^+, Cyd^+, VHb^+)	6.8			
ECL936:pMS421 (Cyo^-, Cyd^+)	6.8	0.19	4.6	0.99
ECL936:pMSV1 (Cyo^-, Cyd^+, VHb^+)	6.7	0.21	5.0	0.98
ECL937:pMS421 (Cyo^+, Cyd^-)	4.2	4.1	33	0.99
ECL937:pMSV1 (Cyo^+, Cyd^-, VHb^+)	6.2	2.6	28	0.95

[a] Cyo denotes cytochrome *o* complex, Cyd cytochrome *d* complex, and VHb *Vitreoscilla* hemoglobin.

[b] Oxygen uptake rate (OUR) was determined from the time required for dissolved oxygen tension in the chamber to drop from 70% to 10% air saturation. No exogenous substrate was added. Experimental error was estimated to be 5% of the listed values.

[c] Variation between duplicate measurements was around 10% for K_m and K_{cat}.

[d] Linear regression correlation coefficient (R) of Hofstee plot for K_m and V_{max} determination.

3.9 Figures

Figure 1 CO-reduced minus reduced intact-cell absorbance spectrum of ECL933 harboring plasmid pMSV1 and its decoupled absorptions. (A) From multiple regression analysis the concentration of each component was determined to be 3.8 μM for VHb (1), 1.8 μM for cytochrome *o* (2), and 2.11 μM for cytochrome *d* (3). A composite spectrum (– – –) consisting of the weighted sum of spectra of individual species is also shown for comparison with the sample spectrum (4).

(B) Absorption of cytochrome *d* (5) from ECL933:pMSV1 in 600-650 nm region is shown.

Figure 2 Effect of VHb and the *vhb* promoter activity on the net synthesis of cytochrome *o* and *d*. Levels of terminal oxidases at different times of bioreactor cultures of ECL933:pMS421, ECL933:pMSV1 and ECL933:pMSC1 were determined from spectral deconvolution analysis. (A) Cytochrome *o* (Cyo) levels (nmol/mg protein) of ECL933:pMS421 (•), ECL933:pMSV1 (o), and ECL933:pMSC1 (x) are shown. VHb production from ECL933:pMSV1 (Δ) is also shown.

(B) Cytochrome *d* (Cyd) levels (nmol/mg protein) from ECL933:pMS421 (•), ECL933:pMSV1 (o), and ECL933;pMSC1 (x) are shown. CAT production from ECL933:pMSC1 (Δ) is also shown. Error bars were estimated from both deconvolution uncertainty and sonication efficiency (for total cellular protein preparation).

Figure 3 Theoretical proton translocation rate of microaerobic *E. coli* utilizing either cytochrome *o* or *d* complex. Theoretical proton translocation rate was calculated from simple Michaelis-Menten kinetics of the oxidases using experimentally determined parameters: $V_{H^+} = \frac{nH^+}{O} \cdot \frac{V'_{max} \cdot [O_2]}{K_m + [O_2]} \cdot \frac{[oxidase]}{g\ cells}$ where K_m is 4.1 μM O_2 for Cyo and 0.19 μM O_2 for Cyd; $[O_2]$ is the oxygen concentration in μM; V'_{max} is 20.5 μM $O_2 \cdot min^{-1} \cdot$nmol cytochrome o^{-1} for Cyo^+ cells and 6.0 μM $O_2 \cdot min^{-1} \cdot$nmol cytochrome d^{-1} for Cyd^+ cells. Cytochrome *o* and *d* concentrations of 38.5 nmol Cyo/g cells and 93.5 nmol Cyd/g cells in cyd^- and cyo^- mutants, respectively, grown under microaerobic conditions were used to calculate V_{H^+}. Reduction of each oxygen atom via Cyo couples 4 proton translocations and the reduction of an oxygen atom via Cyd couples 2 protons; therefore, *n* is taken to be 4 for Cyo and 2 for Cyd.

Figure 1

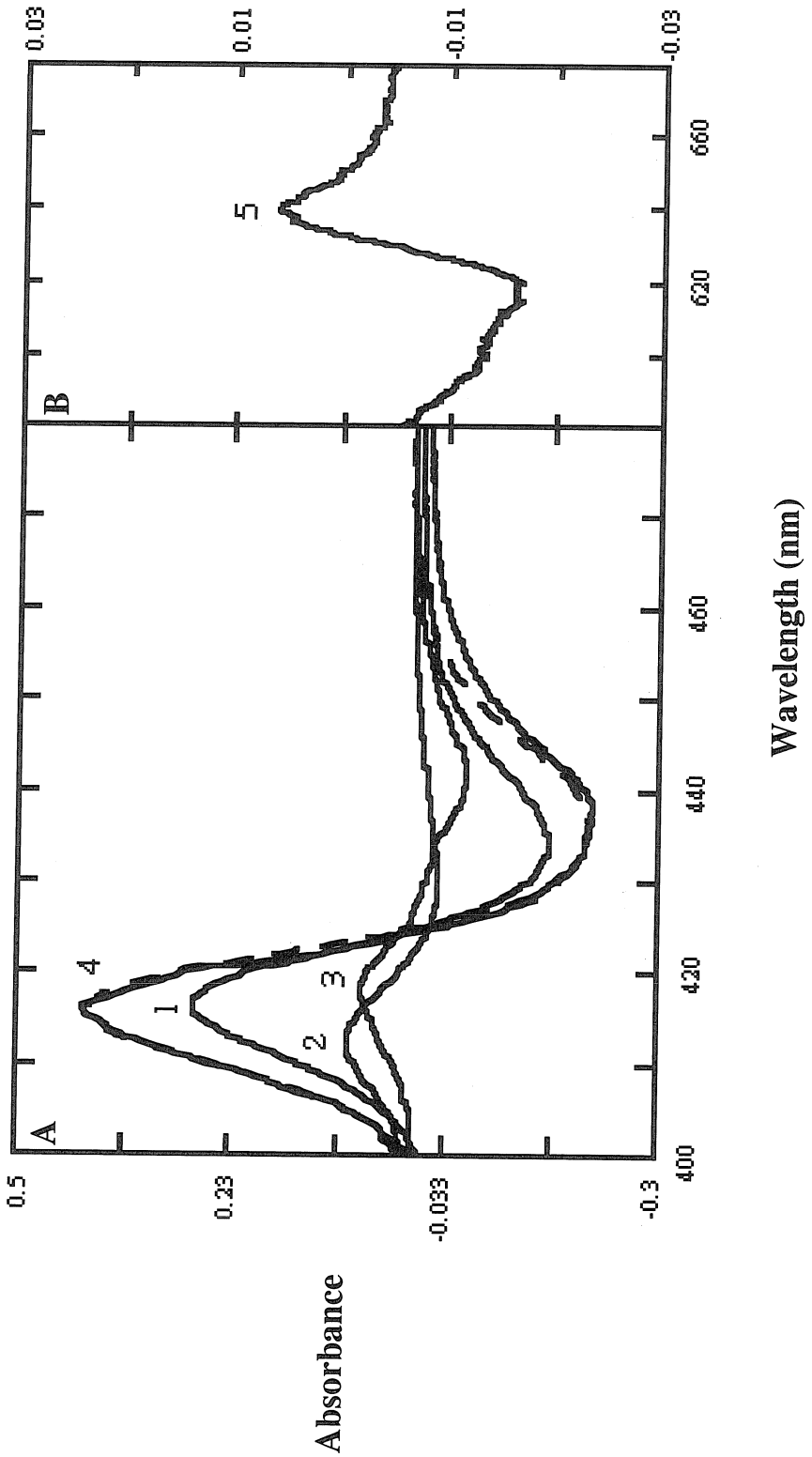
A
B
1
2
3
4
5
0.5
0.23
-0.033
-0.3
0.03
0.01
-0.01
-0.03
400
420
440
460
620
660
Absorbance
Wavelength (nm)

Figure 2

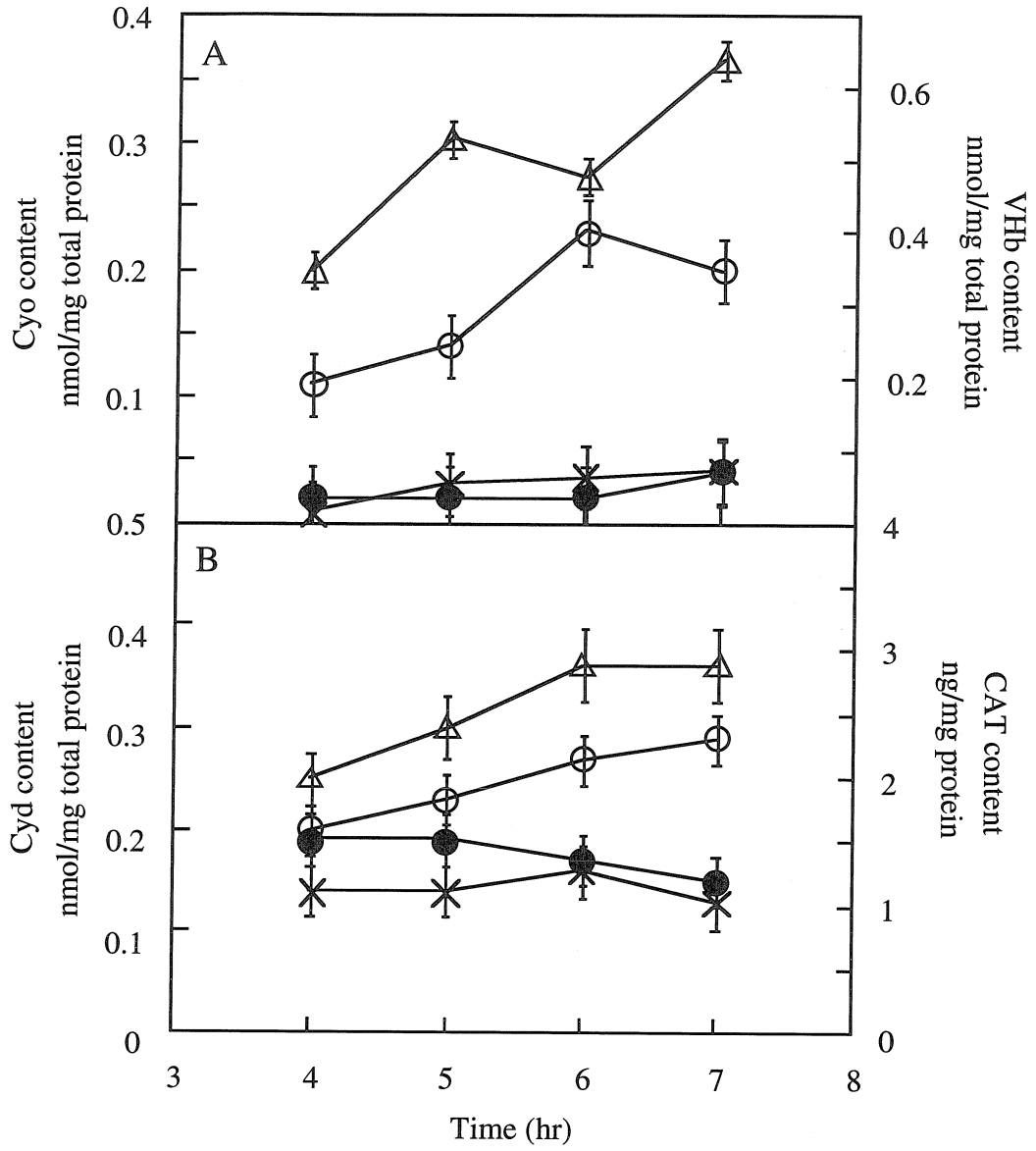
A
B
Cyo content
nmol/mg total protein
VHb content
nmol/mg total protein
Cyd content
nmol/mg total protein
CAT content
ng/mg protein
Time (hr)
0.4
0.3
0.2
0.1
0.5
0.6
0.4
0.2
4
0.4
0.3
0.2
0.1
0
3
2
1
0
3
4
5
6
7
8

Figure 3

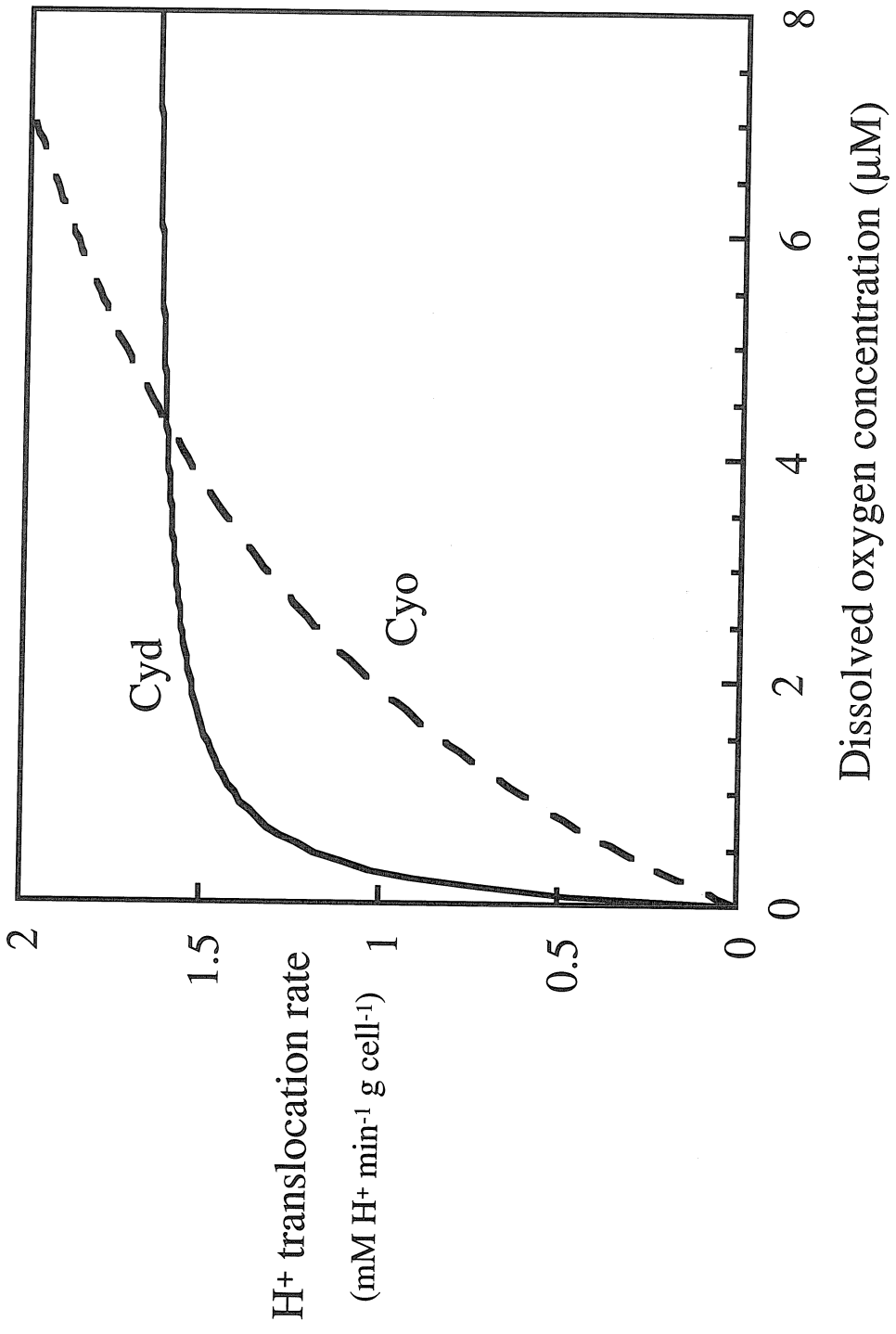
Cyd
Cyo
H+ translocation rate
(mM H+ min-1 g cell-1)
Dissolved oxygen concentration (µM)
0
0.5
1
1.5
2
0
2
4
6
8

CHAPTER 4:

Altered NAD(P)H Fluorescence and Redox Potential of Microaerobic *Escherichia coli* Synthesizing *Vitreoscilla* Hemoglobin

Source: Tsai, P. S.; Rao, G.; Bailey, J. E. Improvement of *Escherichia coli* microaerobic oxygen metabolism by *Vitreoscilla* hemoglobin: New insights from NAD(P)H fluorescence and culture redox potential. 1995. Accepted for publication in *Biotechnology and Bioengineering*.

4.1 Abstract

On-line NAD(P)H fluorescence and culture redox potential (CRP) measurements were utilized to investigate the role of *Vitreoscilla* hemoglobin (VHb) in perturbing oxygen metabolism of microaerobic *Escherichia coli*. Batch cultures of a VHb–synthesizing *E. coli* strain and the isogenic control under fully aerated conditions were subject to several high/low oxygen transitions, and the NAD(P)H fluorescence and CRP were monitored during these passages. The presence of VHb decreased the rate of net NAD(P)H generation by 2.4–fold under diminishing oxygen tension. In the absence of aeration, the strain producing VHb maintained a steady NAD(P)H level 1.8–fold less than that of the control, indicating that the presence of VHb keeps *E. coli* in a more oxidized state under oxygen-limited conditions. Estimated from CRP, the oxygen uptake rates near anoxia were 25% higher for cells with VHb than those without. These results suggest that VHb-expressing cells have a higher microaerobic electron transport chain turnover rate. To examine how NAD(P)H utilization of VHb-expressing cells responds to rapidly changing oxygen tension which is common in large-scale fermentations, we pulsed air intermittently into a cell suspension and recorded the fluorescence response to the imposed dissolved oxygen (DO) fluctuation. Relative to the control, cells containing VHb had a sluggish fluorescence response to sudden changes of oxygen tension, suggesting that VHb buffers intracellular redox perturbations caused by extracellular DO fluctuations.

Key words: NADH fluorescence, Culture redox potential, *Vitreoscilla* hemoglobin, Oxygen fluctuation.

4.2 Introduction

Recently, a genetic engineering technology designed to compensate for oxygen limitation in aerobic bioprocesses has been described based on intracellular expression of *Vitreoscilla* hemoglobin (VHb). VHb expression in *Escherichia coli* improves microaerobic cell growth and overall recombinant protein production (16, 18, 19). Product yield enhancements by VHb have been achieved in several different processes in which oxygen plays a direct or indirect role in the product formation pathway. For example, production of the antibiotics actinorhodin from *Streptomyces coelicolor* and cephalosporin C from *Acremonium chrysogenum*, both of which involve oxygen in precursor formation, are increased 10-fold and 4-fold, respectively, when VHb is expressed (8, 30).

Few biochemical and physiological details are known about VHb-engineered strains relative to their unmodified parents. Improved understanding of the intracellular consequences of VHb expression in various hosts is important to guide future applications and refinement of VHb technology. Most detailed information about VHb effects are available for engineered *E. coli*. Analysis of ^{31}P NMR spectra indicates that *E. coli* synthesizing VHb have higher ATP content than the control strain (15). An on-line ^{31}P NMR and saturation transfer study demonstrated that the net ATP accumulation rate and ATPase–catalyzed P_i-ATP flux are 65% and 30%, respectively, higher in VHb–expressing cells relative to the control (5). In addition, the number of protons extruded from cells per oxygen consumed was 50% higher in cells with VHb (15). It is likely that VHb increases the efficiency and/or the activity of the *E. coli* aerobic electron transport chain under low oxygen tensions.

The nicotinamide adenine dinucleotide couple (NAD^+/NADH), which serves as an electron carrier in many biological redox systems, has important functions in energy metabolism. In fueling pathways, NAD^+ is reduced to NADH with concomitant substrate degradation. Oxidation of NADH is coupled to electron transfer to oxygen and proton translocation through the cytoplasmic membrane which generates a membrane electrochemical gradient which drives many cellular activities such as ATP synthesis through ATPase. During anaerobiosis, NADH couples electron transfer to reducible intermediates leading to formation of end metabolites such as lactate and ethanol. Therefore, NADH content is expected to decrease with substrate exhaustion and increase with oxygen depletion. This connection is consistent with the findings of Harrison and Chance (12) that cells are in a more reduced state when oxygen supply is reduced. Based on previous research, it is plausible that the presence of VHb in *E. coli* will increase electron flux through the respiratory chain under low oxygen tension. Therefore, valuable information on the physiological consequences of VHb expression might be gained by measuring changes in the NAD^+/NADH ratio in response to external stimuli.

Utilization of fluorescence measurement in monitoring intracellular NAD(P)H content to understand cell metabolism has become a valuable tool. Here the notation NAD(P)H refers to the sum of NADH and NADPH. Harrison and Chance (12) have shown that the observed culture fluorescence is based on the reduced form of nicotinamide pyridine dinucleotides [NAD(P)H]. NADH concentration in *E. coli* is about ten times higher than NADPH (29) and so the majority of culture fluorescence can typically be assigned to NADH. In addition, London and Knight (29) have shown that the total NAD(P) pool [NAD(P)H + $NAD(P)^+$] in *E. coli* stays relatively constant with respect to biomass. This allows attribution of an increase in the culture

fluorescence signal to a decrease in the turnover rate of NADH to NAD^+. Since the advent of on-line fluorescence probes (12), applications of fluorescence measurement in bioreactors have included biomass estimation (32), reactor mixing characterization (11), and analyses of substrate uptake kinetics (10), substrate exhaustion (24), and acidogenic/solventogenic pathway switchover (37, 38).

Culture redox potential (CRP) measurement is based on the assumption that extracellular redox potential is a function of intracellular redox potential. Therefore, a change in a major redox couple such as the respiration-linked (oxygen/water) NAD redox system during aerobiosis should be reflected in the CRP measurement [for review of redox potentiometry, see Dutton and Wilson (9)]. Because of a strong contribution from the respiratory redox couple, CRP has been used to estimate oxygen tension (22, 45) and oxygen transfer rate (1) near anoxia. Like fluorescence measurement, CRP has gained increasing importance as an on-line monitoring technique in detecting subtle changes in metabolic state such as substrate exhaustion in amino acid–producing *Corynebacterium glutamicum* fermentations (23, 25). Controlling CRP by varying agitation (36) or by adding reducing agents (26) have also been employed in efforts to regulate cell physiology.

In this study, both culture fluorescence and CRP measurements were employed in order to expand understanding of the consequences of VHb expression in *E. coli*. We examined whether the presence of VHb increases the activity of the respiration-coupled redox system by comparing the $NAD(P)^+$/NAD(P)H turnover rate and ratio for cells synthesizing VHb with these properties for a VHb-free control strain under several oxygen transients. In addition, we estimated the oxygen uptake

rate of both types of cells from their CRP time trajectories under non-aerated conditions.

It has been shown that nonideal mixing in large-scale bioreactors leads to dissolved oxygen (DO) fluctuations as cells circulate among oxygen-rich and oxygen-poor microenvironments within the fermentor (31, 35). This DO heterogeneity can have profound effects on microorganism growth and metabolism (34, 35, 43). Given the oxygen-binding characteristics of VHb, it would be interesting to see how VHb-engineered cells behave when subjected to dissolved oxygen oscillations. We therefore devised a simple scale-down scheme for simulating in a laboratory bioreactor oxygen fluctuations with a time-scale comparable to those expected in a large-scale aerobic process, and we compared NAD(P)H fluorescence signals of VHb^+ cells with those of the control under these conditions.

4.3 Materials and Methods

4.3.1 Microorganism, Plasmid Construction, and Cultivation Conditions

Escherichia coli K-12, strain W3110 (2) harboring either the *Vitreoscilla* hemoglobin expression plasmid, pKTV1 or the control plasmid, pKT1, was used to study the effects of VHb expression on culture fluorescence and redox potential. Plasmid pKT1 was constructed by digesting pBR322 (3) with *Eco*RI and *Ssp*I, and ligating with the 1.1 kb *Eco*RI-*Hind*III fragment [*Hind*III–digested fragment post-treated with DNA polymerase I large (Klenow) fragment (Promega Inc.)] containing the *lac* repressor gene, $lacI^q$, from pMJR1560 (Amersham International). Plasmid pKTV1 was constructed by subcloning the 1.2 kb *Hind*III-*Sal*I fragment containing

the *tac* promoter-*vhb* gene fusion from pINT1 (17) into the corresponding sites in pKT1. *E. coli* strain W3110 was transformed with either pKTV1 or pKT1 according to the calcium chloride method (39).

Cells were cultivated overnight in one–liter shake flasks containing 300 mL of buffered LB medium (10 g/L Bacto-tryptone, 5 g/L Bacto-yeast extract, 10 g/L NaCl, 3 g/L K_2HPO_4, 1 g/L KH_2PO_4, adjusted to pH 7) at 37°C and 250 rpm in a New Brunswick Scientific Innova 4000 shaker. Ampicillin (100 mg/L) was added to both W3110:pKTV1 and W3110:pKT1 for plasmid maintenance. Prior to fluorescence and redox measurements, 100 mL of the overnight culture was mixed with 100 mL of fresh LB medium and incubated for 4 hr at 37°C, and 250 rpm. VHb expression was achieved by inducing W3110:pKTV1 with 0.5 mM IPTG at the beginning of the cultivation and again when fresh LB medium was added. For comparison, 0.5 mM IPTG was also added to the W3110:pKT1 culture.

4.3.2 Fluorescence and CRP Measurements

Fluorescence and redox potential measurements were performed in a 200 mL working volume glass vessel fitted with a water jacket. Cells were withdrawn from the vessel by a peristaltic pump and circulated through a flow cell attached to an Ingold Type 25 101 300 Fluorosensor which has excitation and emission wavelengths at 360 and 450 nm, respectively. The distance between the vessel and the flow cell was minimized (8 cm) and the pump speed was set to maximum to minimize the recycle loop residence time, which was 5 sec under these conditions. This is much shorter than the time scale of culture fluorescence transients which is in the range of 2-3 minutes. The use of a recycle loop/flow cell to measure NAD(P)H transients was validated in another study (6) in which the advantage of using a flow cell to reduce

fluorescence artifacts caused by foaming, aeration and agitation was also described. No significant differences in culture physiology, including intracellular redox state, are expected in the sampling loop. In a closed environment for 5 seconds, the maximum estimated oxygen depletion (the most potential limiting factor) is 10% of the entering dissolved oxygen, assuming a specific oxygen uptake rate of 5 mmol/g DCW/hr and a cell density of 1 g DCW/L.

After additions of glucose (to a final concentration of 0.15%) and 2 drops of antifoam, cells were aerated with 0.6 L/min of air and agitated by a magnetic stirrer. Before data logging, culture pH was adjusted to pH 7 with either 1 M NaOH or 1 M HCl solution. During measurement, the temperature of the vessel was maintained at 25°C by a circulating water bath. Dissolved oxygen tension and redox potential were monitored by a pO_2 electrode (Ingold Electrodes Inc.) and a redox electrode (Amagruss Electrodes Limited), respectively. Process parameter data were recorded every minute via an LH bioreactor system (Inceltech Inc.). Culture DO and fluorescence were also monitored with a chart recorder to capture details missed by intermittent data acquisition. Fluorescence intensity was normalized by dry cell weight (DCW) for each experiment and is reported as Specific Fluorescence Units (SFU).

To rule out inner filter effect artifacts (see Results section) stemming from the presence of VHb, fluorescence and redox potential under transient oxygenation conditions of broken cells extracts from W3110:pKTV1 and W3110:pKT1 were examined. Cells were cultivated under the same conditions as those for the *in vivo* assay. At harvest, 200 mL of cells was resuspended in 10 mL sonication buffer (100 mM Tris-HCl, 50 mM NaCl, 1 mM EDTA) and disrupted by passage twice through a French press (SLM-Aminco). Following removal of cell debris by centrifugation, the

soluble fraction was added back to 190 mL of the used LB medium without cells. Two drops of antifoam and glucose (to 0.15% of final concentration) were added to the suspension before fluorescence and redox potential measurements commenced. The vessel temperature and the air flow were maintained at 25°C and 0.6 L/min, respectively, as in the *in vivo* assay.

4.3.3 Analytical Procedure

For DCW measurement, 10 mL samples were centrifuged at 3000 x *g* and washed once with phosphate buffer saline (8 g/L NaCl, 0.2 g/L KCl, 1.44 g/L Na_2HPO_4, 0.24 g/L KH_2PO_4, adjusted to pH 7). Wet pellets were dried in a 80°C oven for three days and then their weights were measured. VHb concentration was assayed by CO–reduced minus reduced difference absorption spectrophotometry using the monomer extinction coefficient ($\varepsilon_{419\ nm} - \varepsilon_{437\ nm}$) of 1.067×10^5 $(Mcm)^{-1}$ for VHb (14). Total protein was determined by Bradford dye binding assay with a Protein Assay kit from Bio-Rad.

For total cellular NAD(P)H quantification, cells were grown in LB medium under the same conditions as those for fluorescence and redox measurement. Glucose (0.15% of final concentration) was added to the culture 30 min prior to harvest. In order to minimize intracellular metabolite loss during typical sampling procedures, samples were fast quenched in –40°C methanol according to the method described by de Koning and van Dam (7) with a slight modification. Briefly, 10 mL of cells was mixed with 40 mL of 60% methanol at –40°C immediately after withdrawn from the shake flask. The subsequent steps of chloroform extraction were performed in a –30°C glycerol/methanol/water shaking bath (Hetofrig Model CB60VS, Heto Lab Equipment) instead of –40°C as previously described (7). NAD^+ and [NADH +

NADPH] concentrations were determined using an enzymatic assay described by de Koning and van Dam (7) and a bioluminescence kit from Boehringer Mannheim Biochemical, respectively, and normalized by DCW estimated from total protein [total protein content = 55% DCW (33)].

4.4 Results

4.4.1 NAD(P)H Fluorescence and Effect of VHb

The NAD(P)H fluorescence time profiles of the VHb–synthesizing *E. coli* strain W3110:pKTV1, and the control W3110:pKT1, in response to changing dissolved oxygen (DO) were examined in an environment with controlled pH and temperature (pH 7, 25°C). Overnight grown cells were mixed 1:1 with fresh LB medium and cultivated for four additional hours before measurement. Prior to fluorescence measurement, concentrated glucose solution was introduced into the vessel to obtain a starting glucose concentration of 0.15 weight %, and cell suspension was aerated with 0.6 L/min of air for 15 minutes to allow the cells to metabolize glucose. Addition of glucose to the cell suspension increased fluorescence intensity and improved reproducibility (result not shown). Glucose levels before and after the transient experiment were measured to verify glucose uptake. During measurement, air flow was interrupted, and the resulting culture DO and fluorescence signals were traced. Air flow was resumed after a period of 20 minutes, and the cycle (air on/air off) was repeated.

Figure 1A and 1B show the DO and normalized NAD(P)H fluorescence signals of W3110:pKT1 and W3110:pKTV1 in response to a step cessation of

aeration. Culture DO plunged instantaneously after aeration was stopped, indicating that the aerobic respiratory pathway of both strains was active and cells were consuming oxygen. The fluorescence signals of both strains rose sharply as DO decreased, but the increase was noticeably reduced after the DO reading reached 0% (all DO values are as a percent of air saturation). The upward shift in fluorescence baselines for both strains was most likely due to increases in cell densities during measurements. The initial and final DCW measured prior to and after oxygen transitions were 1.24 g/L and 1.66 g/L, respectively, for W3110:pKT1 and 1.43 g/L and 1.62 g/L, respectively, for W3110:pKTV1. The presence of VHb in W3110:pKTV1 culture was verified by CO-reduced minus reduced spectroscopic assay (spectrum not shown), and the amount of VHb detected at the end of experiment was 1 nmole/mg protein. Comparing Figure 1A and 1B, it is apparent that the difference in the NAD(P)H fluorescence signals between aeration and non-aeration [$\Delta NAD(P)H_{air\ off-air\ on}$] of the control strain W3110:pKT1 was larger than that of the VHb^+ strain W3110:pKTV1. The magnitude of $\Delta NAD(P)H_{air\ off-air\ on}$ during each oxygen transition (air on/off) of W3110:pKT1 was on the average 1.8-fold larger than that of W3110:pKTV1 (45 SFU for W3110:pKT1 and 25 SFU for W3110:pKTV1). Similar results were obtained in replicate experiments.

Li and Humphrey (28) showed that cellular fluorophors such as riboflavin can interfere with NAD(P)H measurement. Since VHb absorbs in a range 400-450 nm overlapping the emission characteristics of NAD(P)H, it is possible that a change in the redox status of VHb, which is influenced by changes in oxygen tension, may affect the overall fluorescence and lead to faulty conclusions. Therefore, to see whether the observed difference in fluorescence magnitude between VHb^- and VHb^+ cells was caused by an inner filter effect artifact from VHb, we repeated the

experiment using extracts of W3110:pKTV1, which contains VHb, and W3110:pKT1, which does not contain VHb. In such extracts, effects of VHb on cytochrome amounts and activities observed in intact cells (unpublished results) will not be coupled to NADH oxidation. Therefore, any differences in NAD(P)H fluorescence between these extracts should be primarily due to a VHb inner filter effect.

Cells were cultivated to similar concentrations under the same conditions as used for the *in vivo* experiment. Extracts of these cells were then prepared, and the NAD(P)H fluorescence of these extracts under aerated and non-aerated conditions were monitored; the normalized signals are displayed in Figure 2. A small increase and a decrease in the fluorescence intensity and DO, respectively, were detected for both cell extracts when the air supply was interrupted. This is presumably due to nonspecific couplings of $NAD(P)^+$/NAD(P)H systems that are still active in cell extract. The fluorescence signals of both strains fluctuated during the oxygen transient. Nevertheless, the NAD(P)H fluorescence profiles of the control cell extract and the VHb^+ cell extract appeared similar. The sizes of $\Delta NAD(P)H_{air\ off\text{-}air\ on}$ were on the average 10 SFU for W3110:pKT1 cell extract and 9 SFU for W3110:pKTV1 cell extract. The difference in $\Delta NAD(P)H_{air\ off\text{-}air\ on}$ between the control and the VHb^+ strain extract was not significant compared with the magnitudes of $\Delta NAD(P)H_{air\ off\text{-}air\ on}$ observed for the *in vivo* system. Thus, result suggests that our *in vivo* fluorescence measurement indicates the physiological effects of VHb on NAD(P)H utilization.

Our finding of a smaller *in vivo* $\Delta NAD(P)H_{air\ off\text{–}air\ on}$ for the VHb-containing strain also raised the question of whether VHb changes the overall NAD(P) pool size in *E. coli.* Therefore, NAD^+ and NAD(P)H concentrations of

W3110:pKT1 and W3110:pKTV1 were measured from overnight cultures pre-incubated 30 min with 0.15% glucose before –40°C methanol quenching (Materials and Methods). $NADP^+$ concentration was not measured in this study because intracellular $NADP^+$ concentration in *E. coli* is on the order of 10-fold less than that of NAD^+ (29), and VHb is not likely to perturb the NADP pool to a level which would significantly affect the total NAD(P) pool. Our enzymatic analyses showed that the total [NAD^+ and NAD(P)H] contents for W3110:pKT1 and W3110:pKTV1 were the same within the experimental error (3.3 ± 0.3 μmole/g DCW). These values are in good agreement with those previously reported for *E. coli* (29).

With the assumption that the intracellular nicotinamide dinucleotide concentration of *E. coli* remains constant with respect to cell mass during cultivation (29), a decrease in fluorescence signal can be interpreted as a decrease in NAD(P)H/$NAD(P)^+$ ratio. Based on the findings that VHb did not interfere with our measurement nor alter the total nicotinamide dinucleotide pool of W3110, we concluded that, with VHb present, cells maintain approximately half of the NAD(P)H level of the control cells, and hence are in a greater oxidized state under very low oxygen tensions.

More information could be gained from monitoring the rate of change of fluorescence following an interruption of aeration because this rate approximates the turnover rate of $NAD(P)^+$ to NAD(P)H. The fluorescence profiles (Figure 1) from the beginning of the second interruption of aeration for the control and the VHb^+ strains were used to calculate the rate of fluorescence change. Upon cessation of aeration, the fluorescence intensity increased rapidly for W3110:pKT1 and reached 82 SFU while the fluorescence of W3110:pKTV1 ascended slower and reached only 61 SFU before

stabilizing. The rate of SFU change, approximated from the time required for the signal to reach its peak value, was 18 SFU/min for W3110:pKT1 and 7.5 SFU/min for W3110:pKTV1. This indicates that the control strain has a 2.4-fold higher net turnover rate of $NAD(P)^+$ to NAD(P)H than the VHb synthesizing strain. Based on the assumption that the dynamics of NAD(P)H are primarily due to changes in NADH level, our results suggest that VHb enhances the conversion rate of NADH to NAD^+, thereby causing a smaller net synthesis rate of NADH during diminishing oxygen transients.

4.4.2 Culture Redox Potential and Effect of VHb

Figure 3A and 3B show the typical redox profiles of W3110:pKT1 and W3110:pKTV1 under different oxygenation conditions. The CRPs of both strains during aeration were similar (~40 mV) and decreased immediately after termination of aeration, indicating an increase in the reduction state of the culture. Upon reaeration, CRPs of both strains ascended immediately along with DO and reached a plateau of 40 mV after DO returned to its original steady-state value of ~95% air saturation. Based on Figure 3, it appeared that cells with or without VHb have similar CRP characteristics under our experimental scheme. However, a closer examination of CRP near zero DO revealed useful information on the effect of VHb.

It is not possible to determine the oxygen uptake rate of cells directly from DO electrode readings under microaerobic conditions due to the insensitivity of the probe in this region. However, CRP data can possibly reveal subtle differences in the oxygen uptake rate of different cells. According to the Nernst equation, CRP is linear with respect to logarithmic DO at constant temperature and pH under extremely low oxygen tensions (36)

$$\log(DO) = a(CRP) + b \qquad [1]$$

where a and b are constants dictated by medium composition and different species in the cells. Constants a and b were determined for each strain independently using CRP and DO signals from the redox and DO probes, respectively, between 1-2% air saturation.

The CRP profiles near anoxia (below DO 1% based on readings from the DO probe) from Figure 3 were used to calculate oxygen concentration using the above relationship. The calculated DO time trajectories are shown in Figure 4. Cells synthesizing VHb have a faster oxygen uptake rate than the control strain. The oxygen uptake rates of W3110:pKTV1 and W3110:pKT1 during the first two minutes shown in Figure 4 were 60 nmole/min·g DCW and 45 nmole/min·g DCW, respectively. Four additional experiments were performed under the same conditions and oxygen uptake rates of the two strains were compared. Unfortunately, the absolute values varied from a low 45 to a high 98 nmole/min·g DCW between experiments (data not shown). However, VHb–containing cells have higher oxygen uptake rates, although by different magnitudes (15%–30% higher in VHb^+ cells), than the control cells in four out of five experiments.

4.4.3 DO, CRP Fluctuations and Effect of VHb

During the course of optimizing conditions for NAD(P)H fluorescence and redox measurements, we occasionally observed an unusual "biphasic" behavior of DO and CRP profiles of cells (both W3110:pKT1 and W3110:pKTV1) when aeration was resumed after a period of interruption. Such biphasic DO and CRP responses are shown in Figure 5. As air supply was re-introduced to the working vessel, DO and

CRP increased immediately until DO reached 5% air saturation, then both DO and CRP signals dropped for a period of 3-5 min before they rose again to their original steady-state values. Harrison and co-workers (12, 13) have also observed similar behavior for a *Klebsiella aerogenes* culture. Upon reaeration, the culture DO increased but then maintained a DO level of 10% for a period of time before it ascended slowly back to its original value. Two distinct respiration rates and ATP/ADP ratios were detected in that study accompanying this biphasic behavior during the oxygen transient. A higher respiration rate and a lower ATP/ADP ratio were found to be characteristics of cells in this low-DO, quasi steady-state (12, 13). It is likely that cells might have utilized different terminal oxidases with different oxygen affinities and energetic efficiencies in these two oxygenation regimes. *E. coli* synthesizes a low oxygen affinity, high energetic efficiency terminal oxidase, cytochrome *o*, during fully aerobic conditions and the lower energy efficient but higher oxygen affinity cytochrome *d* under low oxygen tensions. In our experiment, perhaps the oxygen-scavenging cytochrome *d* dominated the respiratory activity when air was first re-introduced to the vessel, thereby causing an increase in respiration rate which corresponds to a drop in DO. When aeration continued and oxygen concentration reached a point above the K_m value of cytochrome *o*, cytochrome *o* activity becomes significant, resulting in a decrease in respiration rate (observed earlier when *E. coli* switches from cytochrome *d* to cytochrome *o* utilization [4]) and an increase in DO. Indeed, Swartz (40) has observed DO instability in a large-scale *E. coli* fermentation in which DO fluctuated under a steady aeration rate. The instability was eliminated when *E. coli* mutants lacking either cytochrome *o* or *d* were cultivated under the same conditions (40).

4.5 Discussion

The observation of VHb improving cellular NAD(P)H utilization suggests a functional role of VHb in microaerobic *E. coli*. Biophysical studies showed that *Vitreoscilla* hemoglobin possess an oxygen affinity similar to those of *E. coli* cytochrome *o* and *d* [VHb K_m=0.25 μM (42); cytochrome *o* K_m=2.9 μM (20); cytochrome *d* K_m=0.38 μM (21)] and that VHb has an unusually high dissociation constant in comparison with most of other hemoglobins (44). Oxygenated VHb was previously conjectured to increase the effective DO and preferentially raise the activity of cytochrome *o* over cytochrome *d* due to the differences in the affinities for oxygen of the two cytochromes (15). An intact-cell spectroscopic analysis also revealed that the expression of VHb increases the amount of cytochrome *o* and, to a lesser extent, the amount of cytochrome *d* (unpublished result). Although this study was not designed to determine the effect of VHb on cytochrome activity, the present findings are in good agreement with the earlier hypothesis. An increase in cytochrome activity due to a higher oxygen availability through VHb would likely accelerate the turnover rate of the electron transport chain which, through its coupling with NADH dehydrogenase, would increase the NADH consumption rate, just as we have observed in this study.

An important, although preliminary, discovery that also emanated from this study is the buffering effect of VHb on NAD(P)H responses during oxygen fluctuations. From our hypothesis on the role of VHb, it can be envisioned that, following a sudden shift from oxygen-rich to oxygen-scarce surroundings in a poorly mixed fermentor, oxygenated VHb molecules would release their oxygen to the

respiratory machinery during the oxygen-depleted period. Taking Michaelis-Menten rate parameters for microaerobic *E. coli* respiration rate of 0.27 μM for K_m and 18.9 μM/mg DCW/min for V_{max} from prior investigations (21), the time required for the initial supply of VHb-stored oxygen to be depleted to a point giving 20% of the original rate is approximately 4 seconds. Thus, when encountering oscillating fields of DO in a large-scale bioreactor with cycle times of the same order of magnitude, VHb–expressing cells may not experience major fluctuations in respiratory activity.

The finding that VHb decreases NADH levels in *E. coli* respiring under microaerobic conditions may have implication for fluxes through other pathways. NADH and NAD^+ are co-substrates in reactions at the beginning and ends of central carbon metabolism, and a shift in the oxidation state of this couple could well have effects on rates of key reactions which determine total carbon flux and flux distribution. The observations reported here suggest that VHb does not exert its effects on metabolism only through previously reported changes in respiratory metabolism and effective intracellular dissolved oxygen level, but also through changed concentrations of NAD^+ and NADH which directly perturb rates of key metabolic reactions.

4.6 Acknowledgments

This research was supported by the Swiss Priority Program in Biotechnology. GR acknowledges support from the National Science Foundation (BCS-9157852) and the hospitality provided by the ETH.

4.7 References

1. Akashi, K., Ikeda, S., Shibai, H., Kobayashi, K., Hirose, Y. 1978. Determination of redox potential levels critical for cell respiration and suitable for L-leucine production. Biotechnol. Bioeng. **20**: 27-41.

2. Bachmann, B. J. 1987. Derivations and genotypes of some mutant derivatives of *Escherichia coli* K-12. p. 1191-1219, In: J. L. Ingraham, K. B. Low, B. Magasanik, M. Schaechter, and H. E. Umbarger (eds.), *Escherichia coli* and *Salmonella typhimurium*: cellular and molecular biology. American Society for Microbiology, Washington, D.C.

3. Bolivar, F., Rodriguez, R. L., Greene, P. J., Betlach, M. C., Heyneker, H. L., Boyer, H. W., Crosa, J. H., Falkow, S. 1977. Construction and characterization of new cloning vehicles. II. A multipurpose cloning system. Gene **2**: 95-113.

4. Calhoun, M. W., Oden, K., Gennis, R. B., de Mattos, M. J. T., Neijssel, O. M. 1993. Energetic efficiency of *Escherichia coli*: Effects of mutants in components of the aerobic respiratory chain. J. Bacteriol. **175**: 3020-3025.

5. Chen, R., Bailey, J. E. 1994. Energetic effect of *Vitreoscilla* hemoglobin expression in *Escherichia coli*: An on-line ^{31}P NMR and saturation transfer study. Biotechnol. Prog. **10**: 360-364.

6. Coppela, S. J., Rao, G. 1990. Practical considerations in the measurement of culture fluorescence. Biotechnol. Prog. **6**: 398-401.

7. de Koning, W., van Dam, K. 1992. A method for the determination of changes of glycolytic metabolites in yeast on a subsecond time scale using extraction at neutral pH. Anal. Biochem. **204**: 118-123.

8. DeModena, J. A., Gutierrez, S., Velasco, J., Fernandez, F. J., Fachini, R. A., Galazzo, J. L., Hughes, D. E., Martin, J. F. 1993. The production of cephalosporin C by *Acremonium chrysogenum* is improved by the intracellular expression of a bacterial hemoglobin. Bio/Technol. **11**: 926-929.

9. Dutton, P. L., Wilson, D. F. 1974. Redox potentiometry in mitochondrial and photosynthetic bioenergetics. Biochim. Biophys. Acta 346: 165-212.

10. Einsele, A., Ristroph, D. L., Humphrey, A. E. 1978. Mixing times and glucose uptake measured with a fluorometer. Biotechnol. Bioeng. **20**: 1487-1492.

11. Gschwend, K., Beyeler, W., Fiechter, A. 1983. Detection of reactor nonhomogeneities by measuring culture fluorescence. Biotechnol. Bioeng. **25**: 2789-2793.

12. Harrison, D. E. F., Chance, B. 1970. Fluoremetric technique for monitoring changes in the level of reduced nicotinamide nucleotides in continuous cultures of microorganisms. Appl. Microbiol. **19**: 446-450.

13. Harrison, D. E. F., Maitra, P. K. 1969. Control of respiration and metabolism in growing *Klebsiella aerogenes*. Biochem. J. **112**: 647-656.

14. Hart, R. A., Bailey, J. E. 1991. Purification and aqueous 2-phase partitioning properties of recombinant *Vitreoscilla* hemoglobin. Enz. Microb. Technol. **13**: 788-795.

15. Kallio, P. T., Kim, D. J., Tsai, P. S., Bailey, J. E. 1994. Intracellular expression of *Vitreoscilla* hemoglobin alters *Escherichia coli* energy metabolism under oxygen-limited conditions. Eur. J. Biochem. **219**: 201-208.

16. Khosla, C., Bailey, J. E. 1988. Heterologous expression of a bacterial haemoglobin improves the growth properties of recombinant *Escherichia coli*. Nature **331**: 633-635.

17. Khosla, C., Bailey, J. E. 1989. Evidence for partial export of *Vitreoscilla* hemoglobin into the periplasmic space in *Escherichia coli*. J. Mol. Biol. **210**: 79-90.

18. Khosla, C., Curtis, J. E., DeModena, J., Rinas, U., Bailey, J. E. 1990. Expression of intracellular hemoglobin improves protein synthesis in oxygen-limited *Escherichia coli*. Bio/Technol. **8**: 849-853.

19. Khosravi, M., Webster, D. A., Stark, B. C. 1990. Presence of bacterial hemoglobin gene improves α-amylase production of a recombinant *Escherichia coli* strain. Plasmid **24**: 190-194.

20. Kita, K., Konishi, K., Anraku, Y. 1984. Terminal oxidases of *Escherichia coli* aerobic respiratory chain, I. J. Biol. Chem. **259**: 3368-3374.

21. Kita, K., Konishi, K., Anraku, Y. 1984. Terminal oxidases of *Escherichia coli* aerobic respiratory chain, II. J. Biol. Chem. **259**: 3375-3381.

22. Kjaergaard, L. 1976. The redox potential: Its use and control in biotechnology. p. 131-149, In: T. K. Ghose, A. Fiechter, and N. Backebrough (eds.), Advances in biochemical engineering, Springer Verlag, N.Y.

23. Kwong, S. C., Randers, L., Rao, G. 1992. On-line assessment of metabolic activities based on culture redox potential and dissolved oxygen profiles during aerobic fermentation. Biotechnol. Prog. **8**: 576-579.

24. Kwong, S. C., Randers, L., Rao, G. 1993. On-line detection of substrate exhaustion by using NAD(P)H fluorescence. Appl. Environ. Microbiol. **59**: 604-606.

25. Kwong, S. C., Rao, G. 1991. Utility of culture redox potential for identifying metabolic state changes in amino acid fermentation. Biotechnol. Bioeng. **38**: 1034-1040.

26. Kwong, S. C., Rao, G. 1992. Effect of a reducing environment in an aerobic amino acid fermentation. Biotechnol. Bioeng. **40**: 851-857.

27. Larsson, G., Enfors, S.-O. 1993. Kinetics of *Escherichia coli* hydrogen production during short term repeated aerobic-anaerobic fluctuations. Bioprocess Engineering. **9**: 167-172.

28. Li, J-K., Humphrey, A. E. 1991. Use of fluorometry for monitoring and control of a bioreactor. Biotechnol. Bioeng. **37**: 1043-1049.

29. London, J., Knight, M. 1966. Concentration of nicotinamide nucleotide coenzymes in micro-organisms. J. Gen. Microbiol. **44**: 241-254.

30. Magnolo, S. K., Leenutaphong, D. L., DeModena, J. A., Curtis, J. E., Bailey, J. E., Galazzo, J. L., Hughes, D. E. 1991. Actinorhodin production by *Streptomyces coelicolor* and growth of *Streptomyces lividans* are improved by the expression of a bacterial hemoglobin. Bio/Technol. **9**: 473-476.

31. Manfredini, R., Cavallera, V., Marini, L., Donati, G. 1983. Mixing and oxygen transfer in conventional stirred fermentors. Biotechnol. Bioeng. **25**: 3115-3131.

32. Meyer, H. P., Beyeler, W., Fiechter, A. 1984. Experiences with the on-line measurement of culture fluorescence during cultivation of *Bacillus subtilis*, *Escherichia coli*, and *Sporotrichum thermophile*. J. Biotechnol. **1**: 341-349.

33. Neidhardt, F. 1987. Chemical composition of *Escherichia coli*, p. 4, In: J. L. Ingraham, K. B. Low, B. Magasanik, M. Schaechter, and H. E. Umbarger (eds.), *Escherichia coli* and *Salmonella typhimurium*: cellular and molecular biology. American Society for Microbiology, Washington, D.C.

34. Onken, U., Leifke, E. 1989. Effect of total and partial pressure (oxygen and carbon dioxide) on aerobic microbial processes. Adv. Biochem. Eng. Biotechnol. **40**: 137-169.

35. Oosterhuis, N. M. G., Kossen, N. W. F. 1984. Dissolved oxygen concentration profiles in a production scale bioreactor. Biotechnol. Bioeng. **26**: 546-555.

36. Radjai, M. K., Hatch, R. T., Cadman, T. W. 1984. Optimization of amino acid production by automatic self-tuning digital control of redox potential. Biotechnol. Bioeng. Symposium No. 14, p. 657-679.

37. Rao, G., Mutharasan, R. 1989. NADH levels and solventogenesis in *Clostridium acetobutylicum*: new insights through culture fluorescence. Appl. Microbiol. Biotechnol. **30**: 59-66.

4.8 Figures

Figure 1 Culture NAD(P)H fluorescence (—) and DO (- - -) time trajectories of the *E. coli* control strain, W3110:pKT1 (1A), and the VHb synthesizing strain, W3110:pKTV1 (1B), under transient oxygenation conditions. Arrows denote the points at which 3 v.v.m. of aeration was interrupted or resumed. Fluorescence signals were normalized by the average dry cell weight (of the samples taken at the beginning and the end of the experiment) and are reported in Specific Fluorescence Units (SFU).

Figure 2 Culture NAD(P)H fluorescence profiles of cell extracts from the control strain, W3110:pKT1 (—), and the VHb– producing strain, W3110:pKTV1 (- - -). Arrows indicate the points at which 3 v.v.m. of aeration was interrupted or resumed. Solid lines were drawn to estimate the baseline drift. Fluorescence signals for both strains were normalized by the dry cell weight determined from a 10 mL sample taken prior to cell disruption. The fluorescence profile of W3110:pKT1 is purposely placed above that of W3110:pKTV1 for clarity.

Figure 3 Culture redox potential, CRP (—), and DO (- - -) time trajectories of the *E. coli* control strain, W3110:pKT1 (3A), and the VHb-synthesizing strain, W3110:pKTV1 (3B), under unsteady oxygenation conditions. Arrows denote the points at which 3 v.v.m. of aeration was interrupted or resumed.

Figure 4 Oxygen concentration profiles of W3110:pKT1(—) and W3110:pKTV1 (- - -) under extremely low DO were calculated from CRP using the logarithmic relationship between DO and CRP, Equation [1], with a and b

equal to, respectively, 0.1132 and –0.9022 for W3110:pKT1 and 0.1320 and –0.7733 for W3110:pKTV1. Sections of DO profiles shown here were determined from the CRP signals of both strains near anoxia (below 1% air saturation). DO was determined and reported in μM from the correlation 4% air saturation = 10 μM.

Figure 5 Biphasic behavior of CRP (—) and DO(- - -) of W3110:pKTV1 during oxygen transitions are shown. Vertical arrows denote the points at which 3 v.v.m. of aeration was interrupted or resumed. Circles indicate the times at which CRP or DO of the culture exhibited fluctuation.

Figure 6 Fluorescence traces of W3110:pKTV1 (+VHb) and W3110:pKT1 (control) in response to oxygen pulses are shown. Cell concentration of both strains were the same at 2.2 g/L. Fluorescence was recorded in 20 sec cycles with 5 sec aeration (3 v.v.m.).

Figure 1

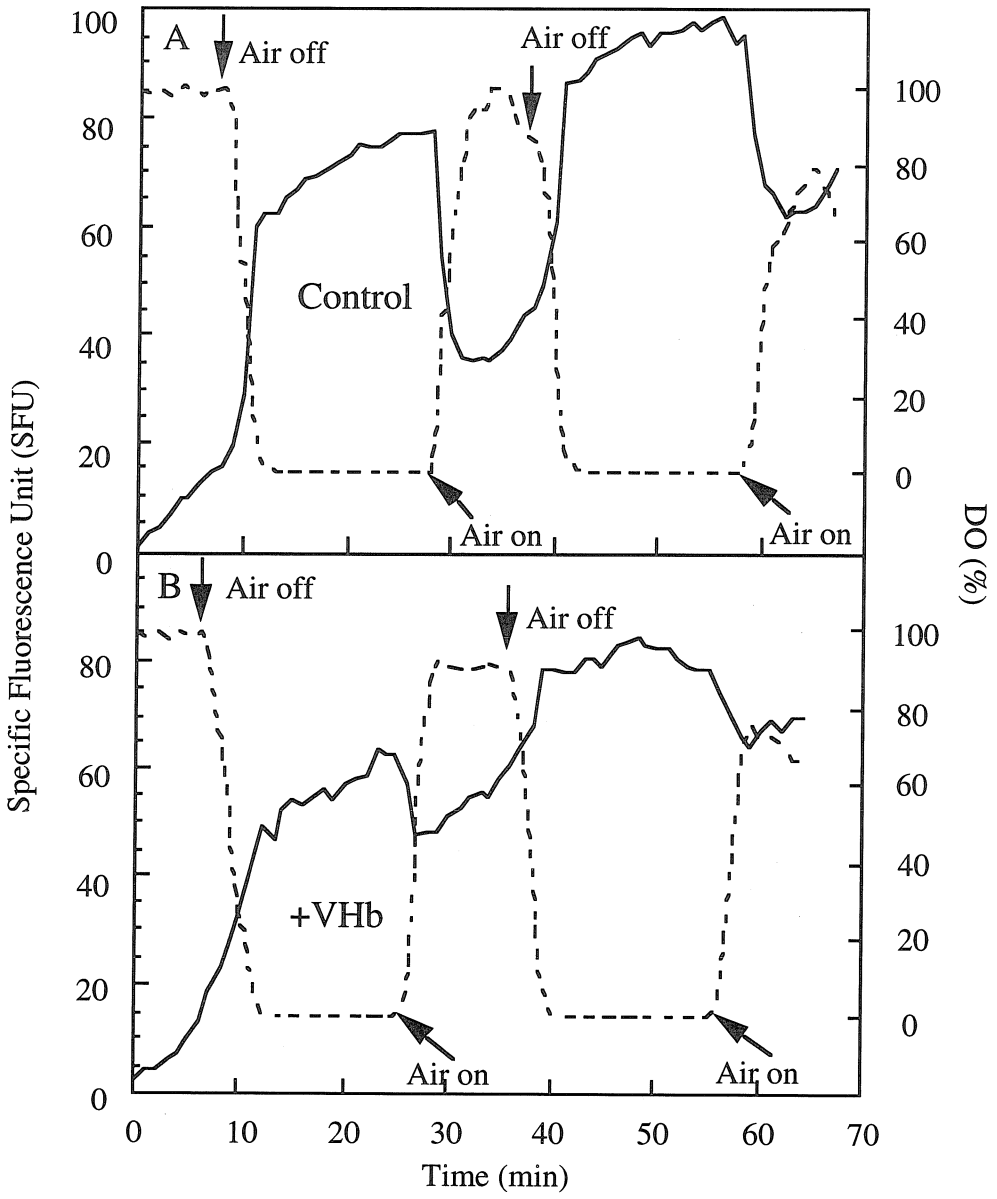
A
Air off
Air off
Control
Air on
Air on
B
Air off
Air off
+VHb
Air on
Air on
Specific Fluorescence Unit (SFU)
DO (%)
Time (min)
0
10
20
30
40
50
60
70
0
20
40
60
80
100

Figure 2

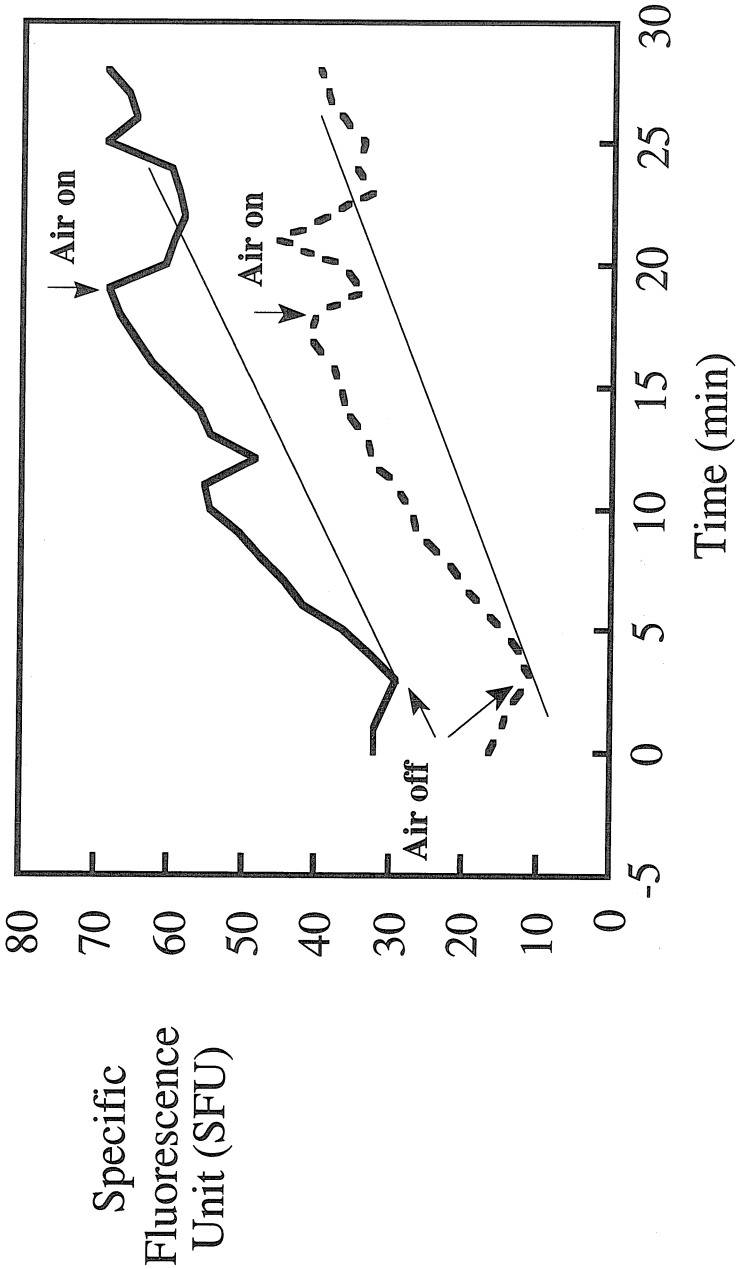
Air on
Air on
Air off
Specific Fluorescence Unit (SFU)
Time (min)
80
70
60
50
40
30
20
10
0
-5
0
5
10
15
20
25
30

Figure 3

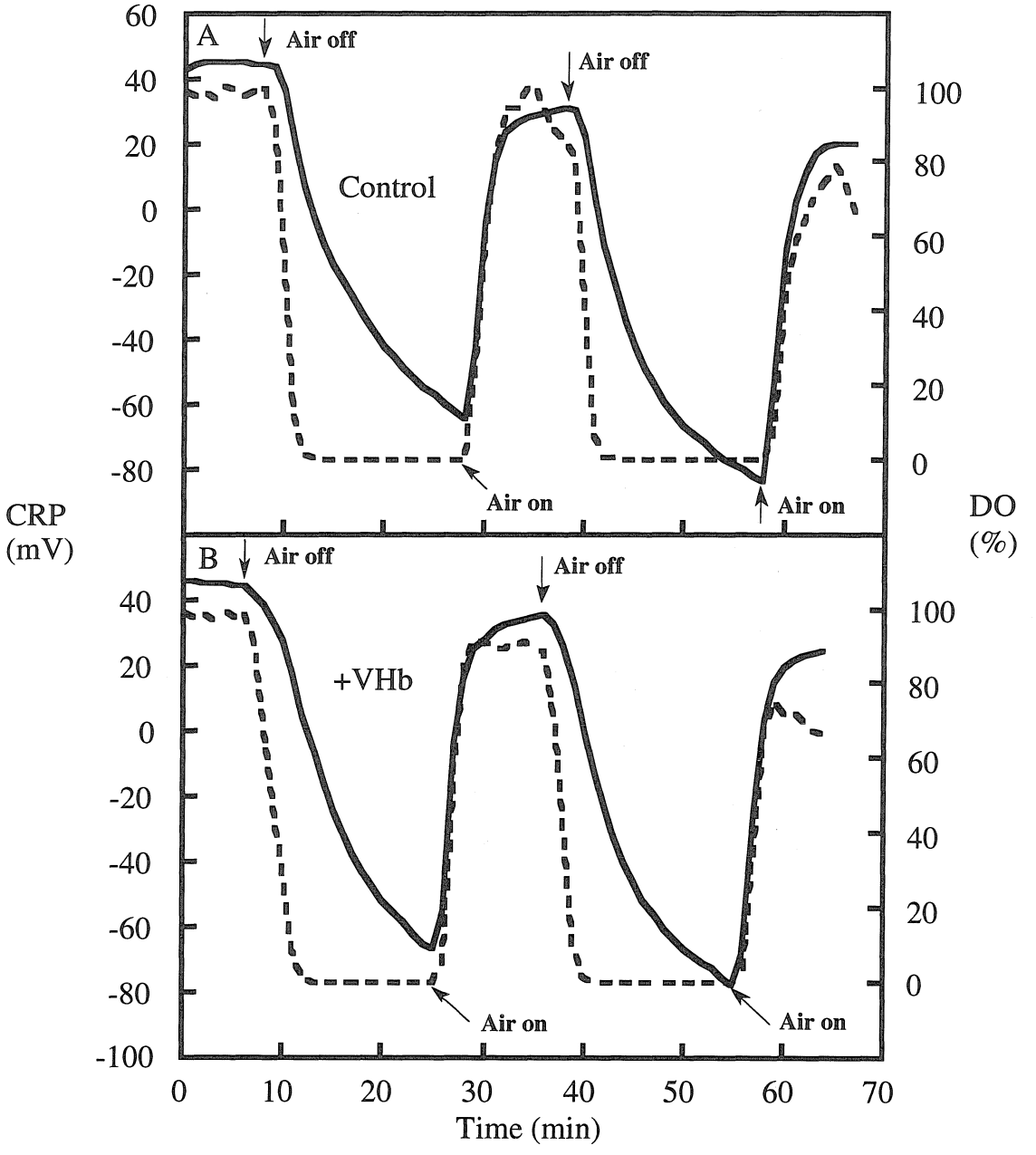
A
Air off
Air off
Control
Air on
Air on
B
Air off
Air off
+VHb
Air on
Air on
CRP
(mV)
DO
(%)
60
40
20
0
-20
-40
-60
-80
100
80
60
40
20
0
-100
0
10
20
30
40
50
60
70
Time (min)

Figure 4

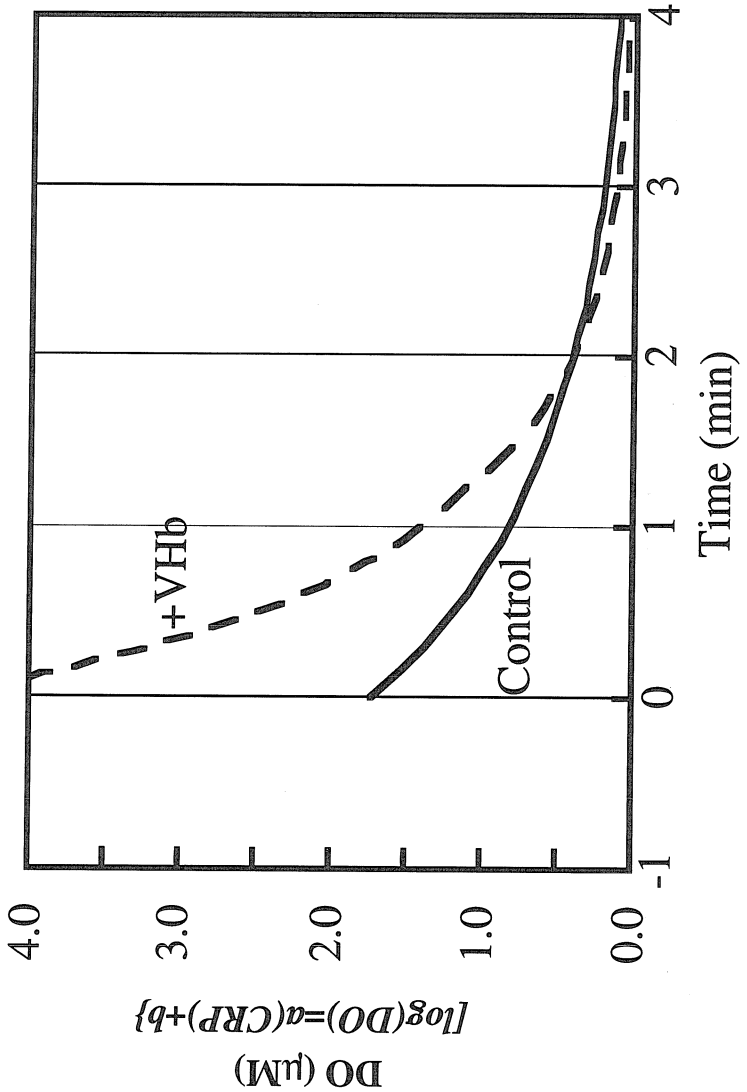

Figure 5

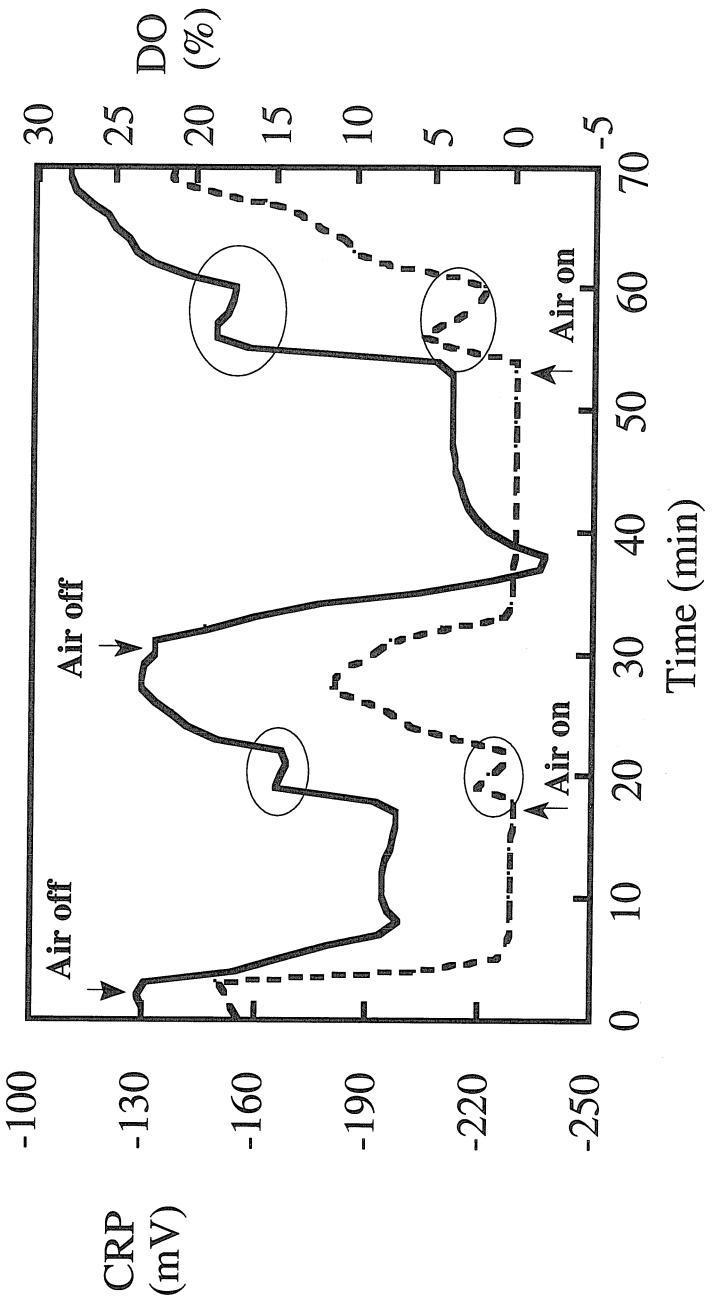
CRP (mV)
-100
-130
-160
-190
-220
-250
DO (%)
30
25
20
15
10
5
0
-5
Time (min)
0
10
20
30
40
50
60
70
Air off
Air on
Air off
Air on

Figure 6

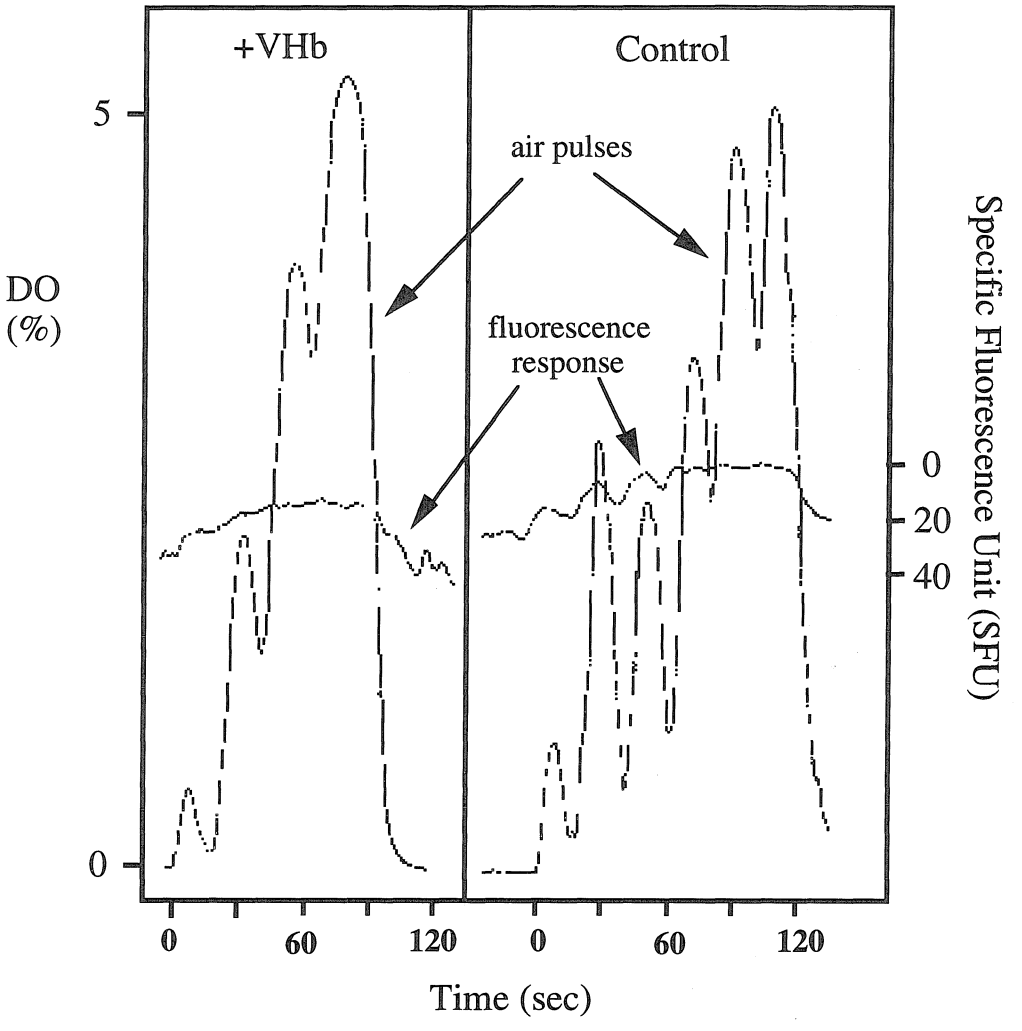
+VHb
Control
5
0
DO
(%)
air pulses
fluorescence
response
0
20
40
Specific Fluorescence Unit (SFU)
0
60
120
0
60
120
Time (sec)

CHAPTER 5:

Factors Influencing the Activity of *Vitreoscilla* Hemoglobin Promoter

Source: Tsai, P. S.; Kallio, P. T.; Bailey, J. E. Fnr, a global transcriptional regulator of *Escherichia coli*, activates the *Vitreoscilla* hemoglobin (VHb) promoter and intracellular VHb expression increases cytochrome *d* promoter activity. 1995. Accepted for publication in *Biotechnology Progress*.

5.1 Abstract

The oxygen-regulated promoter (P_{vhb}) of the *Vitreoscilla* hemoglobin gene has been applied to direct high-level expression of several cloned proteins, including *Vitreoscilla* hemoglobin (VHb) which improves productivity of many aerobic processes. In an effort to gain a better understanding of the regulation of P_{vhb} and to guide further optimization of this technology, we investigated whether the *E. coli* global regulatory molecules Fnr and the Arc system (ArcA and ArcB), which control expression of various genes under either aerobic or anaerobic conditions, also regulate P_{vhb} activity in *E. coli*. The activity of P_{vhb} and the expression of VHb in *E. coli* were activated by Fnr but relatively unaffected by the Arc system under microaerobic conditions (DO less than 2% air saturation). We also examined the possibility of VHb affecting the cytochrome *d* promoter activity during microaerobiosis. The presence of VHb increased the activity of ß-galactosidase from a cytochrome *d* promoter-*lacZ* fusion by 1.5-fold. This indicates that VHb affects oxygen-regulated transcription of *E. coli* genes and may contribute to the modified physiology observed in VHb-expressing *E. coli*.

5.2 Introduction

Convenient regulated promoter systems for expression of recombinant proteins in *Escherichia coli* find application in both academic research and industrial processes. Recently, Hughes et al. (1989) described a technologically interesting promoter system under which a bioprocess can be easily switched to recombinant protein production by limiting oxygen supply to a bioreactor. This promoter, and the naturally adjacent structural gene which encodes a hemoglobin (VHb), were isolated from the aerobic bacterium *Vitreoscilla* (Khosla and Bailey, 1988 a&b; Dikshit et al., 1988). Transcription from this promoter is initiated when dissolved oxygen concentration becomes sufficiently low but transcription does not occur under anoxic conditions; P_{vhb} activity is maximal under microaerobic conditions (defined as dissolved oxygen concentration in the range of 2% air saturation or less) (Khosla and Bailey, 1988a, 1989; Joshi and Dikshit, 1994). Use of this oxygen-dependent promoter of the *Vitreoscilla* hemoglobin gene (*vhb*) for high-level recombinant protein expression in *E. coli* and its potential advantages over other expression systems such as *tac* (de Boer et al., 1983) and bacteriophage lambda p_L (Remaut et al., 1981) have been documented (Hughes et al., 1989; Khosla et al., 1990a).

Intracellular expression of VHb in oxygen-limited *E. coli* cultures improves cell growth and recombinant protein production (Khosla and Bailey, 1988a; Khosla et al., 1990b; Khosravi et al., 1990). Other examples of bioprocess productivity enhancement by VHb, such as increasing antibiotic production from *Streptomyces coelicolor* and *Acremonium chrysogenum*, have also been demonstrated (Magnolo et al., 1991; DeModena et al., 1993). VHb expression in *Corynebacterium glutamicum* enhances the titer and yield on glucose of lysine (Sander et al., 1993).

Clearly, in the first class of applications, the properties of the *vhb* promoter and the regulatory species which determine its activity are important and, in the second class, possible effects of VHb on transcription of other cellular genes may contribute to the altered physiology observed in VHb-expressing constructs. Thus, key features in both cases are the interactions between those genetic elements of *Vitreoscilla* and *E. coli*, and their protein products, which are implicated in response to oxygen limitation. This work examines some of these interactions through monitoring of reporter enzyme expression in different pertinent genetic backgrounds.

The Fnr (fumarate nitrate reduction) protein and the Arc (aerobic respiration control) system are two global transcriptional activators of *E. coli* which sense the presence of oxygen and elicit a cascade of metabolic changes within the cell by regulating transcription of many oxygen-regulated genes (for reviews, see Anraku, 1988; Ingledew and Poole, 1984; Spiro and Guest, 1991). The product of the *fnr* gene, Fnr, is a sequence-specific DNA-binding protein (Green et al., 1991) which regulates synthesis of various enzymes such as the increased and decreased expression of cytochrome *d* and NADH dehydrogenase II, respectively, in anaerobic conditions (Fu et al., 1991; Spiro et al., 1989). Fnr also autoregulates its own expression under anoxia (Spiro and Guest, 1987). The Arc system consists of two genes, *arcA* and *arcB*. The proteins ArcA and ArcB have been identified as a sensor-regulator system; ArcB is the membrane bound sensor and ArcA is the cytoplasmic regulator that recognizes signals from ArcB (Iuchi and Lin, 1991; Spiro and Guest, 1991; Stock et al., 1989).

Many oxygen-regulated genes are subject to dual controls by Fnr and the Arc system. Expression of the genes encoding the aerobic terminal oxidases of *E. coli*, cytochrome *o* and cytochrome *d*, for example, is switched on and off by the overlapping controls of Fnr and the Arc system (Frey et al., 1989; Fu et al., 1991).

Although Fnr and the Arc system are known for their anaerobic modulations of gene expression, respectively, the difference in the strength of their regulatory activities allow an enzyme such as cytochrome *d* to be maximally expressed under microaerobic conditions (Fu et al., 1991; Cotter and Gunsalus, 1992).

The fact that the transcriptional activity of P_{vhb} is oxygen-regulated and that VHb is maximally expressed under microaerobic conditions in *E. coli* suggest the possibility of Fnr and/or Arc involvement in regulating P_{vhb} activity. Analysis of the *vhb* DNA sequence (Khosla and Bailey, 1989) reveals a nucleotide sequence resembling the consensus binding site of Fnr in a region about 45 bp upstream of the transcription initiation site P1 in P_{vhb} . This suggests that Fnr might recognize this sequence and regulate the activity of P_{vhb}. In this investigation, we determined the effects of *fnr* and *arc* mutations on the activity of P_{vhb} and VHb expression level to gain insights into the mechanism by which P_{vhb} is controlled in *E. coli.* The possibility that VHb affects other oxygen-regulated promoters was also examined by comparing the activity of the cytochrome *d* promoter (P_{cyd}) in *E. coli* synthesizing VHb and in control cells not expressing VHb. The data presented in this study provide evidence that the transcriptional activity of P_{vhb} is modulated by Fnr and that the activity of the cytochrome *d* promoter is altered in *E. coli* containing a VHb expression vector.

5.3 Materials and Methods

5.3.1 Bacteria and Plasmids

E. coli strains and plasmids used are given in Table 1. To study the regulation of P_{vhb} activity by the Arc system, *E. coli* strains ECL942, ECL943, and ECL944

were transformed with the control plasmid pMS421, the VHb expression plasmid pMSV1, or plasmid pMSC1 which contains P_{vhb} fused with the *cat* gene. For study of *fnr* regulation, *E. coli* strains MC4100 and PC2 were also transformed with plasmids pMS421, pMSV1, or pMSC1. Plasmid pMSC1 was constructed by isolating the 1 kb *Hind* III-*BamH* I fragment containing P_{vhb}-*cat* from pOX2 (Khosla and Bailey, 1989) and ligated with pMS421 (*Hind* III-*BamH* I). The construction of pMSV1 was described elsewhere (Kallio et al., 1994).

5.3.2 Chemicals, Reagents, and DNA Manipulations

All restriction endonucleases, modifying enzymes (T4 DNA ligase and calf intestinal phosphatase) were purchased from either New England BioLabs or Boehringer Mannheim Biochemicals. All DNA manipulations were done according to standard methods (Sambrook et al., 1989). DNA fragments were eluted from agarose gels using a Geneclean Kit (Bio 101, Inc.).

5.3.3 Cultivation Conditions

Shake flask cultivations for preliminary analyses of P_{vhb} regulation by Fnr and the Arc system were done in buffered LB medium (10g/L Bacto-tryptone, 5 g/L Bacto-yeast extract, 10 g/L NaCl, 3 g/L K_2HPO_4, 1 g/L KH_2PO_4, adjusted to pH 7) at 37°C and 250 rpm in a New Brunswick Scientific G24 Environmental shaker. To study the effect of P_{vhb} induction, which occurs at low oxygen tensions, *E. coli* strains ECL942, ECL943, ECL944, MC4100, and PC2 containing plasmids pMS421 or pMSV1 were cultivated in 250 ml non-baffled shake flasks containing 50 ml buffered LB media at 37°C and 75 rpm.

Batch bioreactor cultivations were performed in Six-fors bioreactors (Infors, Inc., Switzerland) with 300 ml working volume. Six milliliters of an overnight culture grown in buffered LB medium were used to inoculate a bioreactor containing the same medium, and the process parameters 37°C, pH 7.0, 300 rpm, and 0.15 L/min of air flow were maintained for the duration of each 15-hour batch fermentation. Spectinomycin (40 mg/L) was added to all fermentations for plasmid maintenance. In addition, ampicillin (100 mg/L) and tetracycline (10 mg/L) were added to ECL strain cultivations, except ECL942 to which only ampicillin was added. Samples were taken every two hours for analyses starting two hours after inoculation.

Additional batch fermentations were performed using buffered LB medium in a New Brunswick Bioflo III fermentor with 2.5 l working volume. Fifty milliliters of an overnight culture in LB medium were used to inoculate each bioreactor cultivation, and the process parameters 37°C, pH 7.0, 250 rpm, and 0.4 L/min of air flow were maintained for the duration of the 12-hour batch fermentation.

5.3.4 Western Immunoblotting of *Vitreoscilla* Hemoglobin

One milliliter samples from the VHb-expressing strains were resuspended in 200 µl lysis buffer (200 µl 50% w/v glycerol, 100 µl 10% SDS, 10 µl ß-mercaptoethanol, 100 µl 0.1% bromophenol blue, 250 µl 0.5 M Tris-pH 6.8, and 340 µl sterile H_2O) and boiled for 5 min in a water bath. The globin content of a sample was assayed by running a 15% SDS-polyacrylamide gel (Laemmli, 1970) followed by Western blotting (Winston et al., 1987) using rabbit anti-VHb antiserum (Cocalico Biologicals) and horseradish peroxidase-conjugated sheep IgG fraction to rabbit IgG (Cappel™). Using a Molecular Dynamics densitometer, the amount of VHb in each sample was estimated by comparing the intensity of its Western blot negative with

that of a hemoglobin standard (4.5 pmole) prepared from *E. coli* JM101:pRED2 (Khosla and Bailey, 1988b) cell extract. Total soluble protein level of each sample was determined using a Protein Assay kit from BioRad. Hemoglobin content is reported in nmole of VHb per mg total protein.

5.3.5 ß-galactosidase Activity Assay

Besides a functional *cyd* gene, each of strains ECL942, ECL943, and ECL944 carries a single chromosomal integration of $\Phi(P_{cyd}\text{-}lac)$ (Iuchi et al., 1990). ß-galactosidase activity levels in these strains were determined using Miller's protocol (Miller, 1972) with the following modification: after 20-fold dilution in Z buffer (Miller, 1972), cells were lysed by adding 50 µl of chloroform and 25 µl of 0.1% SDS. ß-galactosidase activity was assayed by measuring the hydrolysis of *o*-nitrophenyl-ß-D-galactoside (4 mg/ml) at $A420$ and $A550$ after 20 min of reaction at 30°C. The specific activity is expressed in Miller units (1 Miller unit = $1000*\Delta A*min^{-1}*ml^{-1}*A_{600}^{-1}$).

5.3.6 Chloramphenicol Acetyltransferase (CAT) Assay

CAT content was determined by an ELISA protocol (CAT ELISA Kit, Boehringer Mannheim). Samples were disrupted by sonication and portions of the soluble fractions were assayed for total protein content using a Protein Assay kit (BioRad). The CAT activity was determined according to the recommended protocol and expressed in µg of CAT per milligram of total soluble protein.

5.3.7 Plasmid Copy Number Determination

Plasmid copy was determined according to the method described by Projan et al. (1983) with the following modifications. The cell pellet was suspended and

incubated for 30 min at 37°C in 50 µl lysis buffer containing 20 mM Tris-HCl, pH 8, 10 mM EDTA, 100 mM NaCl, 20% sucrose, 75 µg/ml lysozyme, and 2 U/ml RNase. Fifty microliters of 2% SDS were added, and the samples were vortexed at maximum setting for 1 min. After the samples were freeze-thawed two times (-70°C to 37°C), 10 µg of proteinase K was added, and the samples were incubated at 37°C for 30 min. Twenty-five microliters of loading buffer (50% glycerol, 1 mM EDTA, pH 8, and 0.1% bromophenol blue) were then added to the samples. 20 µl of the mixture was loaded on a 0.9% agarose gel for plasmid DNA determination. The remainder samples (for chromosomal DNA determination) were diluted 20-fold and loaded on the same agarose gel. The gel was electrophoresed for 3 hr at 80 V and was subsequently stained for 40 min with 1 mg/ml ethidium bromide and destained once for 10 min with water. The gel was illuminated using a UV lamp and photographed with Polaroid type 665 film. The plasmid copy number per chromosomal equivalent was estimated by scanning the negatives using a densitometer from Molecular Dynamics and comparing the intensity of the chromosomal DNA band to that of the plasmid DNA. The calculated plasmid copy numbers relative to that of the strain ECL942:pMSV1 are reported.

5.4 Results and Discussion

In this study, we explored the roles of Fnr and the Arc system in the regulation of P_{vhb} by studying the VHb expression level in *E. coli* using a low copy number VHb expression plasmid and hosts with either *fnr* and *arcA* or *arcB* mutations (Table 1). In order to identify whether the effects of Fnr and the Arc system on VHb production are at the transcriptional level and are not connected with post-

transcriptional processing and assembly of the heme-containing VHb dimer, we also transformed *fnr* and *arc* mutants with a plasmid containing the *cat* gene fused with P_{vhb} ($\Phi(P_{vhb}$-*cat*)) and analyzed the synthesis of the reporter enzyme chloramphenicol acetyltransferase (CAT). Studies were performed under controlled environment in bioreactors, and the effects of Fnr and Arc on VHb expression and P_{vhb} activity were quantified under microaerobic conditions where the activity of P_{vhb} is maximum (Khosla and Bailey, 1989).

5.4.1 Fnr Increases VHb Expression and P_{vhb} Activity

From an *in vitro* DNaseI footprinting study, Fnr was shown to be a DNA-binding protein that binds to a synthetic Fnr consensus-site (Green et al., 1991). Figure 1 shows a comparison of the DNA sequences near a region upstream of *vhb* P1 and the suggested Fnr binding site consensus sequence (Khosla and Bailey, 1989; Spiro and Guest, 1990). The consensus nucleotide-binding sequence of Fnr, excluding one nucleotide, matches identically with a region 48 bp upstream of the P_{vhb} transcription initiation site P1.

Figure 2 shows the VHb time trajectory in cultures of the *fnr*$^+$ strain (MC4100:pMSV1) and the *Δfnr* strain (PC2:pMSV1) monitored by Western blotting. In the absence of Fnr, VHb contents were two-fold less than those of the control cells throughout the cultivation. Both cultivations became microaerobic three hours after inoculation and remained microaerobic until the 10th hr and the 12th hr for MC4100:pMSV1 and PC2:pMSV1, respectively. The specific growth rates decreased and the dissolved oxygen rose toward the end of cultivations. Under our cultivation scheme, a deletion in *fnr* did not seem to have a detrimental effect on cell growth, since the final cell densities of the two strains were similar ($A_{600} = 3.4 \pm 0.1$). A

40% drop in the VHb level was observed for MC4100:pMSV1 when oxygen tension increased sharply toward the end of fermentation, indicating the oxygen-dependent nature of VHb expression. However, VHb concentration in PC2:pMSV1 also decreased with an increase in the dissolved oxygen, suggesting that Fnr is not the only species which regulates P_{vhb}.

In order to examine whether the target of Fnr regulation lies within the promoter of *vhb*, we constructed a plasmid, pMSC1 which contains P_{vhb} upstream of a reporter gene encoding CAT. No sequence deletion of P_{vhb} was done to localize the binding region of Fnr because deletions from the 5' end of P_{vhb} led to instability of *vhb* insert (Khosla and Bailey, 1989). The accumulation of CAT in strains MC4100:pMSC1 and PC2:pMSC1 were monitored under the same conditions as those shown in Figure 2. Cells with the *fnr* gene synthesized twice as much CAT as the cells containing an *fnr* deletion (Figure 3). The amount of CAT in MC4100:pMSC1 was on the average 5.0 μg CAT/mg protein compared with the average of 2.5 μg CAT/mg protein for PC2:pMSC1.

The observation of a two-fold increase by Fnr in either VHb content or CAT production from $\Phi(P_{vhb}\text{-}cat)$ was modest compared with the usual regulation pattern of Fnr which activates or represses gene expression on the order of 5-fold or larger under anaerobic conditions (Kiley and Reznikoff, 1991). However, our studies were performed under microaerobic conditions which could result only in partial activation of Fnr. In order to differentiate whether the increase in P_{vhb} activity is solely due to regulation by Fnr or artifacts stemming from variation in gene dosage, we measured the plasmid copy number of samples from the bioreactor cultivations. The plasmid copy numbers of all strains remained relatively stable during the course of cultivation and thus only the average numbers are reported (Table 2). The measured copy number

per chromosomal equivalent of pMSV1 was the same in MC4100 and PC2, and the number of copies of pMSC1 also did not vary significantly in MC4100 and PC2. Therefore, assuming the transcriptional efficiency from P_{vhb} was the same in either MC4100 or PC2, our results indicated that P_{vhb} activity is not fully induced in the absence of the Fnr protein; Fnr is a trans-acting activator of P_{vhb} under microaerobic conditions.

It is possible that a small change in oxygen tension could shift the regulation regimes of Fnr and Arc. Difference in oxygen transfer resulting from variations in vessel and stirrer geometry may play a role in the regulation of Fnr and Arc on P_{vhb}. We examined this possibility by repeating experiments using a different bioreactor (NBS Bioflow III). Results showed the same Fnr regulation on P_{vhb} as before: a two-fold decrease in CAT production and VHb content from PC2:pMSC1 and PC2:pMSV1, respectively, when *fnr* was deleted (results not shown).

While the present manuscript was in review, a communication by Joshi and Dikshit (1994) appeared which also indicates influence of Fnr on P_{vhb} in *E. coli*. Two independent observations of this interaction are significant since different host strains, expression vectors, and cultivation conditions were used in their work compared to the present study. The current experiments are distinguished in particular by copy number measurements and by bioreactor cultivation with controlled temperature, pH, and monitored DO.

5.4.2 Arc Exerts No Effect on VHb Expression and P_{vhb} Activity

A recent DNA footprinting analysis shows that ArcA protects P_{sodA} in a stretch of 61 bp nucleotides which overlaps both -10 and -35 of promoter regions (Tardat and Touati, 1993). However, no significant sequence homology between the

ArcA binding region of *sodA* and the promoters of 12 genes which are also regulated by ArcA was found (Tardat and Touati, 1993). Using a computer package for sequence analysis (Devereux et al., 1984), we also did not find significant sequence similarity between the *vhb* promoter, the *cyoA* promoter, the *sdhC* (regulated by ArcA) promoter, and the ArcA binding region of *sodA* promoter (data not shown). Nevertheless, the findings of the Arc system regulating a wide spectrum of oxygen-dependent genes in *E. coli* (Cotter and Gunsalus, 1992; Iuchi et al., 1990) prompted us to study the effects of *arc* mutations on VHb expression and P_{vhb} activity. Preliminary screening in shake flask cultures suggested that *arcB*, not *arcA*, might regulate VHb expression and P_{vhb} activity (data not shown). Therefore, bioreactor studies were performed on $arcA^+$, $arcB^+$ (ECL942) and $arcA^+$, $arcB^-$(ECL944) genetic backgrounds only. The time trajectory of VHb in ECL942:pMSV1 and ECL944:pMSV1 fluctuated but did not differ significantly (Figure 4). A deletion in the *arcB* gene did not affect cell growth; the final cell density for ECL944:pMSV1 was comparable to that of ECL942:pMSV1 (A_{600} = 2.20 ± 0.1). We also examined CAT synthesis from $\Phi(P_{vhb}\text{-}cat)$ in strains ECL942:pMSC1 and ECL944:pMSC1 under microaerobic bioreactor cultivations. A deletion in *arcB* did not have a substantial effect on the synthesis of CAT driven by the *vhb* promoter (Figure 5). In view of the above observations and the marginal difference in the copy number of pMSV1 and pMSC1 between the control and the mutant strains (Table 2), we concluded that ArcA and ArcB exert no notable regulation on P_{vhb} activity.

5.4.3 Expression of VHb Increases P_{cyd} Activity

We have previously conjectured the role of VHb in *E. coli* is to raise the effective dissolved oxygen tension within the cells by scavenging and releasing oxygen to the terminal oxidases during oxygen-limited growth conditions (Kallio et

al., 1994). The effectiveness of VHb in increasing intracellular dissolved oxygen is thus inversely proportional to the culture oxygen concentration and is most amplified in the region of nearly anoxia to 4% air saturation (Kallio et al., 1994). It is possible that VHb might shift the regulation regime of the Arc system by increasing the effective dissolved oxygen concentration. Results from a study by Fu et al. (1991), who investigated the effects of ArcA on the transcriptional activity of Arc-regulated promoters under different oxygen concentrations, suggest that the range of ArcA regulation lies within 0 – 5% air saturation for P_{cyd}, P_{frd}, and P_{sdh}, and the most sensitive control of ArcA on P_{cyd} activity is around and below 1% air saturation but not anoxia. The presence of VHb may influence the activity of P_{cyd} indirectly through a change in regulation of Arc and Fnr by raising the effective DO.

Iuchi et al. (1990) showed, as implied by their promoter-*lacZ* gene fusion study, that regulation of *cyo* and *cyd* expression is mainly at the level of mRNA synthesis. For that reason we chose expression of $\Phi(P_{cyd}\text{-}lac)$ as a reporter for possible effects of VHb on the activity of the cytochrome *d* promoter. Investigations were conducted in an NBS Bioflow III bioreactor with strains ECL942, ECL943, and ECL944 in which $\Phi(P_{cyd}\text{-}lac)$ was introduced into the genome without altering the functional *cyd* operon (Iuchi et al., 1990). These strains were transformed with pMS421, pMSV1, or pMSC1 (Table 1). In a background with functional Fnr and Arc, the production of ß-galactosidase in ECL942:pMSV1 was increased by almost 1.5-fold when VHb is synthesized compared with the control strain ECL942:pMS421 (Figure 6). ß-galactosidase activities assayed at the end of batch fermentations were 1000 and 700 Miller units for strains ECL942:pMSV1 and ECL942:pMS421, respectively. This increase in ß-galactosidase activity indicates that the presence of VHb increases the transcriptional activity from P_{cyd} under microaerobic conditions.

Perhaps the presence of VHb raised the effective DO to a level which triggers the regulatory mechanism of the Arc system, and then activated ArcA which, in combination with other regulatory molecules such as Fnr, gave rise to an increase in the activity of P_{cyd}.

To determine whether the increase in $\Phi(P_{cyd}\text{-}lac)$ expression is due to some interaction involving P_{vhb} itself or due to the presence of VHb itself, we examined the expression of $\Phi(P_{cyd}\text{-}lac)$ in strain ECL942:pMSC1. To our surprise, the production of ß-galactosidase in ECL942:pMSC1 was lower (approximately 3.5-fold) than that of the control strain ECL942:pMS421 (Figure 6). This suggests a possible effect of the presence of P_{vhb} on the activity of P_{cyd}, but also suggests a more significant effect of VHb on P_{cyd} since ß-galactosidase activity was substantially increased when both P_{vhb} and VHb are present.

How might the presence of P_{vhb} decrease the transcriptional activity from P_{cyd}? Introducing even a few copies of one oxygen-regulated promoter may titrate critical regulators and alter the activity of other oxygen-regulated promoters. Our results indicate that the transcription of the *vhb* promoter decreased the activity of the cytochrome *d* promoter. Without the presence of VHb, which may interact with Fnr and the Arc system, the transcriptional activity of P_{cyd} in ECL943 and ECL944 harboring the $\Phi(P_{vhb}\text{-}cat)$ expression plasmid pMSC1 was always lower than that of the same cells carrying the control plasmid pMS421 (result not shown).

5.5 Conclusions

Application of P_{vhb}-driven recombinant protein production and intracellular expression of VHb as a means to enhance process productivity are novel, economical, and easily practiced technologies. Yet, the mechanism by which P_{vhb} is regulated and the effects of VHb expression on other cellular enzymes in *E. coli* are not well understood. The main findings of this study are therefore valuable information for the further advancement of P_{vhb} and VHb technology. We have demonstrated that the global oxygen-sensing, trans-acting regulator of *E. coli*, Fnr, activates the transcriptional activity of the *vhb* promoter, and intracellular expression of VHb in *E. coli* increases activity of the cytochrome *d* promoter. Varying dosage of *fnr* in cells may provide additional control of the *vhb* promoter. The presence of VHb may also increase expression of other oxygen-regulated genes.

5.6 Acknowledgments

This work was supported by the Swiss Priority Program in Biotechnology. We thank Dr. E. C. C. Lin for generously supplying *E. coli* strains ECL942, ECL943, and ECL944 , and Dr. R. P. Gunsalus for *E. coli* strains MC4100 and PC2.

5.7 References

Anraku, Y. Bacterial Electron Transport Chains. *Ann. Rev. Biochem.* **1988**, *57*, 101-132.

Cotter, P. A.; Gunsalus, R. P. Contribution of the *fnr* and *arcA* Gene Products in Coordinate Regulation of Cytochrome *o* and *d* Oxidase (*cyoABCDE* and *cydAB*) Genes in *Escherichia coli*. *FEMS Microbiol. Lett.* **1992**, *91*, 31-36.

de Boer, H. A.; Comstock, L. J.; Vasser, M. The *tac* Promoter: a Functional Hybrid Derived from the *trp* and *lac* Promoters. *Proc. Natl. Acad. Sci. USA*. **1983**, *80*, 21-23.

DeModena, J. A.; Gutierrez, S.; Velasco, J.; Fernandez, F. J.; Fachini, R. A.; Galazzo, J. L.; Hughes, D. E.; Martin, J. F. The Production of Cephalosporin C by *Acremonium chrysogenum* is Improved by the Intracellular Expression of a Bacterial Hemoglobin. *Bio/Technol.* **1993**, *11*, 926-929.

Devereux, J.; Haeberli, P.; Smithies, O. A Comprehensive Set of Sequence-analysis Programs for the VAX. *Nucleic. Acid Res.* **1984**, *12*, 387-395.

Dikshit, K. L.; Webster, D. A. Cloning, Characterization and Expression of the Bacterial Globin Gene from *Vitreoscilla* in *Escherichia coli*. *Gene* **1988**, *70*, 377-386.

Frey, B.; Janel, G.; Michelson, U.; Kersten, H. Mutations in the *Escherichia coli fnr* and *tgt* Genes: Control of Molybdate Reductase Activity and the Cytochrome *d* Complex by *fnr*. *J. Bacteriol.* **1989**, *171*, 1524-1530.

Fu, H.-A.; Iuchi, S.; Lin, E. C. C. The Requirement of ArcA and Fnr for Peak Expression of the *cyd* Operon in *Escherichia coli* under Microaerobic Conditions. *Mol. Gen. Genet.* **1991**, *226*, 209-213.

Green, J.; Trageser, M.; Six, S.; Unden, G.; Guest, J. R. Characterization of the FNR Protein of *Escherichia coli*, an Iron-binding Transcriptional Regulator. *Proc. R. Soc. Lond. B.* **1991**, *244*, 137-144.

Hughes, D. E.; Curtis, J. E.; Khosla, C.; Bailey, J. E. A New Oxygen-regulated Promoter for the Expression of Proteins in *Escherichia coli*. *BioTechniques* **1989**, *7*, 1026-1028.

Ingledew, J. W.; Poole, R. K. The Respiratory Chain of *Escherichia coli*. *Microbiol. Rev.* **1984**, *48*, 222-271.

Iuchi, S.; Chepuri, V.; Fu, H.-A.; Gennis, R. B.; Lin, E. C. C. Requirement for Terminal Cytochromes in Generation of the Aerobic Signal for the *arc* Regulatory System in *Escherichia coli*: Study Utilizing Deletions and *lac* Fusions of *cyo* and *cyd*. *J. Bacteriol.* **1990**, *172*, 6020-6025.

Iuchi, S.; Lin, E. C. C. Adaptation of *Escherichia coli* to Respiratory Conditions: Regulation of Gene Expression. *Cell* **1991**, *66*, 5-7.

Joshi, M.; Dikshit, K.L. Oxygen-dependent Regulation of *Vitreoscilla* Globin Gene–Evidence for Positive Regulation by FNR. *Biochem. Biophy. Res. Commun.* **1994**, *202*, 535-542.

Kallio, P. T.; Kim, D. J.; Tsai, P. S.; Bailey, J. E. Intracellular Expression of *Vitreoscilla* Hemoglobin Alters *Escherichia coli* Energy Metabolism under Oxygen-limited Conditions. *Eur. J. Biochem.* **1994**, *219*, 201-208.

Khosla, C.; Bailey, J. E. Characterization of the Oxygen-dependent Promoter of the *Vitreoscilla* Hemoglobin Gene in *Escherichia coli. J. Bacteriol.* **1989**, *171*, 5995-6004.

Khosla, C.; Bailey, J. E. Heterologous Expression of a Bacterial Haemoglobin Improves the Growth Properties of Recombinant *Escherichia coli. Nature* **1988a**, *331*, 633-635.

Khosla, C.; Bailey, J. E. The *Vitreoscilla* Hemoglobin Gene: Molecular Cloning, Nucleotide Sequence and Genetic Expression in *Escherichia coli. Mol. Gen. Genet.* **1988b**, *214*, 158-161.

Khosla, C.; Curtis, J. E.; Bydalek, P.; Swartz, J. R.; Bailey, J. E. Expression of Recombinant Proteins in *Escherichia coli* Using an Oxygen-responsive Promoter. *Bio/Technol.* **1990a**, *8*, 554-558.

Khosla, C.; Curtis, J. E.; DeModena, J.; Rinas, U.; Bailey, J. E. Expression of Intracellular Hemoglobin Improves Protein Synthesis in Oxygen-limited *Escherichia coli. Bio/Technol.* **1990b**, *8*, 849-853.

Khosravi, M.; Webster, D. A.; Stark, B. C. Presence of Bacterial Hemoglobin Gene Improves α-Amylase Production of a Recombinant *Escherichia coli* Strain. *Plasmid* **1990**, *24*, 190-194.

Kiley, P.; Reznikoff, W. S. Fnr Mutants that Activate Gene Expression in the Presence of Oxygen. *J. Bacteriol.* **1991**, *173*, 16-22.

Laemmli, U. K. Cleavage of Structural Proteins During the Assembly of the Head of Bacteriophage T4. *Nature* **1970**, *227*, 680-685.

Magnolo, S. K.; Leenutaphong, D. L.; DeModena, J. A.; Curtis, J. E.; Bailey, J. E.; Galazzo, J. L.; Hughes, D. E. Actinorhodin Production by *Streptomyces coelicolor* and Growth of *Streptomyces lividans* are Improved by the Expression of a Bacterial Hemoglobin. *Bio/Technol.* **1991**, *9*, 473-476.

Miller, J. H. In *Experiments in Molecular Genetics*; Cold Spring Harbor Laboratory, Cold Spring Harbor, N.Y., 1972; pp. 352-355.

Projan, S. J.; Carleton, S; Novick, R. P. Determination of Plasmid Copy Number by Fluorescence Densitometry. *Plasmid* **1983**, *9*, 182-190.

Remaut, E.; Stanssens, P.; Fiers, W. Plasmid Vectors for High-efficiency Expression Controlled by the *pL* Promoter of Coliphage Lambda. *Gene* **1981**, *15*, 81-93.

Sambrook, J.; Frisch, E. F.; Maniatis, F. E. In *Molecular Cloning: a laboratory manual*; Cold Spring Harbor Laboratory, Cold Spring Harbor, N.Y.; 1989.

Sander, F. C.; Fachini, R. A.; Hughes, D. E.; Galazzo, J. L.; Bailey, J. E. Expression of *Vitreoscilla* Hemoglobin in *Corynebacterium glutamicum* Increases Final Concentration and Yield of L-lysine. *ECB6: Proceedings of the 6th European Congress on Biotechnology* **1993**; pp. 607-610.

Spiro, S.; Guest, J. R. Adaptive Responses to Oxygen Limitation in *Escherichia coli*. *Trends in Biochem. Sci.* **1991**, *16*, 310-314.

Spiro, S.; Guest, J. R. FNR and Its Role in Oxygen-regulated Gene Expression in *Escherichia coli*. *FEMS Microbiol. Rev.* **1990**, *75*, 399-428.

Spiro, S.; Guest, J. R. Regulation and Over-expression of the *fnr* Gene of *Escherichia coli*. *J. Gen. Microbiol.* **1987**, *133*, 3279-3288.

Spiro, S.; Roberts, R. E.; Guest, J. R. FNR-dependent Repression of the *ndh* Gene of *Escherichia coli* and Metal ion Requirement for FNR-regulated Gene Expression. *Mol. Microbiol.* **1989**, *3*, 601-608.

Stock, J. B.; Ninfa, A. J.; Stock, A. M. Protein Phosphorylation and Regulation of Adaptive Responses in Bacteria. *Microbiol. Rev.* **1989**, *53*, 450-490.

Tardat, B.; Touati, D. Iron and Oxygen Regulation of *Escherichia coli* MnSOD Expression: Competition between the Global Regulators Fur and ArcA for Binding to DNA. *Mol. Microbiol.* **1993**, *9*, 53-63.

Winston, S. E.; Fuller, S. A.; Hurrell, J. G. R. Western blotting. In *Current Protocols in Molecular Biology*; F. M. Ausubel, R. Brent, R. E. Kingston, D. D. Moore, J. G. Seidman, J. A. Smith, and K. Struhl (ed.), John Wiley & Sons, Inc., N.Y.; 1987; pp. 10.8.1-10.8.6.

5.8 Tables

Table 1. ***Escherichia coli*** **strains and plasmids**

Bacterium or plasmid	Relevant properties	Source or reference
Bacteria		
ECL942	Φ(P_{cyd}-*lac*) *bla*$^+$ *cyd*$^+$ *cyo*$^+$	Iuchi et al., 1990
ECL943	Φ(P_{cyd}-*lac*) *bla*$^+$ *cyd*$^+$ *cyo*$^+$ *arcA1 zij*::Tn*10*	Iuchi et al., 1990
ECL944	Φ(P_{cyd}-*lac*) *bla*$^+$ *cyd*$^+$ *cyo*$^+$ *arcB1 zgi*::Tn*10*	Iuchi et al., 1990
MC4100	F$^-$ *araD139* Δ(*argF-lac*) *U169 rpsL150 relA1 flb-5301 deoC1 ptsF25 rbsR*	R.P. Gunsalus
PC2	F$^-$ *araD139* Δ(*argF-lac*) *U169 rpsL150 relA1 flb-5301 deoC1 ptsF25 rbsR* Δ*fnr*	R.P. Gunsalus
Plasmids		
pMS421	pSC101 Spc^r *lacI*^{q}	Cold Spring Harbor Laboratory
pRED2	pUC19 Amp^r *vhb*	Khosla and Bailey, 1988b
pOX2	pBR322 Amp^r Φ(P_{vhb}-*cat*)	Hughes et al., 1989
pMSV1	pSC101 Spc^r *lacI*^{q} *vhb*	Kallio et al., 1994
pMSC1	pSC101 Spc^r *lacI*^{q} Φ(P_{vhb}-*cat*)	This study

Table 2. Plasmid copy number

Strain	Relative Copy No.*	Strain	Relative Copy No.*
MC4100:pMSV1	1.8	ECL942:pMSV1	1.0
PC2:pMSV1	1.8	ECL944:pMSV1	1.1
MC4100:pMSC1	1.5	ECL942:pMSC1	1.5
PC2:pMSC1	1.7	ECL944:pMSC1	1.0

* Method of plasmid copy number determination is described in Materials and Methods. Plasmid copy number per chromosomal equivalent of each strain remained relatively constant throughout the cultivation in a Six-fors bioreactor; therefore, the average number is reported. Plasmid copy number of each strain was normalized with that of ECL942:pMSV1. The error range of this assay is 20%.

5.9 Figures

Figure 1 A). The consensus DNA sequence of the Fnr binding site. The potential Fnr binding site was determined by comparing and locating the consensus nucleotides of the 5' non-coding region of genes which are regulated by Fnr (Spiro and Guest, 1990). The sequence for the Fnr binding site shown here is the collection of nucleotides found to be the most conserved from the sequence comparison. An inverted repeat element is shown here with arrows. B). A segment of the nucleotide sequence (Khosla and Bailey, 1989) of the oxygen-regulated promoter P_{vhb} is shown for comparison with the Fnr binding site. The homologous regions to the Fnr binding sequence are boxed. The arrow designated P2 corresponds to the second transcription start site in the *vhb* promoter. –30 denotes the nucleotide 30 bp upstream of the transcription start site P1.

Figure 2 The effect of *fnr* mutation on VHb synthesis. Western detection of VHb time trajectory of the *vhb* gene containing strains MC4100:pMSV1 (o) and PC2:pMSV1 (•) are reported as nmole of VHb per mg total protein. Dissolved oxygen concentration (DO) of MC4100:pMSV1 (– – –) and PC2:pMSV1 (———) are also shown. Growth conditions in Six-fors bioreactor and Western blotting are described in Materials and Methods.

Figure 3 The effect of *fnr* mutation on expression of $\Phi(P_{vhb}\text{-}cat)$. Specific CAT content (in μg CAT/mg total protein) of strains MC4100:pMSC1 (o) and PC2:pMSC1 (•), and DO profile of MC4100:pMSC1 (– – –) and PC2:pMSC1 (———) are shown at different time points during batch

cultivation. Growth conditions in Six-fors bioreactor and CAT assay are described in Materials and Methods.

Figure 4 The effect of *arcB* mutation on VHb synthesis. Western detection of VHb time trajectory of the *vhb* gene containing strains ECL942:pMSV1 (o) and ECL944:pMSV1 (•) are reported as nmole of VHb per mg total protein. Dissolved oxygen concentration (DO) of ECL942:pMSV1 (– – –) and ECL944:pMSV1 (——) are also shown. Growth conditions in Six-fors bioreactor and Western blotting are described in Materials and Methods.

Figure 5 The effect of *arcB* mutation on $\Phi(P_{vhb}\text{-}cat)$ expression. Specific CAT content (in µg CAT/mg total protein) of strains ECL942:pMSC1 (o), ECL944:pMSC1 (•), and DO profile of ECL942:pMSC1 (– – –) and ECL944:pMSC1 (——) are shown at different time points during batch cultivation. Growth conditions in Six-fors bioreactor and CAT assay are described in Materials and Methods.

Figure 6 The effect of VHb production on the expression of $\Phi(P_{cyd}\text{-}lac)$. ß-galactosidase level at different time points of cultivation for the fnr^+, $arcA^+B^+$ strain ECL942:pMS421 (o), the *vhb* expressing strain ECL942:pMSV1 (•), and the P_{vhb}-*cat* fusion strain ECL942:pMSC1 (Δ) are shown. Dissolved oxygen profiles in the NBS Bioflow III bioreactor for the three constructs were similar and thus only one is shown (——).

Figure 1

A

Consensus DNA sequence for Fnr binding:

B

Partial *vhb* promoter sequence:

Figure 2

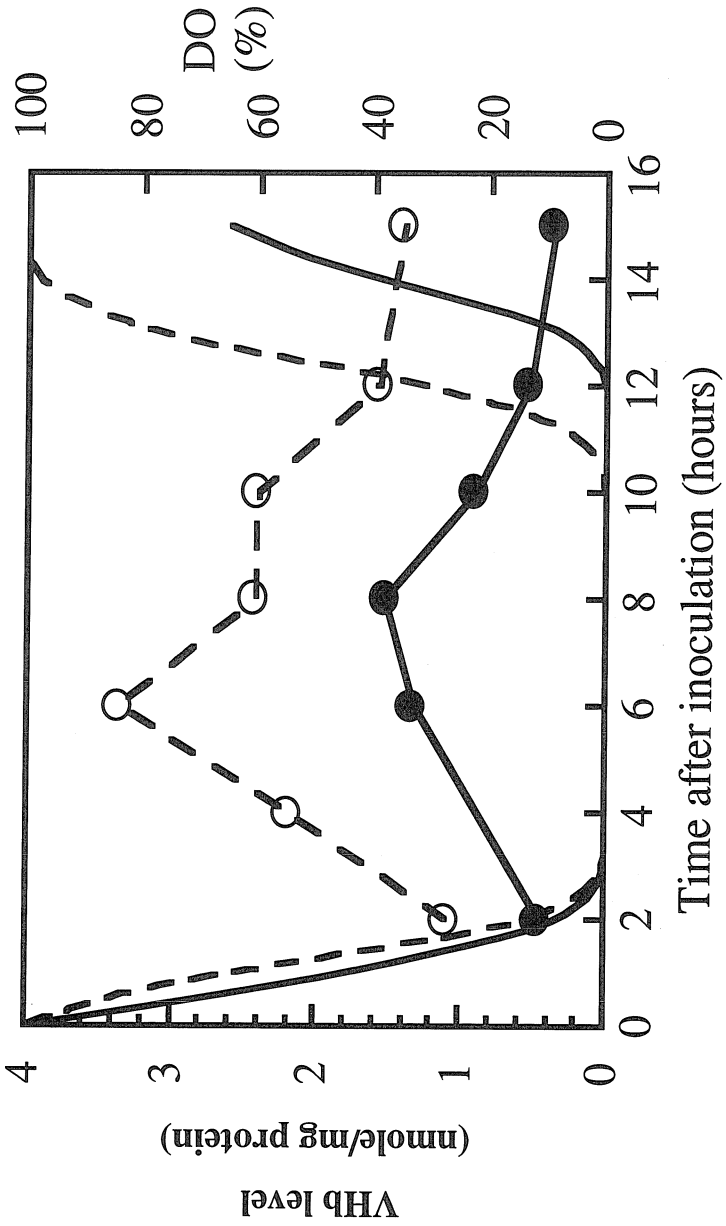
VHb level
(nmole/mg protein)
0
1
2
3
4
0
2
4
6
8
10
12
14
16
Time after inoculation (hours)
DO (%)
0
20
40
60
80
100

Figure 3

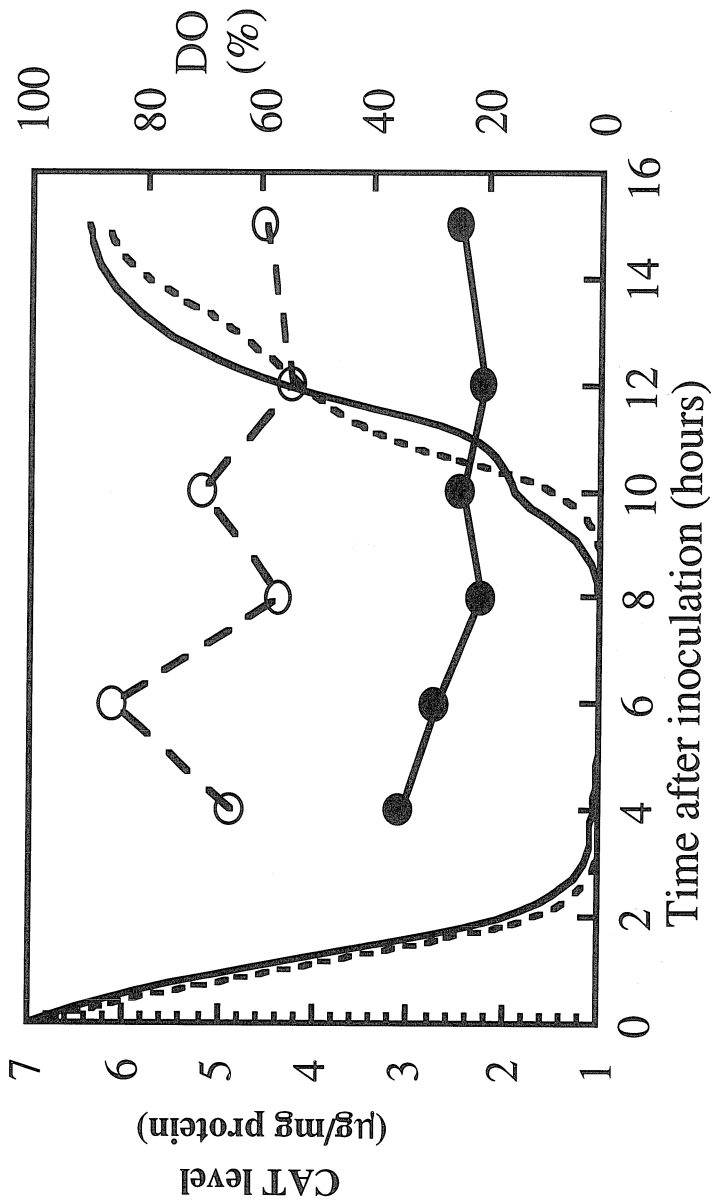
CAT level
(μg/mg protein)
7
6
5
4
3
2
1
DO (%)
100
80
60
40
20
0
0
2
4
6
8
10
12
14
16
Time after inoculation (hours)

Figure 4

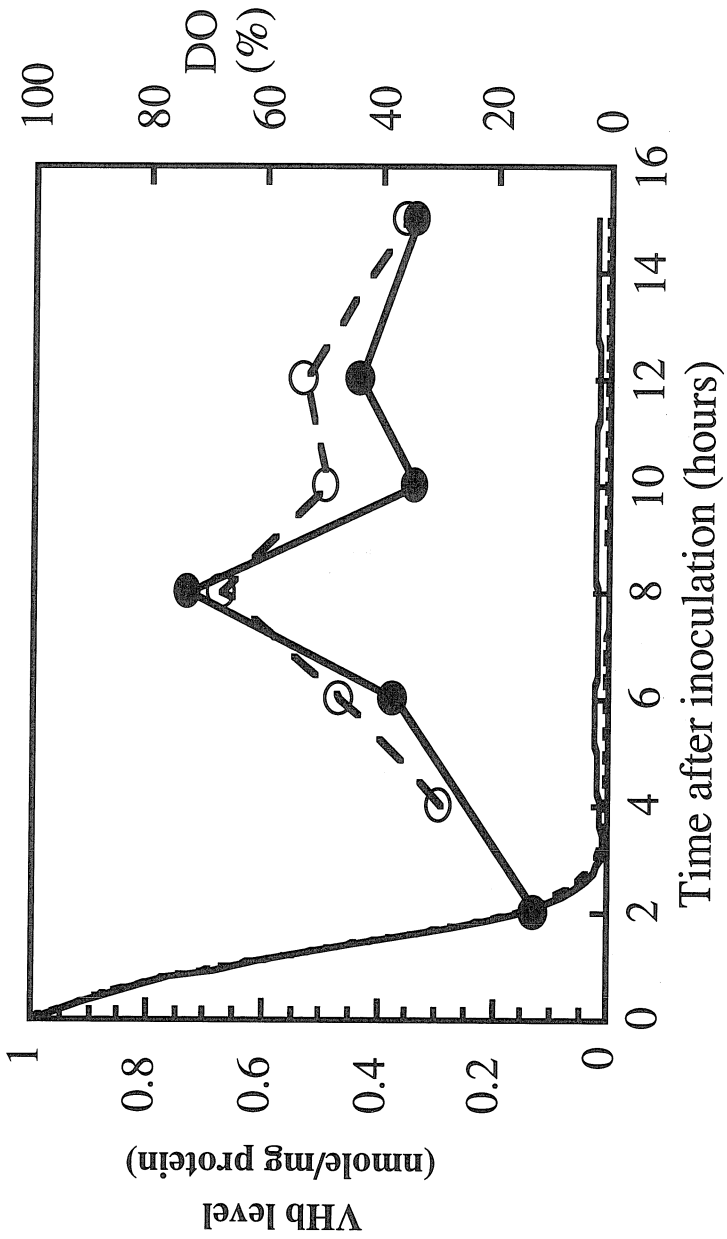
VHb level
(nmole/mg protein)
1
0.8
0.6
0.4
0.2
0
0
2
4
6
8
10
12
14
16
Time after inoculation (hours)
100
80
60
40
20
0
DO
(%)

Figure 5

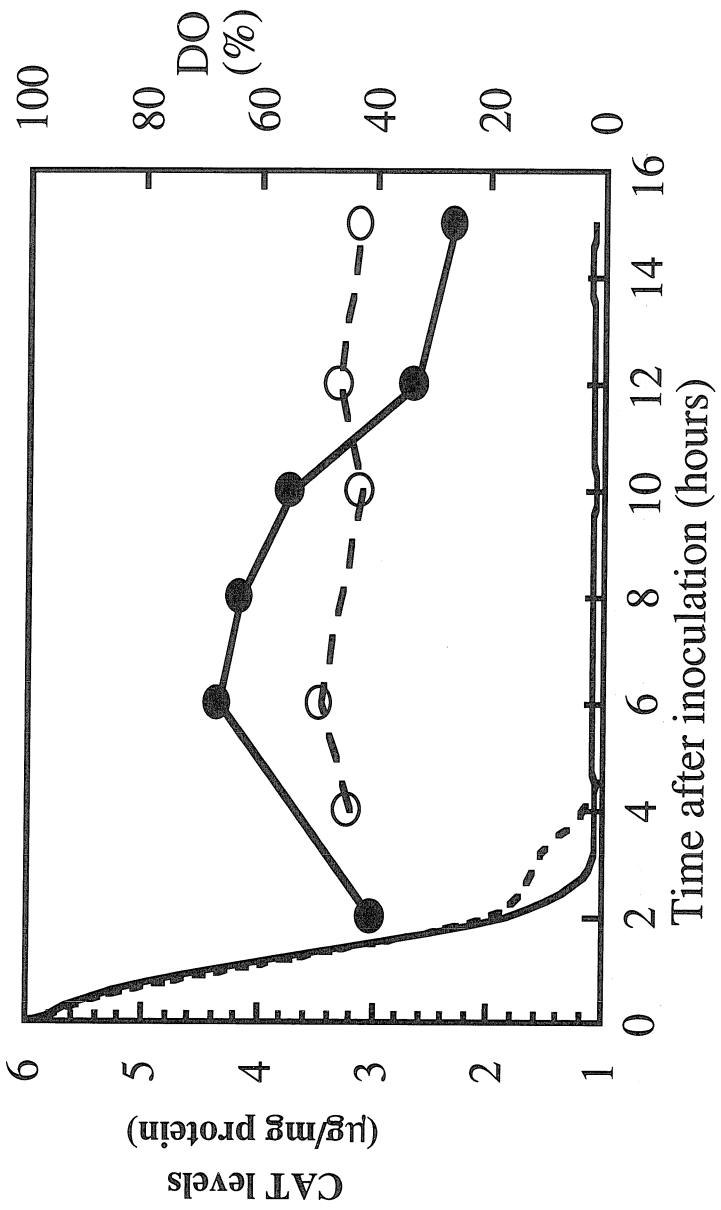
CAT levels
(μg/mg protein)
6
5
4
3
2
1
DO
(%)
100
80
60
40
20
0
0
2
4
6
8
10
12
14
16
Time after inoculation (hours)

Figure 6

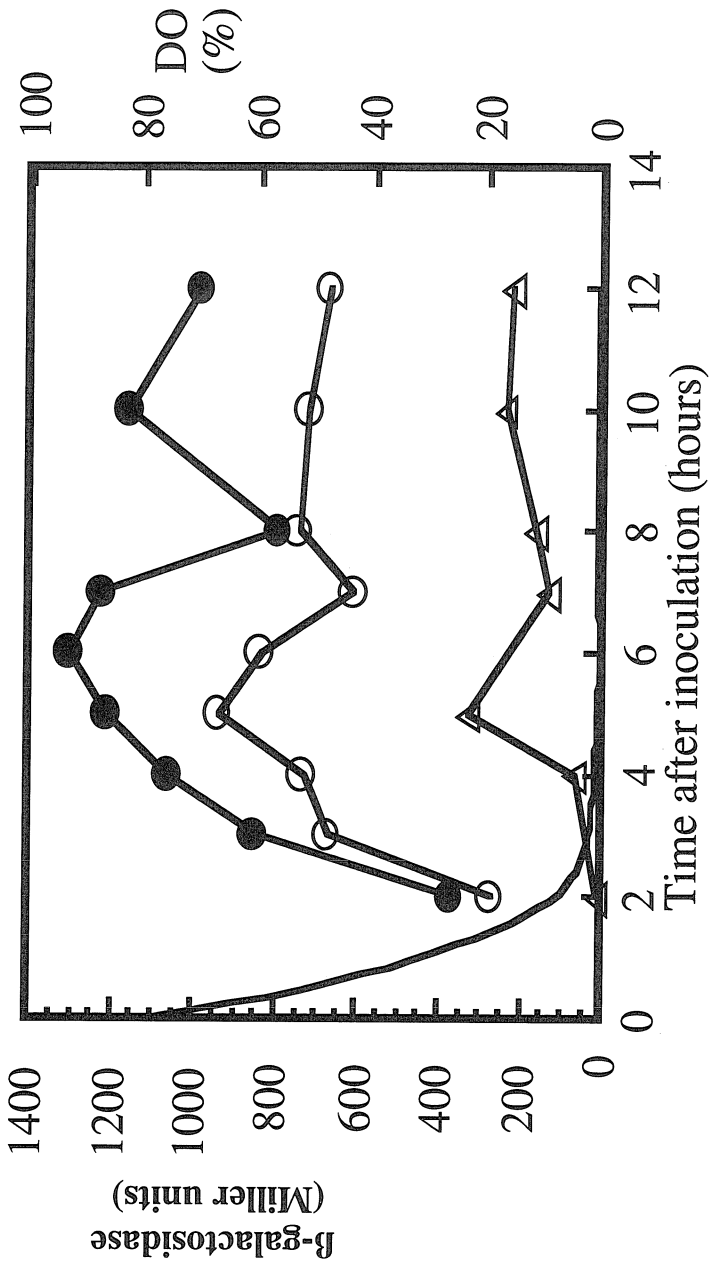
β-galactosidase
(Miller units)
0
200
400
600
800
1000
1200
1400
DO
(%)
0
20
40
60
80
100
0
2
4
6
8
10
12
14
Time after inoculation (hours)

CHAPTER 6:

Vitreoscilla Hemoglobin Dosage and Physiological Response of *Escherichia coli*

Source: Tsai, P. S.; Bailey, J. E. Effect of *Vitreoscilla* hemoglobin dosage on microaerobic *Escherichia coli* carbon and energy metabolism. 1995. Submitted to *Biotechnology and Bioengineering*.

6.1 Summary

The amount of *Vitreoscilla* hemoglobin (VHb) expression was modulated over a broad range with an IPTG-inducible plasmid, and the consequences on microaerobic *Escherichia coli* physiology were examined in glucose fed-batch cultivations. The effect of VHb dosage on growth under oxygen–limited conditions was most visible during late fed-batch phase where the final cell density increased initially linearly with increasing VHb concentrations, ultimately saturating at a 2.7–fold increase over the VHb–negative (VHb^-) control. During the same growth phase, excretion of fermentation by-products, acetate, ethanol, formate, lactate, and succinate from the culture expressing the highest amount of VHb were reduced by 25%, 49%, 68%, 72%, and 50%, respectively, relative to the VHb^- control. During exponential growth phase, VHb exerted a positive but smaller control on growth rate, growth yield and respiration. Varying the amount of VHb from 0 to 3.8 μmol/g dry cell weight (DCW) increased the specific growth rate, the growth yield and the oxygen consumption rate by 33%, 35% and 60%, respectively. Increasing VHb concentration to 3.8 μmol/g DCW suppressed the rate of carbon dioxide evolution in the exponential phase by 30%. A metabolic flux distribution analysis incorporating data from these cultivations discloses that VHb^+ cells direct a larger fraction of glucose towards the pentose phosphate pathway and a smaller fraction of carbon through the tricarboxylic acid cycle from acetyl coenzyme A. The overall NADH flux balance indicates that VHb-expressing cells generate a net NAD^+ flux while the VHb^- cells yield a net NADH flux under the same growth conditions, and thus are under more reduced state. Flux distribution analysis also reveals that VHb^+ cells have a smaller ATP synthesis rate

from substrate level phosphorylation but a larger overall ATP production rate under microaerobic conditions.

Key words: *Vitreoscilla* hemoglobin, Flux distribution, Dose-response, Microaerobic metabolism.

6.2 Introduction

Escherichia coli (*E. coli*), a microbe capable of switching between multiple metabolic networks for energy generation, thrives on energetically most favorable pathways in a particular environment. When cells are grown aerobically with glucose as carbon and energy substrate, glucose is efficiently dissimilated into cellular materials. Metabolic energy is generated in the form of proton motive force across the cytoplasmic membrane with concomitant recycling of redox carriers using oxygen as an exogenous electron acceptor. In the absence of oxygen, energy synthesis depends on substrate-level phosphorylation, and redox reactions are balanced internally by discomposition of glucose into wasteful metabolites which are then excreted into the environment. The biochemistry and genetics of both aerobic and anaerobic pathways in *E. coli* are now well understood and characterized. Unfortunately, in most industrial bioprocesses involving *E. coli* or other microorganisms, problems arise mostly not with aerobiosis or anaerobiosis, but with microaerobiosis in which aspects of both respiration and fermentative metabolisms are active and rival for accomplishing energy synthesis and redox balance. During microaerobic conditions, environmental factors such as nonideal mixing result in fluctuations of culture dissolved oxygen tension (DO) between hypoxic and anoxic (Manfredini et al., 1983; Oosterhuis et al., 1984). Internally, global and specific oxygen regulation mechanisms

activate and repress key enzymes to prepare cells for aerobic or anaerobic survival (Spiro and Guest, 1991; Iuchi and Lin, 1991). Accordingly, the product pattern changes dramatically during microaerobiosis (Onken and Leifke, 1989).

It has been demonstrated, through genetic engineering, that intracellular expression of a bacterial hemoglobin from *Vitreoscilla* (VHb) into different hosts elicits *in vivo* effects of reduced oxygen starvation, improved cell growth and product formations (Khosla and Bailey, 1988; Khosravi et al., 1990; DeModena et al., 1993; Magnolo et al., 1991). Recent studies aimed at understanding the mechanism of VHb action indicate that VHb increases the number of protons extruded across the cytoplasmic membrane per oxygen atom reduced and enhances the ATPase–catalyzed ATP synthesis rate in microaerobic *E. coli* (Kallio et al., 1994; Chen and Bailey, 1994). Kallio et al. (1994) suggest that VHb improves the electron transport chain through a catalytic role in raising the activity of the terminal oxidase cytochrome *o*. Given the intricate interactions between respiratory and fermentative metabolisms under microaerobic conditions, a perturbed respiratory pathway could have an effect on central carbon metabolism and the flux distribution. Unfortunately, the effect of VHb on carbon metabolism as well as effect of VHb dosage on physiological responses are unknown for any of the organisms reported. Studying these consequences of VHb expression will enhance understanding of interactions of VHb with microaerobic physiology. This will expand the foundation of information useful in guiding future applications of VHb technology.

Models that predict intracellular flux distribution and its perturbation as a result of enzymatic or environmental manipulations have been developed and applied in different organisms in recent years (Galazzo and Bailey, 1990; Papoutsakis and Meyer, 1985). Straightforward yet informative methods such as stoichiometric flux

balancing analysis that demands knowledge only on biochemical stoichiometry, biosynthesis requirements, and a few measurable parameters find increasing applications in metabolic engineering (Holms, 1986; Stephanopoulos and Vallino, 1991; Varma and Palsson, 1994). Based on experimental data, this mass balancing method interprets the observed physiology by providing a quantitative analysis of flux distribution within the defined network of reactions.

In this work we addressed the two previously posed questions of 1) how microaerobic *E. coli* physiology responds to VHb dosage and 2) how VHb perturbs microaerobic *E. coli* carbon and energy flux distributions. We compared different growth parameters and by–product excretion patterns of six VHb-expressing *E. coli* cultures under oxygen–limited conditions. Using the gathered information a metabolic flux distribution model based on stoichiometric balancing of *E. coli* glucose metabolism was applied, and the effect of VHb on flux distribution was studied. Based on this information, the implications of VHb expression on microaerobic physiology and indications concerning the mechanism of VHb action were discussed.

6.3 Materials and Methods

6.3.1 Microorganism, Plasmid Construction, and Cultivation Conditions

The effects of different intracellular VHb concentrations on cell physiology was studied using *Escherichia coli* K-12, strain W3110 (Bachman, 1987) transformed with the IPTG-inducible VHb expression plasmid, pKTV1. Plasmid pKT1 was constructed by digesting pBR322 (Bolivar et al., 1977) with *Eco*RI and *Ssp*I, and

ligating with the 1.1 kb *Eco*RI-*Hind*III fragment [*Hind*III–digested fragment post-treated with DNA polymerase I large (Klenow) fragment (Promega Inc.)] containing the *lac* repressor gene, $lacI^q$, from pMJR1560 (Amersham International). Plasmid pKTV1 was then created by subcloning the 1.2 kb *Hind*III-*Sal*I fragment containing the *tac* promoter–*vhb* gene fusion from pINT1 (Khosla and Bailey, 1989) into the corresponding sites in pKT1. Different levels of VHb expression were achieved by varying doses of IPTG. Ampicillin (100 mg/L) was added to all W3110:pKTV1 cultivations for plasmid maintenance.

Seeding cultures for bioreactor cultivations were grown for 12 hr in 500 mL shake flasks containing 100 mL of buffered LB medium (10 g/L Bacto-tryptone, 5 g/L Bacto-yeast extract, 10 g/L NaCl, 3 g/L K_2HPO_4, 1 g/L KH_2PO_4, adjusted to pH 7) at 37°C and 250 rpm in a New Brunswick Scientific Innova 4000 shaker. Glucose fed-batch cultivations were performed in a Six fors bioreactor (Infors, AG) with working volume of 310 mL. Bioreactor cultivations were inoculated with 6.2 mL of seed culture, and process parameters were maintained at 37°C, pH 7 (adjusted with either 3 M NaOH or 3 M H_3PO_4), 400 rpm, and 0.4 v.v.m. (volume gas per volume liquid per minute) of air supply. Glucose defined batch medium consisted of 4 g/L glucose, 0.4 g/L $(NH_4)_2SO_4$, 4.35 g/L K_2HPO_4, 1.5 g/L KH_2PO_4, 1 mL/L trace metal mix (8.3 mM Na_2MoO_4, 7.6 mM $CuSO_4$, 8 mM H_3BO_3), 1 mL/L vitamin mix (0.042% riboflavin, 0.54% panthothenic acid, 0.6% niacin, 0.14% pyridoxin, 0.006% biotin, 0.004% folic acid), 1 mM $MgSO_4$, 0.05 mM $CaCl_2$, 0.2 mM $FeCl_3$, and 100 mg/L ampicillin. Induction of VHb was achieved by adding the indicated concentration of IPTG to the culture when dissolved oxygen (DO) dropped below 5% of air saturation which generally occurred approximately 10 h post inoculation. The fed-batch mode was commenced with 1 mL/h of feed medium when the culture

reached an A_{600} of 1.5, and 2 mL/h when A_{600} reached 3.0. Thereafter the feeding was kept constant at 2 mL/h until the end of cultivation. Feed medium consisted of 250 g/L glucose, 110 g/L $(NH_4)_2SO_4$, 8 g/L $MgSO_4$, 1 mL/L vitamin mix, 1 mL/L trace metal mix, 0.05 mM $CaCl_2$, and 0.2 mM $FeCl_3$. DO was monitored with a pO_2 electrode (Ingold, Inc.) and exhaust gas (CO_2 and O_2) from the bioreactor was monitored using an emission monitor (Brüel & Kjaer, Emissions Monitor Type 3427). Samples for VHb, total protein and excreted metabolite measurements were taken periodically throughout cultivations and stored at –20°C until analysis.

6.3.2 Analytical Procedures

Metabolite analyses for formate, D-lactate, L-lactate, succinate, and pyruvate were performed enzymatically as described in Bergmeyer (1985a & b). Assays were performed at 37°C on a Beckman SYNCHRON CX5CE autoanalyzer by coupling reactions to NAD(P) and following changes in NAD(P)H at 340 nm ($\varepsilon_{NAD(P)H}$ = 6.22 cm^{-1} mM^{-1}). Biochemicals and enzymes were of analytical grade and were obtained from Boehringer Mannheim or Sigma. Acetate concentration was measured with a gas chromatograph (GC; Hewlett-Packard 5890 Series II with a flame ionization detector) with a Carbovac CW 20 M 0.25 (25 m x 0.25 mm) column. GC analysis was performed on a 3-ramp oven temperature program: the initial temperature was held at 70 °C for 1 min, then the temperature was raised 10°C/min to 95°C; thereafter the temperature was increased to 131°C with a rate of 40°C/min, and then to 190°C with a rate of 70°C/min where it was maintained for 4 min. The detector and the inlet temperatures were 300°C and 220°C, respectively; helium and nitrogen gas flow rates were 1 mL/min and 100 mL/min, respectively. 5 mM butyric acid was added as an internal standard to samples for acetate determination. Glucose and ethanol concentrations in culture medium were measured with GLU and ALC

assays (Beckman), respectively, using a Beckman SYNCHRON CX5CE autoanalyzer.

Samples for protein assay were prepared by resuspending harvested cells 1:1 in a sonication buffer (100 mM Tris pH 8, 50 mM NaCl, 1 mM EDTA pH 8). Cells were disrupted by sonication on ice in a sonifier (Branson Model 450) under continuous mode for 12 min at 100% output, followed by centrifugation at 4°C, 15,000 rpm in an Eppendorf centrifuge. Total soluble protein of the supernatant was determined from a M-TP assay (Beckman) using a Beckman SYNCHRON CX5CE autoanalyzer. For dry cell weight (DCW) determination, 10 mL of culture samples were centrifuged at 3,000 x *g* and washed once with phosphate buffer saline (8 g/L NaCl, 0.2 g/L KCl, 1.44 g/L Na_2HPO_4, 0.24 g/L KH_2PO_4, adjusted to pH 7). Wet pellets were dried in an 80°C oven for three days and then their weights were measured. DCW measurement has an error margin of 5%.

6.3.3 VHb Quantification

VHb activity was assayed by CO–reduced minus reduced difference absorption spectrophotometry using the monomer extinction coefficient ($\varepsilon_{419\ nm} - \varepsilon_{437\ nm}$) of 1.067×10^5 $(M\ cm)^{-1}$ for VHb (Hart and Bailey, 1991). VHb time–profiles of different IPTG inductions were monitored and quantified by Western blotting. 15% SDS/PAGE and the subsequent Western blotting were performed according to the method of Laemmli (1970) and the standard Western protocol (Winston et al., 1987), respectively, with rabbit anti-VHb antiserum (Cocalico Biologicals) and horseradish peroxidase-conjugated sheep IgG fraction to rabbit IgG (Cappel™, Organon Teknika Corp.). Using a Molecular Dynamics densitometer, the amount of VHb in each sample was estimated by comparing the intensity of its

Western blot negative with that of a hemoglobin standard (4.5 μM) prepared from *E. coli* JM101:pRED2 cell extract (Khosla and Bailey, 1988). Hemoglobin content was normalized with DCW and is reported as μmol/g DCW.

6.4 Results

6.4.1 Control Expression of VHb and Its Effect on Growth

Effect of VHb dosage on microaerobic cell physiology was studied with controlled expression of VHb from a medium copy number, *tac*–driven VHb expression plasmid pKTV1. A copy of the *lac* I^q gene was also subcloned on this plasmid to ensure an adequate basal level of repressor to prevent *vhb* transcription in the absence of inducer IPTG. Plasmid pKTV1 was transformed into *E. coli* wild type strain W3110 to obtain the recombinant strain W3110:pKTV1. Different levels of VHb synthesis were achieved by varying concentration of IPTG added to the culture in the range of 0 to 0.5 mM. To examine the effect of VHb dose under the most relevant physiological conditions, namely microaerobic growth, VHb synthesis was induced only when the culture DO dropped below 5% of air saturation. The maximal level of VHb, judged from antiserum binding to VHb on Western blots, was 3.8 μmol/g DCW after 31 h of fed-batch cultivation (Figure 1). This level of synthesis is comparable to VHb expression from a pUC–based, high copy-number plasmid such as pRED2 (Khosla and Bailey, 1988; result not shown). The data in Figure 1 disclose that accumulation of VHb increased with increasing concentration of IPTG, and no VHb was detected when no inducer was added.

Six different IPTG–induced, glucose fed–batch W3110:pKTV1 fermentations were performed to study the effect of VHb dosage on cell growth (Figure 2A). The air flow rate was purposely set low at 0.4 v.v.m. so that cultures became microaerobic (DO equal to or below 2% of air saturation) at the beginning of exponential growth. DO profiles of all cultivations were similar and therefore only one is shown in Figure 2A. After 40 h of growth, the cells with increasing VHb concentrations grew to higher densities than the uninduced, VHb-free cells (Figure 1). Although it has been demonstrated that the expression of VHb improves microaerobic cell growth (Khosla and Bailey, 1988; Khosla et al., 1990), these data show for the first time that the growth enhancement is proportional to VHb concentration up to a saturation level at a VHb concentration of 3.4 μmol/g DCW (Figure 2A). Beyond 3.4 μmol VHb/g DCW, no further increase in final cell density was observed (Figure 2B). The final cell density of the highest VHb-expressing culture was 2.7–fold of that of the uninduced, VHb-free culture. From Figure 2A it is apparent that VHb exerted the most notable effect on cell growth not during the exponential growth phase but during the late fed–batch phase. The specific growth rate of cells in the exponential phase, although also increased with increasing VHb concentrations, was raised only by 33% from 0.12 h^{-1} without VHb to 0.16 h^{-1} with 3.8 μmol VHb/g DCW (Table I). The specific glucose uptake rate remained similar with and without VHb, and thus the yield on glucose increased with increasing VHb concentrations (Table I). Similar growth patterns and effects of VHb dosage were observed when W3110:pKTV1 was cultivated in glycerol defined medium under identical conditions (results not shown).

6.4.2 Effect of VHb Levels on Respiration

The oxygen uptake (OUR, Q_{O_2}) and carbon dioxide evolution (CER, Q_{CO_2}) rates of cells in the exponential phase were calculated from exhaust gas measurements

and are summarized in Table I. Although these measurements have an estimated error of around 10%, results showed a significant 60% increase and a 30% decrease in OUR and CER, respectively, of the highest VHb expressing W3110:pKTV1 relative to the uninduced, VHb-free control. A closer examination of the data revealed that a small amount of VHb was sufficient to cause a 30% increase on the respiration rate of *E. coli* W3110:pKTV1; only 0.5 μmol VHb/g DCW raised OUR from 1.7 to 2.2 mmol O_2/g DCW/h. Overall, expression of VHb in the range studied exerted a positive effect on OUR and, to a lesser extend, a negative effect on CER of cells. As a consequence, increasing VHb decreased the RQ (ratio of CER and OUR). This result suggests that the presence of VHb may direct microaerobic *E. coli* to utilize more of its respiratory pathways and less of fermentative pathways.

6.4.3 Effect of VHb Levels on Extracellular Metabolite Concentration

The effect of VHb dosage on fermentative pathways of *E. coli* was studied by monitoring the production of several important fermentation by-products during cultivations. The use of an automated analyzer improved precision and reduced the uncertainty of assays to about 5 mg/L. Table II summarizes the specific metabolite production of the different IPTG–induced W3110:pKTV1 cultures measured after 31 h of growth. L-lactate concentrations of all cultures were very low and therefore only D-lactate concentrations are reported. Synthesis of VHb greatly reduced all of the measured metabolites excreted by cells relative to the uninduced, VHb-free control. VHb has the smallest effect on the repression of acetate production compared with the other metabolites. Increasing VHb concentrations decreased levels of acetate by a maximal 25% from 62.6 to 47.0 mmol/g DCW over the VHb concentrations tested. Expression of VHb had a strong negative effect on formate and D-lactate

concentrations as the presence of as little as 0.5 μmol VHb/g DCW drastically depressed the production of formate and D-lactate by 45% and 70%, respectively. Further increments of VHb reduced the excretion of formate and D-lactate to 68% and 72%, respectively, of the uninduced W3110:pKTV1 levels. Concentrations of ethanol and succinate were decreased monotonically with increasing VHb dosage; ethanol and succinate measured from cultures with 3.8 μmol VHb/g DCW were about 50% of those of the uninduced culture values. Extracellular pyruvate was only measurable toward the end of cultivation where a two to three–fold difference was observed between the uninduced, VHb-free and the VHb^+ cultures (Table II). Because of the small amount of pyruvate detected compared with other metabolites, extracellular pyruvate was excluded from further analyses (except for carbon balance, see below).

6.4.4 Carbon and Redox Balances

To examine whether all the carbon input was accounted for, a carbon balance analysis was performed on each cultivation after 31 h of cell growth. When cells are grown in minimal media with glucose as the carbon and energy source, the incoming substrate can be recovered in the form of biomass, by–products, and carbon dioxide. Table III shows the distribution of glucose into recovered biomass, excreted metabolites, and evolved CO_2 (from exhaust gas measurement) in mmol of carbon. Based on cell composition reported by Neidhardt (1987), the cellular carbon content of *E. coli* grown in minimal media can be calculated as 39.8 mmol carbon per g DCW. After summing the glucose input over 31 h of cultivation and multiplying the biomass and metabolite concentrations (in Table II) by their respective carbon contents, the extents of carbon recovery of all W3110:pKTV1 cultures were found to be 93% or higher of the total carbon input.

A redox, or electron, balance was also performed as a consistency check for the carbon balance and, in addition, to cross–examine the accuracy of our CER measurement since it potentially carries the largest error (10%) of all assays reported in this study. For the electron balance, the net metabolic reactions of cells grown on glucose as the sole substrate can be expressed in mmol carbon as follows:

$$x \cdot C_6H_{12}O_6 + y \cdot O_2 \rightarrow z \cdot C_{biomass} + w \cdot CO_2 + \sum v_i \cdot C_{i_{metabolite}} \qquad (1)$$

where x, y, z, w, and v_i are the oxidation numbers of glucose, oxygen, biomass, CO_2 and metabolites, respectively. The average oxidation state of cellular carbon (z) was estimated to be –0.20 based on the oxidation of nitrogen and the reduction of sulfur that occur in cells grown in minimal media containing NH_4^+ and SO_4^{2-} (Jensen and Michelsen, 1992). Using the method described in Neidhardt et al. (1990), the other oxidation numbers were calculated to be: x, 0; y, –4; w, +4; $v_{acetate}$, 0; $v_{ethanol}$, –2; $v_{formate}$, 1; $v_{succinate}$, 1; $v_{lactate}$, 0. The amount of oxygen consumed (in mmol) was determined from exhaust gas measurement. The theoretical CO_2 production was calculated from Equation 1 and compared with CO_2 evolution from exhaust gas measurement (Table III). Analysis showed that all CERs calculated from the redox balance of the different IPTG–induced cultures, except one, were within 93% or higher of the measured CO_2. Results of carbon and redox balances indicate that our CER measurements were accurate and that our findings of improved growth yield and suppressed by–product excretion by VHb of microaerobic *E. coli* are correct.

6.4.5 Effect of VHb Levels on Metabolic Flux Distribution

Reduction of by–product formation indicates altered carbon metabolism. To gain insight on the effect of VHb on the flux distribution within central carbon

metabolism, a metabolic flux analysis was performed on these cultures. The theory behind such analysis has been described extensively elsewhere (Holms, 1986; Varma et al., 1993; Vallino and Stephanopoulos, 1990 and 1993); therefore, only the principle will be summarized below. Metabolic flux analysis enables one to estimate the carbon flow through metabolic pathways by solving mass balances on pertinent precursor metabolites. To construct a suitable metabolic map for flux distribution elucidation, the biochemistry of the metabolic reactions is first systematically incorporated. Then a metabolic quasi-steady state (QSS), in which the sum of the fluxes involved in the formation and degradation of a metabolite equals zero, is assumed (see Vallino and Stephanopoulos (1993) for a discussion of the validity of this assumption in this context). The metabolic flux distribution within the network is then calculated from the following system of equations:

$$S \cdot v = b \tag{2}$$

where S is a matrix consisting of stoichiometric coefficients from the metabolic map, v is a vector of unknown metabolic fluxes, and b is a vector of known fluxes for measurable metabolite synthesis and for biomass formation.

In our analysis, the reaction network was constructed primarily from established biochemistry in literature (Gottschalk, 1987); included in this network were fluxes that lead to and depart from precursor metabolites that appear in the glycolytic pathway, the pentose phosphate pathway, and the tricarboxylic acid (TCA) cycle. In addition, the anaplerotic reaction catalyzed by phosphoenolpyruvate carboxylase for the conversion of phosphoenolpyruvate to oxaloacetate and the reaction catalyzed by pyruvate-formate lyase for the conversion of pyruvate to formate were included in the network of reactions. Fluxes leading to precursors for

heme biosynthesis (to account for VHb) were insignificant (in μmol/g DCW/h) compared to typical catabolic fluxes (in mmol/g DCW/h) and were not included. The extra protein synthesis capacity needed for VHb expression was lumped into precursor metabolite fluxes to biosynthesis. NADPH was included in the mass balance to make the rank of S equal to the rank of v, or the number of linear-independent equations equal to the number of unknown fluxes. Fluxes for NADH and ATP generation, which are coupled with the reaction network, were calculated after Equation 2 was solved. The Appendix presents the set of 14 mass balance equations from which S, v, and b were constructed and a metabolic map which details the location of all the reactions.

The effect of VHb dosage on *E. coli* carbon flux distribution was analyzed using parameters measured during the late exponential growth phase (between the 13th and the 19th h) of the six glucose fed-batch cultivations (Figure 2A). Flux to biosynthesis from each precursor metabolite was derived by multiplying the specific growth rate of cells by the molar requirement of each precursor for synthesis of 1 g biomass (Neidhardt et al., 1990). Fluxes to extracellular metabolite excretions were obtained by dividing the rate of metabolite accumulation by the cell density. Metabolite fluxes are expressed in mmol/g DCW/h and listed in Table IV. Similar to our findings in the late fed–batch phase of cultivation, VHb has a negative effect on by–product formation during the exponential phase, although by a smaller magnitude than that during the late fed–batch phase (Table II). Increasing VHb concentrations monotonically decreased the accumulation rates of all but one metabolite, from a maximal reduction of 35% in ethanol and succinate to 25% in formate and lactate. VHb did not appear to affect acetate flux during exponential phase since acetate accumulation rates of different cultures fluctuated around a mean. Table IV also

shows that at least 95% of the carbon influx was recovered in the form of biomass, CO_2 and by–product fluxes from all six cultivations.

The flux distributions of the uninduced, VHb-free control and the highest VHb-expressing cultures normalized to a same glucose consumption rate of 2.5 mmol/g DCW/h are presented in Figure 3. A first inspection of these flux distributions confirms the biochemical and thermodynamic reasonability of the model, since no irreversible reactions exhibit negative fluxes. Our model also indicates that the conversion of pyruvate to acetyl coenzyme A is catalyzed mainly by pyruvate–formate lyase and not by pyruvate dehydrogenase. The calculated pyruvate dehydrogenase–catalyzed flux were very small values which are negligible compared to the major fluxes in the network.

Examination of the overall flux distributions revealed two dramatic differences between the control and the VHb-expressing cultures. In the presence of VHb, fluxes through the pentose phosphate pathway are increased and, as a result, fluxes through the Embden–Meyerhof–Parnas pathway are decreased. Fluxes entering the TCA cycle are also decreased with VHb expression. Comparing the two cases shown in Figure 3, the percentage of glucose that enters the pentose phosphate pathway, calculated by dividing f_1 by the sum of $f_{glucose}$, f_3 and f_6, is 15% for the uninduced W3110:pKTV1 culture and 38% for the induced culture. This increase is possibly due to an increased demand for NADPH of VHb^+ cells as consequences of increased biosynthesis and decreased TCA flux.

The effect of VHb on fluxes leading to the TCA cycle can be studied by examining changes in the split–ratios of carbon flux at important branch points, or nodes (Stephanopoulos and Vallino, 1991). The OAA–branch split–ratio at the PEP

node, calculated by taking the ratio of f_{11} and f_9 (Figure 3), are 12% and 14% for the uninduced VHb-free control and the highest VHb dose cells, respectively. The IsoCit–branch split–ratio at the AcCOA node, ratio of f_{12} and $f_{formate}$, is 37% for the control and 17% for the VHb^+ cells.

To check whether VHb dosage exerts a trend on the flexibility of the PEP and AcCOA nodes, we compared the split–ratios of these nodes under different VHb expression levels. Table V and VI present the flux distributions and the split–ratios at the PEP and AcCOA nodes, respectively, for the six cultivations. The location of each flux can be found in Figure 3. Results show that the node at PEP is rigid with respect to VHb concentration; the OAA–branch split–ratio at PEP remains relatively unaffected between 12% and 14%. The node at AcCOA, on the other hand, is flexible under high VHb concentrations. The IsoCit–branch split–ratio at AcCOA stays high around 35% with increasing VHb levels up to 2.3 μmol/g DCW, but the ratio drops to 21% and 17% with 3.4 μmol/ g DCW and 3.8 μmol/g DCW of VHb, respectively. This analysis suggests that attempts to modify enzymatic activities at PEP are unlikely to bring changes in the fraction of carbon channeled to the TCA cycle at any VHb concentration. In contrast, the AcCOA node, which is flexible at high VHb levels, might be explored for possibilities of enzymatic modifications if a changed TCA flux is desired. Table VI also indicates that the fraction of fluxes to the pentose phosphate pathway increases with increasing VHb concentration from 22% with 0.5 μmol VHb/g DCW to 38% with 3.8 μmol VHb/g DCW.

Flux distribution analysis shows that the net NADH flux ($f_{NADH\ net}$) from the reaction network considered, which does not include the respiratory pathway, is higher in uninduced, VHb-free cells than in VHb-containing cells (5.96 vs. 4.41 mmol/g DCW/h; in Figure 3). This indicates that cells are already less reduced in the

presence of VHb without considering contributions from the respiratory chain. Taking respiration into account, with VHb^+ cells consuming oxygen faster with coupled oxidation of NADH, VHb has an even larger effect on the redox state of cells. Cells that do not produce VHb have an overall NADH flux ($f_{NADH\ overall}$) of 2.58 mmol/g DCW/h while those synthesizing 3.8 μmol VHb/g DCW have an overall NAD^+ flux of 1.03 mmol/g DCW/h. Other concentrations of VHb also result in a negative relationship with the net ($f_{NADH\ net}$) and overall ($f_{NADH\ overall}$) NADH fluxes (Table V). Unexpectedly, cells synthesizing 2.3 μmol/g DCW of VHb or more do not produce enough ATP from substrate level phosphorylation to support growth, as indicated by the negative fluxes ($f_{ATP\ net}$) for three of the higher VHb–dose cultures (Table V). However, the ATP synthesis rate from oxidative phosphorylation, calculated from the oxygen consumption rate and assuming a P/O ratio of 2, is more than enough to compensate for this deficiency. Cells with VHb afford on the average an overall (reaction network plus respiration) ATP flux ($f_{ATP\ overall}$) of 9.5 mmol/g DCW/hr, 20% higher than that of the control (Table V). The calculated values for $f_{ATP\ overall}$ may seem high, but we did not consider in the analysis futile cycles and slippage or leakage of protons from the cytoplasmic membrane which might very well claim a large portion of the estimated overall ATP fluxes.

6.5 Discussion

In this study we have demonstrated that, by modulating the synthesis of VHb over a wide range from zero to a level comparable to expression from high copy number plasmids, cell growth was improved and by–product excretion was reduced with increasing VHb concentrations. Saturation of growth improvement due to VHb

was readily observed from VHb concentration profiles of final cell density and specific oxygen consumption rate, which show that beyond 3.4 μmol VHb/g DCW, only marginal enhancements of these qualities were obtained. A metabolic distribution analysis revealed increasing VHb expression changed flux patterns to the pentose phosphate, TCA, NADH, and ATP pathways.

Alleviating oxygen limitation has been a prime interest of research for bioprocesses involving high density growth of aerobic cultures (Delacruz et al., 1992; O'Connor et al., 1992; Konstantinov et al., 1991). Shortage of oxygen not only reduces the rate of an efficient oxidative energy generation pathway, but also promotes undesirable by–product formation, thus slowing down cell growth and diminishing growth yield. The finding that VHb decreases *E. coli* by–product formation has implication for the oxidation–reduction and energetic state of cells under microaerobic conditions. Indeed, fermentative pathways for production of reduced metabolites are coupled with synthesis of ATP and/or oxidation of reducing equivalent NADH. Formation of ethanol and succinate result in production of 2 mol of NAD^+ per mol of metabolite. Lactate fermentation recycles 1 NADH to NAD^+. Synthesis of acetate, although coupled to generation of 1 NADH, provides 1 molecule of ATP per molecule of acetate. The fact that *E. coli* grown under our experimental scheme produced large quantities of by–products indicates that cells were under heavily reduced conditions and were seeking a redox sink in the form of reduced metabolites. The observation that the presence of VHb greatly depressed the formation of ethanol and succinate by more than 50% relative to the control suggests that VHb^+ cells could regenerate somewhere else the reducing equivalents that would otherwise originate from by–product synthesis. In fact, our metabolic flux distribution analysis showed that VHb^+ cells are already under a less reduced state by affording a

smaller NADH flux from central carbon metabolism, even though they synthesize less of reduced metabolites. Taking into account NADH turnover by respiration, uninduced VHb-free cells yield an even higher NADH flux than that of VHb^+ cells. This is similar to our previous observation from culture fluorescence measurement of cells subjected to diminishing oxygen transients (Tsai et al., 1995).

A decrease in acetate excretion and an increase in growth yield on glucose from VHb-expressing *E. coli* imply that cells are more competent in providing ATP in the presence of VHb, possibly through a more active and/or efficient oxidative phosphorylation pathway. Our metabolic flux analysis indicates that VHb-producing cells do not synthesize enough ATP from substrate level phosphorylation but rely on the oxidative phosphorylation pathway as a major contributor in energy synthesis. With a more active respiratory pathway, VHb producers can support a higher ATP synthesis rate. This analysis is consistent with an NMR study which demonstrated a 30% increase in net ATP synthesis rate for the VHb-expressing *E. coli* over its isogenic control (Chen and Bailey, 1994).

Judging from the growth patterns (Figure 2A), VHb appears to play a role in prolonging cell growth during oxygen–limited conditions. Without VHb, cells ceased to grow after the end of exponential phase. The higher the VHb concentration, the longer the growth was sustained. Cells with the highest VHb concentration continued to grow beyond the endpoint of investigation. Suppressed by–product synthesis and enhanced respiration observed in VHb-expressing cells resemble characteristics of cells growing under elevated DO tensions. Our experimental data suggests that the degree of "oxygenation" in VHb-expressing cultures increases with increasing VHb concentrations until a saturation level is attained. In a metabolic performance optimization study in which the flux distributions under different dissolved oxygen

tensions were computed with the objective of optimal growth rate, Varma et al. (1993) showed that the percentage of glucose entering the pentose phosphate pathway increases with increasing oxygenation rates, from 2% under anaerobic conditions, to 15% with 7 mmol O_2/g DCW/h, and to 45% with 12 mmol O_2/g DCW/h. Coincidentally, our metabolic distribution analysis also reveals a more active pentose phosphate pathway under increasing VHb concentrations. A proposed mechanism of VHb action in enhancing intracellular effective dissolved oxygen tension by providing additional oxygen to the terminal oxidases of *E. coli* has been discussed elsewhere (Kallio et al., 1994).

The finding of VHb perturbs the flux distribution of central carbon metabolism in addition to the previously reported enhancements in microaerobic respiratory pathway suggests new perspectives for the application of VHb. The pentose phosphate pathway is important not only for its function in generation of NADPH as reducing agent for biosynthesis but also in production of precursors for aromatic amino acid synthesis. An increase in the flow of carbon through the pentose phosphate pathway by VHb might affect key enzymes and enhance synthesis of aromatic amino acids. In contrast, the predicted decrease in fluxes through oxaloacetate and a–ketoglutarate, which serve as precursor metabolites for 10 amino acids, may discourage cloning of VHb for the sole purpose of improving yields of TCA cycle–derived amino acids.

6.6 Acknowledgments

This research was supported by the Swiss Priority Program in Biotechnology. P.T. is grateful to V. Hatzimanikatis for his assistance on flux distribution analysis.

6.7 Appendix

This appendix contains the mass balances and the flux distribution map used to construct the metabolic network of *E. coli* W3110:pKTV1.

Metabolite Flux Vector

Fluxes were determined by solving the 14 x 14 matrix consisting of mass balances around the following metabolites. Location of each flux can be found in the accompanying metabolic map. Fluxes with numeral subscripts denote unknown fluxes, and fluxes with letter subscripts denote either measurable fluxes or biosynthesis fluxes calculated from the biomass synthesis requirements of each precursor metabolite.

1. NADPH: $2f_1 + f_{13} = f_{biosyn/nadp}$
2. Glc6-P: $f_a - f_b - f_2 - f_1 = 0$
3. Ribu5P : $f_1 - f_5 - f_4 = 0$
4. Xyl5P: $f_4 + f_3 - f_6 = 0$
5. Rib5P: $f_5 - f_q - f_6 = 0$
6. Fru6P: $f_2 - f_c - f_7 - f_3 + f_6 = 0$
7. T3P: $2f_7 - f_d - f_8 - f_3 + f_6 - f_6 = 0$
8. E4P: $f_3 + f_6 - f_p = 0$
9. 3PG: $f_8 - f_e - f_9 = 0$

10. PEP: $f_9 - f_f - f_{11} - f_a - f_{10} = 0$

11. Pyr: $f_{10} - f_g + f_a - f_{12} - f_k - f_l = 0$

12. AcCOA: $f_{12} - f_h - f_i - f_j + f_k - f_{13} = 0$

13. OAA: $f_{11} + f_{14} - f_{13} - f_m - f_n = 0$

14. aKG: $f_{13} - f_o - f_{14} = 0$

NADH: $f_8 + 2f_{14} - f_l - 2f_m - 2f_j - f_{biosyn/nadh} = f_{NADHnet}$

ATP: $f_8 + f_{10} - f_a - f_7 + f_i + f_{14} - f_{biosyn/atp} = f_{ATPnet}$

Abbreviations: Glc6P, glucose-6-phosphate; Ribu5P, ribulose-5-phosphate; Xyl5P, xylulose-5-phosphate; Rib5P, ribose-5-phosphate; Fru6P, fructose-6-phosphate; T3P, triose-3-phosphate; E4P, Erythrose-4-phosphate; Sed7P, sedoheptulose–7–phosphate; 3PG, 3-phosphoglycerate; PEP, phosphoenolpyruvate; Pyr, pyruvate; AcCOA, acetyl coenzyme A; OAA, oxaloacetate; aKG, a-ketoglutarate; IsoCit, isocitrate; Suc, succinate; Form, formate; ETOH, ethanol; Acet, acetate; Lac, lactate.

Flux Distribution Map

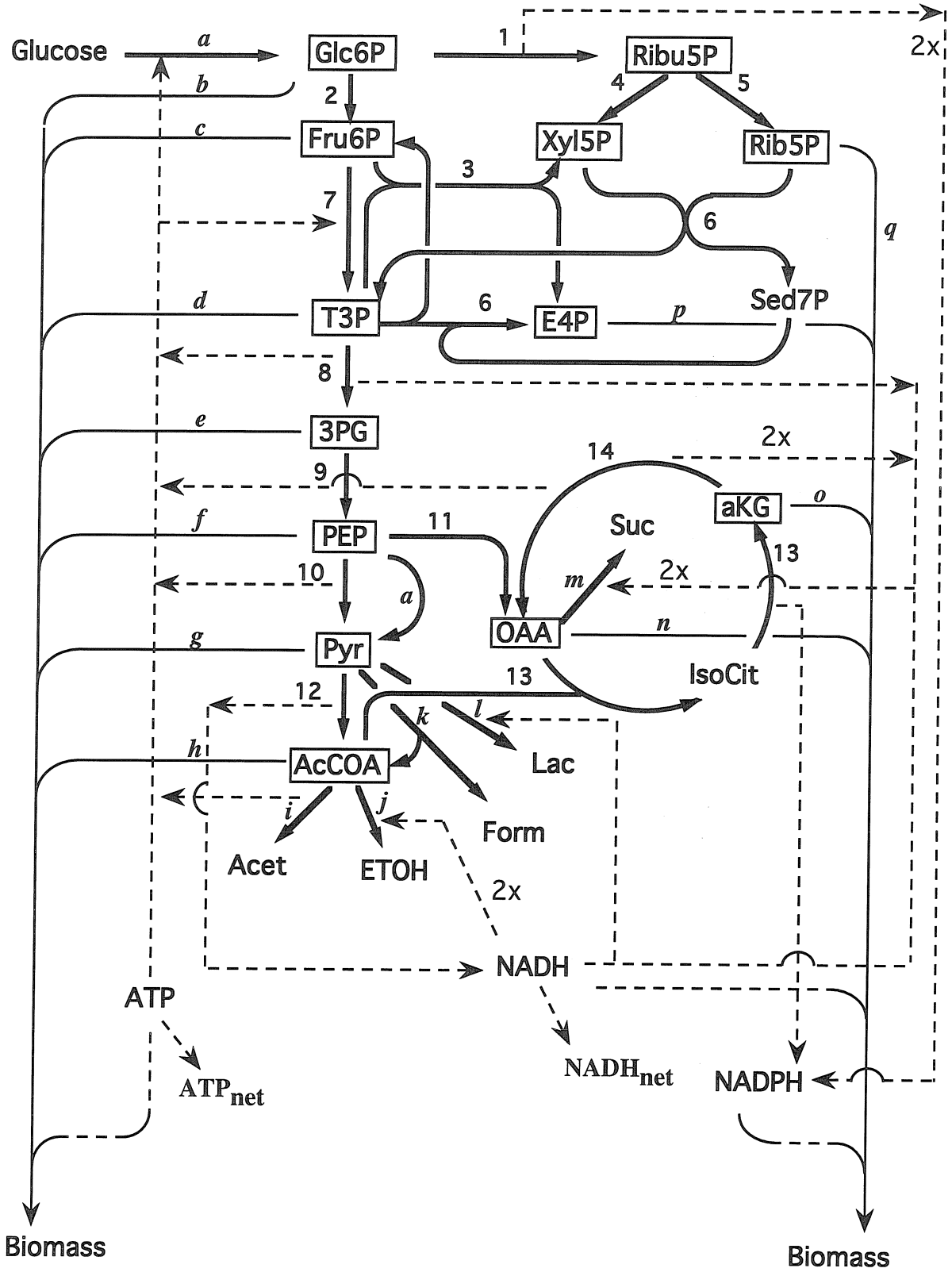

6.8 References

Bachmann, B. J. 1987. Derivations and genotypes of some mutant derivatives of *Escherichia coli* K-12. p. 1191-1219, In: J. L. Ingraham, K. B. Low, B. Magasanik, M. Schaechter, and H. E. Umbarger (eds.), *Escherichia coli* and *Salmonella typhimurium*: cellular and molecular biology. American Society for Microbiology, Washington, D.C.

Bergmeyer, H. U. 1985a. In: Methods of enzymatic analysis, vol. VI, VCH Publishers, Deerfield Beach, FL.

Bergmeyer, H. U. 1985b. In: Methods of enzymatic analysis, vol. VII, VCH Publishers, Deerfield Beach, FL.

Bolivar, F., Rodriguez, R. L., Greene, P J., Betlach, M. C., Heyneker, H. L., Boyer, H. W., Crosa, J. H., Falkow, S. 1977. Construction and characterization of new cloning vehicles. II. A multipurpose cloning system. Gene **2**: 95-113.

Chen, R., Bailey, J. E. 1994. Energetic effect of *Vitreoscilla* hemoglobin expression in *Escherichia coli*: An on-line ^{31}P NMR and saturation transfer study. Biotechnol. Prog. **10**: 360-364.

Delacruz, N., Payne, G. F., Smith, J. M., Coppella, S. J. 1992. Bioprocess development to improve foreign protein production from recombinant *Streptomyces*. Biotechnol. Biotech. **8**: 307-315.

DeModena, J. A., Gutierrez, S., Velasco, J., Fernandez, F. J., Fachini, R. A., Galazzo, J. L., Hughes, D. E., Martin, J. F. 1993. The production of

cephalosporin C by *Acremonium chrysogenum* is improved by the intracellular expression of a bacterial hemoglobin. Bio/Technol. **11**: 926-929.

Galazzo, J., Bailey, J. E. 1990. Fermentation pathway kinetics and metabolic flux control in suspended and immobilized *Saccharomyces cerevisiae*. Enz. Microb. Technol. **12**: 162-172.

Gottschalk, G. 1986. Bacterial metabolism. 2nd edition. Springer–Verlag, New York.

Hart, R. A., Bailey, J. E. 1991. Purification and aqueous 2-phase partitioning properties of recombinant *Vitreoscilla* hemoglobin. Enz. Microb. Technol. **13**: 788-795.

Holms, W. H. 1986. The central metabolic pathways of *Escherichia coli*: Relationship between flux and control at a branch point, efficiency of conversion to biomass, and excretion of acetate, pp. 69–105. In: Current topics in cellular regulation, vol. 28. Academic Press, Inc.

Iuchi, S., Lin, E. C. C. 1991. Adaptation of *Escherichia coli* to respiratory conditions: Regulation of gene expression. Cell **66**: 5-7.

Jensen, P. R., Michelsen, O. 1992. Carbon and energy metabolism of *atp* mutants of *Escherichia coli*. J. Bacteriol. **174**:7635-7641.

Kallio, P. T., Kim, D. J., Tsai, P. S., Bailey, J. E. 1994. Intracellular expression of *Vitreoscilla* hemoglobin alters *Escherichia coli* energy metabolism under oxygen-limited conditions. Eur. J. Biochem. **219**: 201-208.

Khosla, C., Bailey, J. E. 1988. Heterologous expression of a bacterial haemoglobin improves the growth properties of recombinant *Escherichia coli*. Nature **331**: 633-635.

Khosla, C., Bailey, J. E. 1989. Evidence for partial export of *Vitreoscilla* hemoglobin into the periplasmic space in *Escherichia coli*. J. Mol. Biol. **210**: 79-90.

Khosla, C., Curtis, J. E., DeModena, J., Rinas, R., Bailey, J. E. 1990. Expression of intracellular hemoglobin improves protein synthesis in oxygen-limited *Escherichia coli*. Bio/Technol. **8**: 849-853.

Khosravi, M., Webster, D. A., Stark, B. C. 1990. Presence of bacterial hemoglobin gene improves a-amylase production of a recombinant *Escherichia coli* strain. Plasmid **24**: 190-194.

Konstantinov, K. B., Nishio, N., Seki, T., Yoshida, T. 1991. Physiologically motivated strategies for control of the fed-batch cultivation of recombinant *Escherichia coli* for phenylalanine production. J. Ferm. Bioeng. **71**: 350-355.

Laemmli, U. K. 1970. Cleavage of structural proteins during the assembly of the head of bacteriophage T4. Nature **227**: 680-685.

Magnolo, S. K., Leenutaphong, D. L., DeModena, J. A., Curtis, J. E., Bailey, J. E., Galazzo, J. L., Hughes, D. E. 1991. Actinorhodin production by *Streptomyces coelicolor* and growth of *Streptomyces lividans* are improved by the expression of a bacterial hemoglobin. Bio/Technol. **9**: 473-476.

Manfredini, R., Cavallera, V., Marini, L., Donati, G. 1983. Mixing and oxygen transfer in conventional stirred fermentors. Biotechnol. Bioeng. **25**: 3115-3131.

Neidhardt, F. 1987. Chemical composition of *Escherichia coli*, p. 4-6, In: J. L. Ingraham, K. B. Low, B. Magasanik, M. Schaechter, and H. E. Umbarger (eds.), *Escherichia coli* and *Salmonella typhimurium*: cellular and molecular biology. American Society for Microbiology, Washington, D.C.

Neidhardt, F. C., Ingraham, J. L., Schaechter, M. 1990. Biosynthesis and fueling, pp. 133-173. In: Physiology of the bacterial cell: A molecular approach. Sinauer Associates, Inc., Sunderland, Massachusetts.

O'Connor, G. M., Sanchezriera, F., Cooney, C, L. 1992. Design and evaluation of control strategies for high cell-density fermentations. Biotechnol. Biotech. **39**: 293-304.

Onken, U., Leifke, E. 1989. Effect of total and partial pressure (oxygen and carbon dioxide) on aerobic microbial processes. Adv. Biochem. Eng. Biotechnol. **40**: 137-169.

Oosterhuis, N. M. G., Kossen, N. W. F. 1984. Dissolved oxygen concentration profiles in a production scale bioreactor. Biotechnol. Bioeng. **26**: 546-555.

Papoutsakis, E. T., Meyer, C. L. 1985. Equations and calculations of product yields and preferred pathways for butanediol and mixed-acid fermentation. Biotechnol. Bioeng. **27**: 50-66.

Spiro, S., Guest, J. R. 1991. Adaptive responses to oxygen limitation in *Escherichia coli*. Trends in Biochem. Sci. **16**: 310-314.

Stephanopoulos, G., Vallino, J. J. 1991. Network rigidity and metabolic engineering in metabolite overproduction. Science **252**: 1675-1681.

Tsai, P. S., Rao, G., Bailey, J. E. Improvement of *Escherichia coli* microaerobic oxygen metabolism by *Vitreoscilla* hemoglobin: New insights from NAD(P)H fluorescence and culture redox potential. Accepted for publication in Biotechnol. Bioeng.

Vallino, J., Stephanopoulos, G. 1990. Flux determination in cellular bioreaction network: application to lysine fermentation, pp. 205-219. In: Frontiers in bioprocessing. CRC Press, Boca Raton, FL.

Vallino, J., Stephanopoulos, G. 1993. Metabolic flux distributions in *Corynebacterium glutamicum* during growth and lysine overproduction. Biotechnol. Bioeng. **41**:633-646.

Varma, A., Boesch, B., Palsson, B. O. 1993. Stoichiometric interpretation of *Escherichia coli* glucose catabolism under various oxygenation rates. Appl. Environ. Microbiol. **59**:2465-2473.

Varma, A., Palsson, B. O. 1994. Metabolic flux balancing: Basic concepts, scientific and practical use. Bio/Technol. **12**: 994-998.

Winston, S. E.; Fuller, S. A.; Hurrell, J. G. R. 1987. Western blotting, pp. 10.8.1-10.8.6. In: F. M. Ausubel, R. Brent, R. E. Kingston, D. D. Moore, J.

G. Seidman, J. A. Smith, and K. Struhl (ed.). Current Protocols in Molecular Biology. John Wiley & Sons, Inc., N.Y.

Table I. Effect of VHb levels on *E. coli* growth parameters (in exponential phase; 13th-19th h of cultivation)

VHb	μ	$Y_{x/gluc}$	Q_{gluc} [a]	Q_{O_2}	Q_{CO_2}	RQ [b]
μmol/g DCW	1/h	mol C / mol C	mmol / g DCW / h			
0	0.12	0.31	2.6	1.7	2.2	1.3
0.5	0.13	0.31	2.7	2.2	1.8	0.81
1.2	0.13	0.34	2.6	2.5	2.0	0.79
2.3	0.14	0.38	2.5	2.2	1.9	0.88
3.4	0.17	0.41	2.7	2.7	1.8	0.67
3.8	0.16	0.42	2.6	2.7	1.5	0.57

a Calculated from medium glucose concentration and feedings of 0.25 g/h after culture A_{600} reached 1.5 and 0.5 g/h after A_{600} reached 3.0.

b $RQ=Q_{CO2}/Q_{O2}$.

Table II. Metabolite excretion of VHb-synthesizing *E. coli* in glucose defined medium (measured after 31 h of cultivation)

VHb µmol/g DCW	Biomass g DCW/L	Excreted metabolite (mmol/g DCW)					
		Acet	ETOH	Form	D-Lac	Suc	Pyr
0	1.71	62.6	18.7	117.6	12.5	6.2	0.06
0.5	2.28	55.3	12.3	64.8	3.8	4.2	0.03
1.2	2.65	56.0	10.1	60.5	3.1	3.3	0.03
2.3	3.24	52.3	10.0	62.4	4.4	2.7	0.03
3.4	3.50	48.5	8.9	37.0	3.7	2.8	0.02
3.8	3.83	47.1	9.5	37.4	3.4	3.2	0.02

Table III. Carbon balance of VHb-producing *E. coli* (after 31 h of cultivation)

VHb µmol/g DCW	Carbon balance (mmol of Carbon)						Recovery (%)
	Glucose[a]	Biomass[b]	Σ(Metabolites)[c]	CO_2 (off gas)	O_2 (off gas)	CO_2 (redox bal.)	
0	271	20.4	177.7	57.0	66.0	58.3	94
0.5	281	27.2	157.9	76.9	86.7	82.5	93
1.2	290	31.6	172.8	74.6	84.6	79.6	96
2.3	341	38.7	207.1	81.4	88.6	82.4	96
3.4	333	41.8	185.2	83.3	94.9	93.7	93
3.8	333	45.7	201.0	91.5	100.0	98.8	102

a Initial glucose concentration of 4 g/L plus 0.25 g/h of feeding after culture A_{600} 1.5 and 0.5 g/h after A_{600} 3.0.

b Based on 39.8 mmol of carbon per g DCW.

c Sum of excreted acetate, ethanol, formate, succinate, D-lactate, and pyruvate in mmol carbon.

Table IV. Carbon flux of VHb-producing *E. coli* (in exponential phase; 13th -19th h)

VHb μmol/g DCW	Carbon flux[a] (mmol of Carbon / g DCW / h)								Recovery (%)
	Gluc	Biomass[b]	CO_2	Acet	ETOH	Form	D-Lac	Suc	
0	15.7	4.8	2.2	1.3	0.43	3.7	0.22	0.20	98
0.5	16.4	5.1	1.8	1.6	0.38	3.5	0.32	0.19	97
1.2	15.7	5.3	2.0	1.2	0.32	3.2	0.27	0.16	95
2.3	14.8	5.7	1.9	1.0	0.34	2.8	0.18	0.13	95
3.4	16.1	6.6	1.8	1.4	0.30	3.0	0.19	0.13	98
3.8	15.4	6.4	1.5	1.4	0.28	2.8	0.16	0.12	97

a Flux calculated from $\mu(\frac{dm}{dt}) / (\frac{dx}{dt})$, where m denotes metabolite and x biomass.

b Calculated from $Q_{gluc}\ Y_{x/gluc.}$

Table V. Summary of flux distribution of VHb-producing *E. coli*

Fluxes (mmol / g DCW / h)	W3110:pKTV1 with different VHb (μmol/g DCW)					
	0	0.5	1.2	2.3	3.4	3.8
f_{glc} [a]	2.50	2.50	2.50	2.50	2.50	2.50
f_{acet}	1.25	1.45	1.17	0.99	1.26	1.35
f_{ETOH}	0.41	0.35	0.31	0.34	0.28	0.27
f_{form}	3.57	3.19	3.03	2.83	2.78	2.70
f_{lac}	0.21	0.29	0.26	0.19	0.18	0.16
f_{suc}	0.19	0.17	0.15	0.13	0.12	0.12
f_1	0.40	0.62	0.63	0.82	1.13	1.20
f_2	2.08	1.86	1.84	1.65	1.34	1.27
f_3	0.07	0.14	0.14	0.19	0.29	0.31
f_4	0.18	0.33	0.33	0.44	0.64	0.68
f_5	0.22	0.29	0.30	0.38	0.49	0.51
f_6	0.11	0.19	0.19	0.25	0.35	0.37
f_7	2.25	2.18	2.17	2.09	1.97	1.95
f_8	4.56	4.49	4.45	4.34	4.22	4.19
f_9	4.39	4.32	4.26	4.13	3.98	3.95
f_{10}	1.28	1.22	1.16	0.97	0.81	0.78
f_{11}	0.52	0.51	0.52	0.55	0.56	0.56
f_{12}	1.32	0.88	1.08	1.00	0.57	0.47
f_{13}	1.20	0.75	0.94	0.85	0.40	0.30
$f_{NADH\ net}$	5.96	5.07	5.60	5.41	4.60	4.41
$f_{ATP\ net}$	1.23	1.09	0.68	–0.10	–0.65	–0.73
$f_{NADH\ resp}$ [b]	–3.24	–4.06	–4.70	–4.38	–5.04	–5.30
$f_{NADH\ overall}$	2.72	1.01	0.90	1.03	–0.44	–0.89
$f_{ATP\ resp}$ [c]	6.48	8.12	9.40	8.76	10.08	10.60
$f_{ATP\ overall}$	7.71	9.21	10.08	8.66	9.43	9.87

a Specific glucose uptake rates from Table I were normalized to 2.5.
b NADH flux from the electron transport chain was calculated by multiplying Q_{O2} (in Table I, after normalization) by 2. Negative flux denotes generation of NAD from NADH.
c P/O of 2.0 was assumed.

Table VI. Effect of VHb levels on flux ratios[a]

VHb µmol/g DCW	% PPP[b]	% OAA[c] at PEP	% IsoCit[d] at AcCOA
0	15	12	37
0.5	22	12	28
1.2	22	12	36
2.3	28	13	35
3.4	36	14	21
3.8	38	14	17

a Location of the fluxes is shown in Figure 3.

b Percentage of carbon through the pentose phosphate pathway: $f_1/(f_{glucose} + f_3 + f_6)$.

c Oxaloacetate–branch split–ratio at phosphoenolpyruvate: f_{11}/f_9.

d Isocitrate–branch split–ratio at acetyl coenzyme A: $f_{12}/f_{formate}$.

6.10 Figures

Figure 1 VHb induction pattern of *E. coli* W3110:pKTV1 grown in glucose defined medium. IPTG was added to culture at the 10^{th} h to induce VHb expression. VHb content of cells, estimated from Western blotting, was normalized with dry cell weight and is reported as μmol/g DCW.

Figure 2 (A) Glucose fed-batch bioreactor growths of W3110:pKTV1 with different VHb concentrations. Different doses of IPTG (0 mM, 0.005 mM, 0.01 mM, 0.05 mM, 0.1 mM, and 0.5 mM) were added to cultivations at the 10^{th} h to achieve different VHb expression levels. Dissolved oxygen profiles of the six cultivations were similar and only the representative one is shown. Glucose feeding strategy is described in Materials and Methods (B) Effect of VHb concentrations on final cell density.

Figure 3 Metabolic map for glucose fed-batch cultivations during exponential growth phase (between 13 – 19 h of fermentation). Fluxes from cultures without VHb (plain numbers) and with 3.8 μmol VHb/g DCW (italic numbers) are shown. Fluxes, in mmol/g DCW/h, were normalized to a same glucose consumption rate of 2.50 mmol/g DCW/h. The actual glucose uptake rates are shown in parentheses. Fluxes of cells with other VHb concentrations are summarized in Table V.

Figure 1

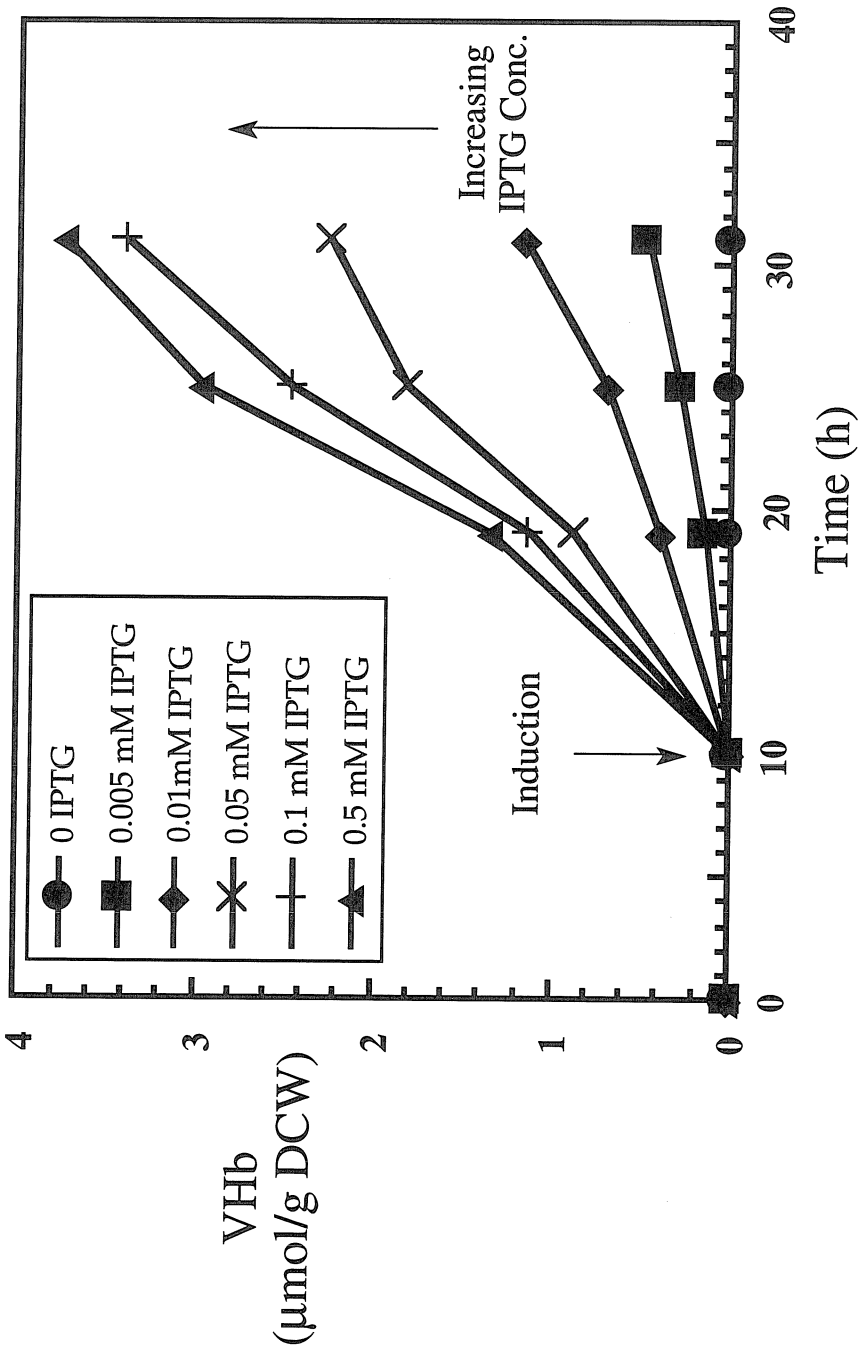
VHb
(µmol/g DCW)
Time (h)
0 IPTG
0.005 mM IPTG
0.01mM IPTG
0.05 mM IPTG
0.1 mM IPTG
0.5 mM IPTG
Induction
Increasing
IPTG Conc.
0
1
2
3
4
0
10
20
30
40

Figure 2A

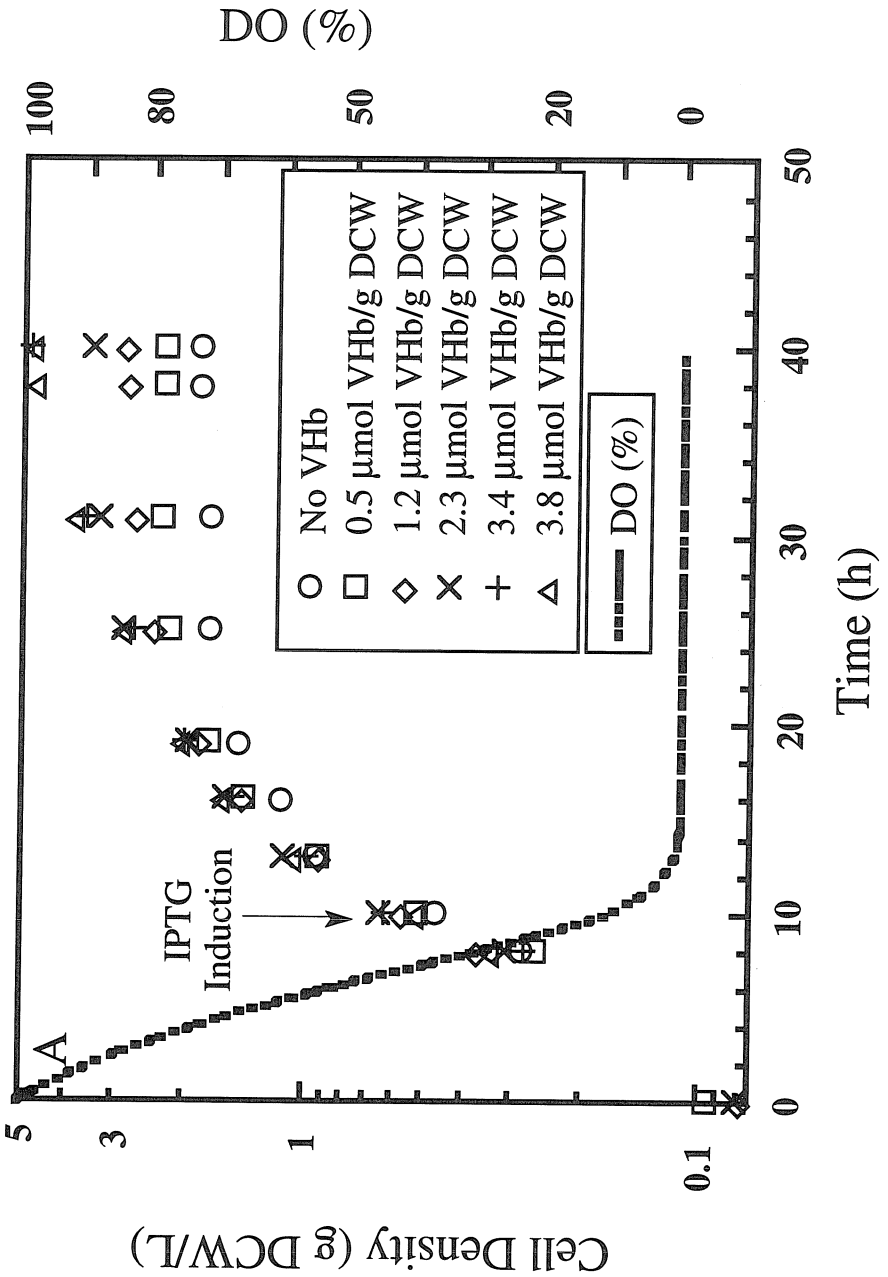
DO (%)
100
80
50
20
0
No VHb
0.5 µmol VHb/g DCW
1.2 µmol VHb/g DCW
2.3 µmol VHb/g DCW
3.4 µmol VHb/g DCW
3.8 µmol VHb/g DCW
DO (%)
IPTG
Induction
A
5
3
1
0.1
0
10
20
30
40
50
Time (h)
Cell Density (g DCW/L)

Figure 2B

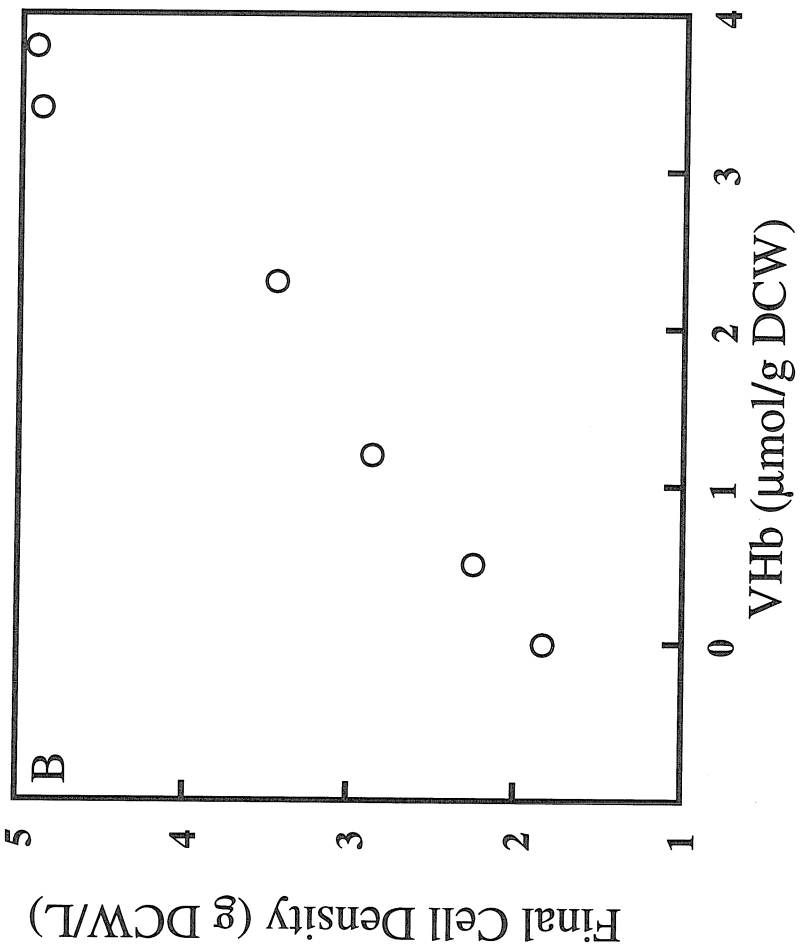

Figure 3

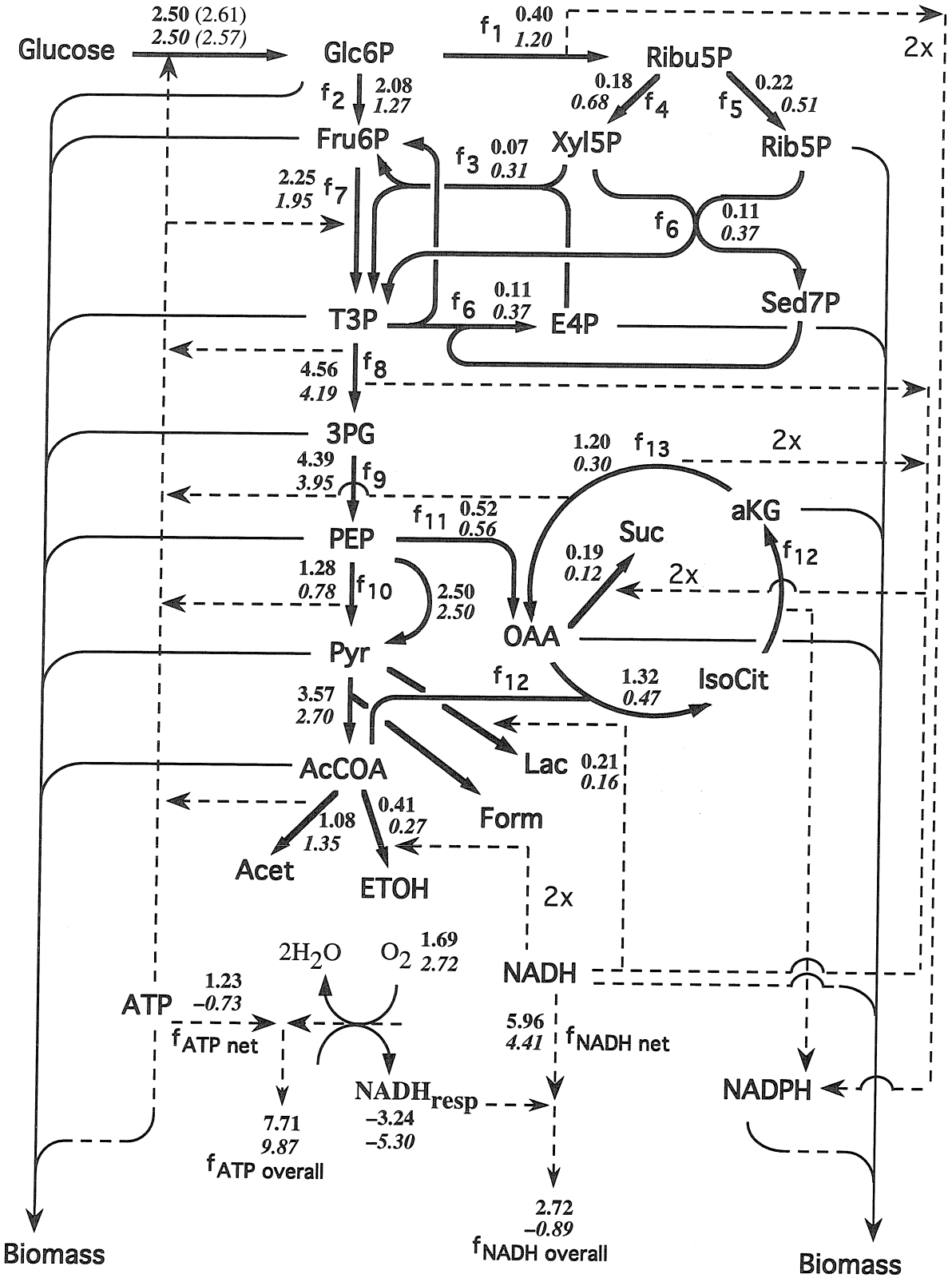
2.50 (2.61)
2.50 (2.57)
Glucose
Glc6P
f1 0.40 1.20
Ribu5P
2x
f2 2.08 1.27
0.18 0.68 f4
f5 0.22 0.51
Fru6P
f3 0.07 0.31
Xyl5P
Rib5P
2.25 1.95 f7
f6 0.11 0.37
T3P
f6 0.11 0.37
E4P
Sed7P
4.56 4.19 f8
3PG
4.39 3.95 f9
1.20 0.30 f13
2x
aKG
f11 0.52 0.56
PEP
Suc
0.19 0.12
f12
1.28 0.78 f10
2.50 2.50
2x
OAA
Pyr
f12
1.32 0.47
IsoCit
3.57 2.70
Lac 0.21 0.16
AcCOA
0.41 0.27
1.08 1.35
Form
Acet
ETOH
2x
2H2O
O2 1.69 2.72
NADH
1.23 −0.73
ATP
fATP net
5.96 4.41
fNADH net
NADH resp
−3.24 −5.30
NADPH
7.71 9.87
fATP overall
2.72 −0.89
fNADH overall
Biomass
Biomass

CHAPTER 7:

Conclusion

7.1 Summary

Significant advancements in knowledge of the physiological effects of *Vitreoscilla* hemoglobin in *Escherichia coli* have been achieved through this work. VHb is now perhaps the most thoroughly examined and characterized hemoprotein of all bacterial hemoglobins. The systematic analysis presented in this work on VHb involvements in *E. coli* central and energy metabolisms establish a foundation for future refinements of VHb technology and set a precedent for studying the function of other bacterial hemoglobins.

This work began with a hypothesized role of VHb in increasing the effective oxygen concentration and enhancing the efficiency of the aerobic electron transport chain of microaerobic *E. coli*. Different aspects of the membrane potential–associated energy synthesis pathway were examined to gain initial insights on the efficacy of the hypothesis. The effect of VHb on the electron transport chain was examined by focusing on the two most likely affected enzymes, cytochrome *o* and cytochrome *d*. These findings then led to a subsequent investigation of VHb effects on the respiratory–linked NADH utilization of cells. Additional insight on VHb function was obtained through further examination of VHb influence on the flux distribution of central carbon metabolism under oxygen–limited conditions. The possibility of the two global oxygen–sensing, trans–acting transcriptional activators of *E. coli*, Fnr and the Arc system, modulating the activity of *vhb* promoter was investigated. The question of whether VHb has special advantages in eliciting the observed physiological changes in microaerobic *E. coli* was addressed by functionally expressing horse heart myoglobin and yeast flavohemoglobin in *E. coli*. Different

VHb mutants were also constructed to generate VHb with altered oxygen–binding properties. Their effects on cell growth under hypoxic conditions were analyzed.

The activity of the *vhb* promoter and the production of VHb are positively regulated by Fnr but not by Arc of *E. coli* under microaerobic conditions. The presence of VHb enhances the activity and the amount of the high energy–efficient, yet low oxygen–affinity terminal oxidase, cytochrome *o*, of microaerobic *E. coli.* Although VHb also increases the amount of the less energy–efficient but high oxygen–affinity cytochrome *d*, the activity of cytochrome *d* is not affected. Improvement of cytochrome *o* activity shifts the electron flow towards cytochrome *o* and results in an increase in the number of protons extruded outside the cell per oxygen consumed by the cells. Increased activity and concentration of cytochrome *o* couple to a concomitant increase in the overall respiratory chain activity and accelerate the oxidation of the cellular electron carrier, NADH. Accelerated NADH turnover relieves cells of electron acceptor shortage that is typical of *E. coli* grown under hypoxic conditions. As a consequence, cells produce less by-products and channel more carbon flux to the pentose phosphate pathway and less through the tricarboxylic acid cycle. These physiological perturbations of VHb explain the previously reported enhancements of microaerobic cell growth, oxygen uptake rate, and recombinant protein synthesis by VHb (Kholsa and Bailey, 1988; Khosravi et al., 1990; Khosla et al., 1990).

7.2 Implications for VHb Technology and Recombinant DNA Bioprocesses

Using VHb expression in *E. coli* as a model system, this work demonstrated the importance and the benefits of understanding the consequences on cell physiology of expressing a metabolically active heterologous protein. Such knowledge allows one to address host–effector interaction problems such as altered protein expression pattern and saturated protein transport capacity that cannot be predicted *a priori*. It also provides directions for "fine tuning" of the cloned protein technology. While some of the results presented here might be actions of VHb specific to *E. coli*, several inferences can be made regarding the applicability of VHb to aerobic bioprocesses in general. First, expression of VHb may exert beneficial effects on organisms that contain branched respiratory pathways similar to those of *E. coli*. The facts that VHb possesses a similar K_m as those of *E. coli* cytochrome *o* and *d* and that our results indicated interactions between VHb and cytochrome *o* suggest the possibility of VHb scavenging and releasing oxygen to the oxygen–reducing molecules of organisms with similar oxygen–uptake properties as those of *E. coli*. Alternatively, cloning globin of other origins with k_{off} comparable to k_{on} of the host respiratory enzymes may also improve microaerobic oxygen transfer to the cell. Second, we have shown that VHb–expressing cells oxidize NADH faster than the VHb–negative controls under microaerobic conditions. Therefore, VHb is likely to increase the product formation of aerobic bioprocesses that are sensitive to changes in the NAD^+/NADH ratio or limited by the availability of NAD^+. Third, VHb may augment yields of pentose phosphate–derived products such as aromatic amino acids; metabolic flux distribution analysis disclosed a higher carbon flux entering the pentose phosphate pathway for the VHb–expressing *E. coli*. Lastly, introducing VHb in large–scale

bioreactor cultivations may eliminate oxygen fluctuations and stabilize cell metabolisms affected by these oxygen oscillations. VHb–containing cells showed dampened fluorescence and oxygen utilization responses to sudden changes of oxygen tension.

7.3 References

Khosla, C.; Bailey, J. E. Heterologous expression of a bacterial haemoglobin improves the growth properties of recombinant *Escherichia coli. Nature*, **1988**, *331*, 633-635.

Khosla, C.; Curtis, J. E.; DeModena, J.; Rinas, U.; Bailey, J. E. Expression of intracellular hemoglobin improves protein synthesis in oxygen-limited *Escherichia coli. Bio/Technol.* **1990**, *8*, 849-853.

Khosravi, M.; Webster, D. A.; Stark, B. C. Presence of bacterial hemoglobin gene improves α-amylase production of a recombinant *Escherichia coli* strain. *Plasmid* **1990**, *24*, 190-194.

APPENDIX A:

Effects of *Vitreoscilla* Hemoglobin Mutations and of Other Heterologous Globin Expression on Microaerobic *Escherichia coli* Growth

A.1 Abstract

The expression of a gene encoding hemoglobin (VHb) from the aerobic bacterium *Vitreoscilla sp.* in several organisms, including *Escherichia coli*, has been shown to improve microaerobic cell growth and enhance oxygen-dependent product formation. The action of VHb in *E. coli* was thought to involve its unique oxygen-binding property. To examine whether hemoproteins of other origins can also elicit the positive effects VHb exerts in microaerobic cells, we subcloned the genes encoding horse heart myoglobin (HMb) and yeast flavohemoglobin (YFb) behind the *tac* promoter on a medium-copy number vector and transformed these globin–expression plasmids into *E. coli*. Functional HMb and YFb were produced from these constructions in *E. coli*, as judged by their ability to abduct carbon monoxide. The presence of HMb increased the final density of cells by 30% relative to the wild–type control not synthesizing HMb, which compares with a cell density increase of 40% provided by VHb under the same cultivation conditions. The expression of YFb reduced the final cell density by 30% relative to the control. Three single amino acid–substituted VHb were also constructed to examine the consequences on oxygen–limited growth. These VHb mutants exhibited CO-binding activities 10-fold lower than that of the wild-type VHb. Replacement of the presumed heme ligand, histidine 85, with arginine abolished the beneficial effect of VHb in improving cell growth under hypoxic conditions; the ^{Arg85}VHb mutant grew to the same final cell density as the VHb–free control.

A.2 Introduction

Achieving desirable or novel catalytic activities through genetic integration of heterologous functions finds increasing applications in bioprocesses (Brennand and Margison, 1986; Khosla and Bailey, 1988a; Stanzak et al., 1986; Bailey, 1991). One such example is the incorporation of *Vitreoscilla* hemoglobin (VHb) in *Escherichia coli* to improve the oxygen utilization property of the cells and to sustain cell growth under hypoxic conditions. Oxygen limitation is a typical problem of large-scale bioreactor cultivations, and the expression of VHb enhances oxygen–limited *E. coli* growth and recombinant protein productions (Khosla and Bailey, 1988a; Khosla et al., 1990b; Khosravi et al., 1990). The beneficial effect of VHb is not limited to *E. coli* only. Antibiotic production from *Streptomyces coelicolor* and *Acremonium chrysogenum*, and the titer and yield of lysine from *Corynebacterium glutamicum* are all augmented in the presence of VHb (Magnolo et al., 1991; DeModena et al., 1993; Sander et al., 1993). Expression of VHb also elicits positive effects on the production of human tissue plasminogen activator from recombinant Chinese hamster ovary cells (Pendse and Bailey, 1994) and ethanol from *Saccharomyces cerevisiae* (Chen et al., 1994).

The success of VHb in relieving oxygen limitation raises the question whether the observed enhancement in microaerobic cell growth and productivity is a special property of VHb or a phenomenon generic for all oxygen-binding proteins. Hemoglobin and globin–like proteins exist ubiquitously in mammals and, less frequently, in plants, eucaryotic cells, and bacteria. Peptide sequence analysis reveals considerable homology between VHb and globins of other origins, including lupin leghemoglobin (Wakabayashi et al., 1986), yeast flavohemoglobin (Zhu and Riggs,

1992), and *E. coli* hemoprotein (Vasudevan et al., 1991). Although hemoglobins of several organisms have been isolated and characterized (Ioannidis, 1992; Oshino et al., 1973; Becana et al., 1991; De Baere et al., 1994), few data support functional roles of these globins in their natural hosts. Given the premise that all globins combine oxygen reversibly, is it possible that the expression of other hemoproteins may duplicate the effects which VHb exerts on the selected microorganisms?

Previous studies on energetic parameters, oxygen metabolism, and NAD(P)H utilization of microaerobic *E. coli* synthesizing VHb (Kallio et al., 1994; Chen and Bailey, 1994; Tsai et al., 1995) indicated involvement of VHb in enhancing the activity and efficiency of the electron transport chain under oxygen–scarce conditions. These findings combining with the fact that VHb has an extraordinary high k_{off} value relative to other globins (k_{off} 5600 s^{-1}; Webster, 1988) are consistent with a conjectured role of oxygenated VHb in releasing oxygen molecules to the terminal oxidases, resulting in an increase in the effective dissolved oxygen tension and enhancement in the activity of the respiratory pathway in *E. coli* (Kallio et al., 1994). Perhaps the oxygen binding properties of VHb make it unique in interacting with the pertinent respiratory enzymes of host organisms, resulting in the enhanced microaerobic activities.

To examine a possible special character of VHb in improving oxygen–limited *E. coli* metabolism, we subcloned and functionally expressed horse heart myoglobin (HMb) and yeast flavohemoglobin (YFb) in *E. coli*. The consequences of their expression on oxygen–limited bioreactor growth were studied. Using site–directed mutagenesis, the presumed proximal heme ligand of VHb was replaced with different amino acids in an attempt to generate VHb with altered oxygen affinity. Oxygen–

limited bioreactor growth of *E. coli* synthesizing wild-type VHb and mutated VHb were examined.

A.3 Materials and Methods

A.3.1 Strains and Plasmids

Escherichia coli DH5α [F', *endA1, hsdR17*($r_K^- m_K^+$), *supE44, thi*, λ^-, *recA1, gryA96, relA1, ϕ80dlacAm15*; Bethesda Research Laboratories] was used as a host for subcloning of genes encoding *Vitreoscilla* hemoglobin (VHb), horse heart myoglobin (HMb), and yeast flavohemoglobin (YFb). In addition, effects of different globins and VHb mutants on cell growth were examined using DH5α. *E. coli* CJ236 [*dut, ung, thi, relA, pCJ105*(Cm^r); BioRad] was used to prepare uracil–containing DNA for site–directed mutagenesis. Plasmid pGYM (Guillemette et al., 1991) was a gift from Dr. Guillemette (University of British Columbia) and contains the horse heart myoglobin synthetic gene based on HMb amino acid sequence and *E. coli* codon usage. Plasmid pRB241c/+ was obtained from Dr. Zhu (University of Texas, Austin) and carries a genomic DNA fragment of *Saccharomyces cerevisiae* encoding yeast flavohemoglobin. Plasmids pRED2 (Khosla and Bailey, 1988b) and pBluescript II SK^+ (Stratagene, Inc.) were employed for site–directed mutagenesis of *vhb*. Plasmid pKQV4 (Strauch et al., 1989), which contains the IPTG–inducible *tac* promoter and the *lac* repressor, $lacI^q$, was used as the expression vector for VHb, HMb, and YFb.

A.3.2 PCR and Subcloning of *Vitreoscilla* Hemoglobin (*vhb*)

The polymerase chain reaction (PCR; Saiki et al., 1988) technique was used to amplify the structural gene of *vhb* for the subsequent cloning of *vhb* into plasmid

pKQV4. Plasmid pRED2 (Khosla and Bailey, 1988b) was used as the template, and Primer 1 and 2 were used to amplify the *vhb* gene. Primer 1, which binds specifically the 5' end of *vhb*, has the following sequence: 5'C **ATG** TTA GAC CAG CAA ACC AT, where **ATG** is the initiation methionine of *vhb*. Primer 2, 5'ACA **TGC ATG** CAT GTC CCA AGT TTT GGC * AAC AG, binds the 3' end of the *vhb* gene (underlined) starting 81 bp downstream of the translational stop codon and creates a new restriction site for *Sph*I (bold letters). A nucleotide C at the indicated position (*) was omitted. PCR amplification was performed using a Perkin Elmer Gene Amp 9600 PCR System and AmpliTag DNA polymerase (Perkin Elmer).

The amplified structural gene of *vhb* was subcloned into pKQV4 by ligating the PCR product with *Sma*I–cleaved pKQV4 (post–treated with calf intestine phosphatase). This construction, which resulted in plasmid pPPC1, positions the *vhb* gene directly behind the *tac* promoter and the Shine-Dalgarno (SD) sequence. Authenticity of the amplified *vhb* and the orientation of *vhb* in pPPC1 were verified by DNA sequencing (Sanger et al., 1977) using an Amersham DNA Sequencing Kit (Sequenase version 2.0).

A.3.3 Subcloning of Horse Heart Myoglobin (*hmb*)

The 470 bp DNA fragment containing *hmb* was isolated from plasmid pGYM digested with *Nco*I and *Pst*I [after *Nco*I digestion the DNA ends were made blunt with DNA polymerase I large (Klenow) fragment]. *Nco*I digestion of pGYM released the 5' end of the *hmb* structural gene with a single nucleotide C preceding the initiation methionine ATG. Plasmid pPPC2 was constructed by subcloning the fragment carrying the *hmb* gene into the *Sma*I–*Pst*I sites of pKQV4. This construction resulted in the same *tac* promoter and spacing between the SD sequence and the start

codon ATG in pPPC2 as in pPPC1. DNA sequencing (Sanger et al., 1977) of pPPC2 was performed to verify the construction.

A.3.4 PCR and Subcloning of Yeast Flavohemoglobin (*yfb*)

Plasmid pRB241c/+ was digested with *Eco*RI to release the 8.4 kb DNA fragment containing the 1.2 kb *yfb* gene. The *yfb* structural gene was then PCR–amplified from the 8.4 Kb *Eco*RI–*Eco*RI fragment using Primer 8 and 9. Primer 8, 5'CGG AAT TCC CCA TGC TAG CCG AAA AAA CCC G, binds to the 5' end of *yfb* (Genbank # L07071) and creates an *Eco*RI restriction site (bold letters). Primer 9, 5'TTA TAC CGC CTA AAC TTG CAC GGT TG, binds specifically to the 3' end of *yfb*. After elution from agarose gel, the PCR product was digested with *Eco*RI to generate an *Eco*RI–blunt fragment for the subsequent subcloning. Plasmid pKQV4 was digested with *Hind*III and *Eco*RI [*Hind*III–end rendered blunt with DNA polymerase I large (Klenow) fragment] and ligated with the amplified *yfb* fragment. This plasmid was named pKLA in which YFb expression is controlled by the *tac* promoter. Primer 8 allows identical spacing between SD sequence and the initiation codon (underlined) as in pPPC1 and pPPC2. The sequence of *yfb* in pKLA was verified by DNA sequencing as described earlier.

A.3.5 Site–directed Mutagenesis of *vhb*

The 0.7 Kb *Hind*III–*Ssp*I fragment containing the *vhb* gene with its native promoter was isolated from pRED2 (Khosla and Bailey, 1988b) and subcloned into *Hind*III–*Hinc*II sites of pBluescript II SK$^+$, thus creating plasmid pBluV. Single–stranded pBluV served as template for site–directed mutagenesis of *vhb* in which histidine 85 was replaced with either tyrosine, alanine, or arginine. The mutagenic oligonucleotide, Oligo 1, 5'GCT TGA CAA TAT TTG ACT GC, was designed to

replace histidine 85 with tyrosine (bold letters). This modification also generates a new restriction site for *Ssp*I (underlined). Similarly, Oligo 3, 5'GCT TGA C**AA GCT** TTG ACT GC, replaces histidine 85 with alanine (bold letters) and creates a new restriction site for *Hind*III (underlined). Oligo 4, 5'GCT TGA C**AA CGT** TTG ACT GC, substitutes arginine (bold letters) for histidine 85 and generates a *Psp*14061 restriction site (underlined). Oligonucleotide mutagenesis, which is based on the method of Kunkel (1985), was performed according to the recommended protocol using an In Vitro Mutagenesis kit (Version 2; BioRad). The single–stranded DNA template was prepared from *E. coli* CJ236 deficient in dUTPase and uracil-N-glycosylase. The mutagenized strand was enriched from subsequent replication of DNA duplex in *E. coli* DH5α which contains functional dUTPase and uracil-N-glycosylase. The resulting plasmids, pBluV1 (Oligo 1), pBluV3 (Oligo 3), and pBluV4 (Oligo 4), carrying the additional restriction sites were selected and the accuracy of mutagenesis was verified by DNA sequencing.

A.3.6 Chemicals, Reagents, and DNA Manipulations

All restriction endonucleases, modifying enzymes [T4 DNA ligase, DNA polymerase I large (Klenow) fragment, and calf intestinal phosphatase] were purchased from commercial suppliers and used according to the recommended protocols. Oligonucleotides used for PCR, DNA sequencing, and site–directed mutagenesis were synthesized by Microsynth (Windisch, Switzerland). [α-^{35}S]–dATP was used for DNA sequencing and was purchased from Amersham International. DNA manipulations were performed according to standard methods (Sambrook et al., 1989). DNA fragments eluted from agarose gels were purified using Sephaglas BandPrep Kit (Pharmacia).

A.3.7 Bioreactor Cultivation

Precultures for bioreactor cultivations were grown at 37°C and 250 rpm for 12 hr in 250 mL shake flasks containing 20 mL of glucose batch medium supplemented with 50 g/L casamino acid and 10 g/L yeast extract. Glucose batch medium consists of 4 g/L glucose, 0.4 g/L $(NH_4)_2SO_4$, 4.35 g/L K_2HPO_4, 1.5 g/L KH_2PO_4, 1 mL/L trace metal mix (8.3 mM Na_2MoO_4, 7.6 mM $CuSO_4$, 8 mM H_3BO_3), 1 mL/L vitamin mix (0.042% riboflavin, 0.54% panthothenic acid, 0.6% niacin, 0.14% pyridoxin, 0.006% biotin, 0.004% folic acid), 1 mM $MgSO_4$, 0.05 mM $CaCl_2$, 0.2 mM $FeCl_3$, and 100 mg/L ampicillin. Fed-batch cultivations were performed in a Sixfors bioreactor (Infors, Switzerland) containing 300 mL of glucose batch medium supplemented with casamino acid and yeast extract. Batch medium for cultivations of *E. coli* producing VHb, HMb, and YFb was supplemented with 5 g/L casamino acid and 1 g/L yeast extract while that for wild–type VHb and VHb mutant cultivations was supplemented with 50 g/L casamino acid and 10 g/L yeast extract. To start bioreactor cultivations, 6.0 mL of seeding culture was added, and process parameters were maintained at 37°C, pH 7 (adjusted with either 3 M NaOH or 3 M H_3PO_4), 300 rpm, and 0.4 vvm of air supply. Expression of VHb, HMb, and YFb were induced by adding IPTG (final concentration of 1 mM) to the culture when dissolved oxygen concentration (DO) dropped below 10% of air saturation. Fed-batch mode was commenced with 1 mL/h of feed medium when the culture reached an A_{600} of 2.5, and 2 mL/h when A_{600} reached 4.0. Thereafter the feeding was maintained constant at 2 mL/h until the end of cultivation. Feed medium consisted of 250 g/L glucose, 110 g/L $(NH_4)_2SO_4$, 8 g/L $MgSO_4$, 1 mL/L vitamin mix, 1 mL/L trace metal mix, 0.05 mM $CaCl_2$, 0.2 mM $FeCl_3$, 5 mg/L thiamine, 50 mg/L arginine, and 100 mg/L ampicillin. DO was monitored with a pO_2 electrode (Ingold, Inc.) and exhaust gas

(CO_2 and O_2) from bioreactors was monitored using an emission monitor (Brüel & Kjaer, Emissions Monitor Type 3427).

A.3.8 Analytical Techniques

Samples for VHb Western blotting were prepared by resuspending 1 mL sample to a final optical density of A_{600} 15 in lysis buffer (200 µl 50% w/v glycerol, 100 µl 10% SDS, 10 µl ß-mercaptoethanol, 100 µl 0.1% bromophenol blue, 250 µl 0.5 M Tris, pH 6.8, and 340 µl sterile H_2O) and boiled for 5 min in a water bath. The subsequent SDS-PAGE, Coomassie blue staining or Western blotting were performed according to the standard protocols (Laemmli, 1970; Winston et al., 1987). Anti-VHb serum was obtained from Cocalico Biologicals.

The soluble fraction of cells (for VHb activity assay) was prepared by resuspending cells 20:1 in a sonication buffer (100 mM Tris-HCl, pH 8, 50 mM NaCl, 1 mM EDTA) and disrupting using a French press (SLM-Aminco). Globin activities were assayed using CO–reduced minus reduced spectroscopy as described previously (Hart and Bailey, 1991). Ethanol assay was performed enzymatically (Bergmeyer, 1985a & b) at 37°C on a Beckman SYNCHRON CX5CE autoanalyzer. Acetate concentration of bioreactor samples was determined by gas chromatography (GC; Hewlett-Packard 5890 Series II with a flame ionization detector) with a Carbovac CW 20 M 0.25 (25 m x 0.25 mm) column. GC analysis was performed on a 3-ramp oven temperature program with an initial temperature of 70°C. The temperature was raised 10°C/min to 95°C, then 40°C/min to 131°C, and 70°C/min to 190°C where it was maintained for 4 min. The detector and the inlet temperatures were 300°C and 220°C, respectively; helium and nitrogen gas flow rates were 1 mL/min and 100 mL/min, respectively.

A.4 Results

A.4.1 Cloning of Horse Heart Myoglobin and Yeast Flavohemoglobin

To examine the effect of expression of different globins on cell physiology, the structural genes encoding *Vitreoscilla* hemoglobin (VHb), horse heart myoglobin (HMb) and *Saccharomyces cerevisiae* flavohemoglobin (YFb) were subcloned in the *E. coli* expression vector, pKQV4 (Strauch et al., 1989). Subcloning of these genes in pKQV4 was designed in such a way that all three genes are under the control of the IPTG–inducible *tac* promoter. The spacing between the *tac* promoter and the ATG initiation methionine codon (including the ribosomal binding site SD sequence) of the three gene constructs was made identical using PCR and incorporating needed restriction sites (See Materials and Methods for detail). Table I lists the plasmids constructed in this study and their relevant genotypes. DNA sequencing was performed to verify the sequences of *vhb*, *hmb*, and *yfb* and the orientation of these genes in pKQV4. DNA sequences of *vhb* and *hmb* in pPPC1 and pPPC2, respectively, were identical to the reported sequences (Khosla and Bailey, 1988b; Guillemette et al., 1991). Sequence verification of *yfb* in pKLA revealed one extra nucleotide C proceeding the initiation start codon. This was most likely due to a mistake in the primer oligonucleotide used for PCR. In addition, three nucleotide mismatches in the structural gene of *yfb* were found with respect to the reported sequence (Genbank #L07071). These mismatches occurred at nucleotide 335 (G instead of T; Asp->Gly), nucleotide 350 (G instead of A; Glu->Gly), and nucleotide 459 (C instead of A; Glu->Asp) downstream from the initiation codon ATG. These mismatches would alter the amino acids encoded and result in a different peptide

sequence. It is not known, however, whether the mismatches are due to mistakes in PCR or errors in the published sequence (Genbank #L07071). As noted below, YFb expression in *E. coli* from this vector did exhibit CO–difference spectrum characteristic of globin activity.

Attempts to clone soybean leghemoglobin A gene (*lba*) in *E. coli* were not successful. The gene *lba* (cDNA of *lba* was obtained from Dr. N. Sandal of the University of Aarhus, Denmark) was PCR amplified and subcloned in pKQV4 using the same strategy as those for *vhb*, *hmb*, and *yfb*. However, for unknown reasons, the resultant plasmid, pPPC4, always generated incorrect restriction patterns and showed incorrect sequence after transformation of *E. coli* with pPPC4.

A.4.2 Functional Expression of HMb and YFb in *E. coli*

Plasmids pKQV4, pPPC1, pPPC2 and pKLA were transformed into *E. coli* DH5α and the expression of VHb, HMb, and YFb were examined. Synthesis of functional globins from these strains was evident from their CO–binding absorbance spectra (Figure 1A) which revealed absorption characteristics analogous to those reported previously (Hart and Bailey, 1991; Guillemette et al., 1991; Oshino et al., 1973). VHb had an absorption peak and a trough at 419 nm and 437 nm, respectively, whereas HMb had a peak at 417 nm and a trough at 438 nm. The maximum and minimum absorption bands of YFb occurred at 420 nm and 438 nm, respectively. The absence of interference from the endogenous *E. coli* hemoprotein was confirmed from the control strain DH5α:pKQV4 whose CO-reduced minus reduced spectrum showed a baseline (Figure 1). Western blotting of DH5α:pPPC2 (HMb^+) and DH5α:pKLA (YFb^+) soluble extracts indicated that HMb and YFb did not cross-react with anti–VHb serum (result not shown). IPTG–induced (to a final concentration of 1 mM)

cultures of DH5α harboring pKQV4, pPPC1, pPPC2, or pKLA were analyzed for their protein contents. SDS/PAGE analysis of total cell extracts indicated that YFb synthesized from DH5α:pKLA migrated electrophoretically with an apparent molecular weight of about 44 kD (Figure 1B, lane 4) similar to that of natural yeast flavohemoglobin (Iwaasa et al., 1992). Unfortunately, neither VHb, monomeric M.W. of 15.7 kD, nor HMb, M.W. of ~17 kD, was visible from the SDS/PAGE (lanes 2 and 3). It is possible that VHb and HMb were not efficiently expressed in these constructs. Nevertheless, active VHb, HMb, and YFb were synthesized from the respective strains, as indicated from their CO–binding absorbance spectra.

A.4.3 Effect of HMb and YFb on Microaerobic Cell Growth

Glucose fed–batch bioreactor cultivations were conducted to examine the effects of YFb and HMb on microaerobic cell growth relative to the VHb and VHb-free controls. Cultivation conditions for bioreactor growth were described in Materials and Methods. Figure 2 shows the cell growth and dissolved oxygen (DO) profiles of DH5α:pKQV4, DH5α:pPPC1, DH5α:pPPC2, and DH5α:pKLA cultivated for 30 hours. The DO profiles of all strains were identical: DO dropped to zero within the first ten hours of fermentation and remained at a non-detectable level for the duration of the cultivations. Expression of the different globins was induced with IPTG (final concentration of 1 mM) when DO dropped below 10% of air saturation. After DO became microaerobic (DO less or equal to 2% air saturation), the strains synthesizing VHb and HMb grew faster than the YFb–producing cells and the globin–negative controls. Optical density (*A600*) of cells at the end of cultivations was 7 for DH5α:pPPC1 (VHb), 6.4 for DH5α:pPPC2 (HMb), 3.6 for DH5α:pKLA (YFb), and 5.0 for DH5α:pKQV4 (control). The effects of VHb and HMb in increasing cell density and YFb in reducing cell density under microaerobic

conditions were reproducible as similar results were obtained from duplicate bioreactor cultivations (not shown). Acetate concentrations measured at the end of cultivations were 70 mM for DH5α:pPPC1, DH5α:pPPC2, and DH5α:pKQV4, and were 15% higher than that of DH5α:pKLA (60 mM). Ethanol concentrations at the end of cultivations were 25 mM for DH5α:pPPC1 and DH5α:pPPC2, and were 25% higher than those of DH5α:pKQV4 and DH5α:pKLA which were similar at 20 mM.

A.4.4 Mutagenesis of VHb

Although there are no structural data of VHb available, alignments of the peptide sequence of VHb hydrophobic residues with those of other globins revealed two invariant residues that are common in all known globins: histidine 85, the proximal ligand that binds covalently to the heme iron, and phenylalanine 43, the residue that forces the heme into its pocket (Wakabayashi et al., 1986). This analysis suggests possible targets for altering VHb oxygen–binding properties. Therefore, site–directed mutagenesis based on the method of Kunkel (1985) was used to change the nucleotide codon for His 85 (CAT) of VHb to ones that encode for tyrosine (TAT; pBluV1), alanine (GCT; pBluV3), or arginine (CGT, pBluV4) (see Materials and Methods for details). Introduction of these mutagenic nucleotides generated additional restriction sites for rapid screening of mutagenized VHb. These single amino acid–substituted *vhb* were subcloned on a high–copy number vector (pBluescript II SK^+) for high level expression. Because these mutants carry the native promoter of *vhb*, the expression of VHb and VHb mutants are induced when the dissolved oxygen tension becomes low. Table I lists the names of the plasmids that carry the mutagenized *vhb* genes.

CO–binding activity assays showed the effect of VHb mutations (Figure 3A). Relative to the wild-type VHb spectrum (curve B), replacement of histidine 85 with either tyrosine (curve A), alanine (curve C), or arginine (curve D) resulted in broad–bands and shifted the position of the absorption maximum and minimum from 419 to 421 nm and 437 to 442 nm, respectively. Concentrations of active globins (VHb and VHb mutants) were estimated from the absorption spectra based on the reported extinction coefficient for VHb (Hart and Bailey, 1991). With a similar cell density used for all strains, the active VHb determined from DH5α:pBluV (wild-type VHb) spectrum was approximately ten times the amount of active globins from either DH5α:pBluV1, DH5α:pBluV3, or DH5α:pBluV4 (Figure 3A). The magnitude of the wild-type VHb absorption band shown in Figure 3A was scaled down to those of the mutated VHb for comparison. Western blotting analysis showed that all three VHb mutants cross–reacted with anti-VHb serum and migrated to the same position on a 15% SDS-PAGE as the VHb standard (Figure 3B). Similar Western blot intensities of VHb mutants with that of wild-type VHb suggested the presence of large fractions of non-functional VHb mutants, possibly due to failure of heme incorporation. Phase–contrast microscopy revealed abnormally elongated cell morphology typical of inclusion body formation (Hart et al., 1990) for DH5α harboring the mutant plasmids pBluV1, pBluV3, and pBluV4. Less than 1% of elongated cells were also observed from DH5α:pBluV cultures.

A.4.5 Effect of VHb Mutation on Microaerobic Cell Growth

Bioreactor cultivations of different VHb mutants were performed to examine the effect of VHb mutations on cell growth. Cells grown under the same batch medium as that for the different globins exhibited a very long lag phase (>10 hr) and grew poorly afterward. Therefore, concentrations of yeast extract and casamino acid

were increased to accelerate culture growth. Results from such bioreactor cultivations of VHb mutants are shown in Figure 4. DO profiles of VHb mutants behaved differently and reached 0% air saturation at different time points of cultivation. This is most likely due to differences in the time of cells exiting lag phase. After the DO of all strains dropped to zero, DH5α:pBluV (wild–type VHb), DH5α:pBluV1 (^{Tyr85}VHb), and DH5α:pBluV3 (^{Ala85}VHb) grew faster than DH5α:pBluescript II SK$^+$ and DH5α:pBluV4 (^{Arg85}VHb). The specific growth rate of DH5α:pBluV, DH5α:pBluV1, and DH5α:pBluV3 were similar (0.123 1/h) and were about 1.5–fold higher than those of DH5α:pBluescript II SK$^+$ and DH5α:pBluV4 (0.082 1/h). The final cell densities of DH5α:pBluV, DH5α:pBluV1, and DH5α:pBluV3 were approximately 50% higher than those of DH5α:pBluescript II SK$^+$ and DH5α:pBluV4. At the end of cultivation, cells harboring pBluV, pBluV1 or pBluV3 produced less acetate and ethanol than cells carrying either pBluescript II SK$^+$ or pBluV4. Acetate concentrations were 75 mM for DH5α with pBluV, pBluV1 or pBluV3, and 100 mM for DH5α with pBluescript II SK$^+$ or pBluV4. Ethanol production from DH5α:pBluescript II SK$^+$ (20 mM) was approximately 30% higher than that from the other four strains (15 mM each).

A.5 Discussion

We have functionally expressed horse heart myoglobin and yeast flavohemoglobin in *E. coli* and shown that the presence of horse heart myoglobin improved cell growth under oxygen-limited conditions. Synthesis of yeast flavohemoglobin, in contrast, reduced cell growth under the same conditions. Replacement of histidine 85 of VHb with arginine altered the carbon monoxide–

binding activity of VHb and eliminated microaerobic cell growth advantage exerts by wild-type VHb.

Although our data are still preliminary to enable suggestion of a functional role of HMb in *E. coli*, a comparison of the kinetic constants of HMb, YFb and VHb may provide insight on possible involvements of HMb's oxygen–binding property in oxygen transfer to the cells. Among the three globins studied, VHb has the lowest oxygen affinity due to a unique combination of a slow on-rate constant [K_{on} 78 (μM s)$^{-1}$] and a very rapid off-rate constant (K_{off} 5600 s^{-1}; Orii and Webster, 1986). These properties make VHb suitable for scavenging oxygen molecules under hypoxic environment and donating them to the respiratory components, thereby causing the beneficial effects of VHb observed in *E. coli* (Kallio et al., 1994). Horse heart myoglobin, with an on-rate similar to the off-rate constant [K_{on} 14 (μM s)$^{-1}$; K_{off} 11 s^{-1}], has a dissociation constant approaching 1 μM (K_D 0.77 μM) (Wittenberg et al., 1985). Therefore, it can be envisioned that, under typical oxygen–scarce conditions (in the range of micromolars), HMb can function similarly to VHb in relaying oxygen molecules to the pertinent oxygen–reducing enzymes of the host. Yeast flavohemoglobin, on the other hand, has a very high oxygen affinity (K_D 0.02 μM) in comparison with VHb and HMb due to a high on-rate constant [K_{on} 850 (μM s)$^{-1}$] and a low off-rate constant (K_{off} 17 s^{-1}) (Oshino et al., 1973). This extraordinary high on-rate of YFb may cause a saturation of oxygenated YFb and allow only minimum contribution to oxygen flux for cell respiration. Therefore, no improvement in oxygen utilization properties of the cells can be expected from YFb expression. As a consequence, cells are burdened with the synthesis of an extra protein and, accordingly, cell growth is reduced. This is what we have observed in this study.

Our site–directed mutagenesis of VHb showed that substitution of the presumed heme ligand with either tyrosine, alanine, or arginine did not abolish completely the heme activity of VHb. The overall carbon monoxide binding activities of the three mutants were approximately 10-fold smaller relative to that of wild-type VHb. This is possibly due to a changed oxygen affinity or improper folding of VHb protein as a consequence of mutation. The fact that ^{Tyr85}VHb and ^{Ala85}VHb still retained the beneficial effect of VHb suggests robustness of VHb in improving in microaerobic cell growth and the possibility of further improvements in VHb protein. However, further biochemical characterization of ^{Tyr85}VHb, ^{Ala85}VHb, as well as ^{Arg85}VHb which eliminated the growth advantage exert by VHb$^+$ cells is needed to understand the role of these amino acid replacements on VHb activity.

A.6 Acknowledgments

This work was supported by the Swiss Priority Program in Biotechnology (SPP Biotech). We gratefully acknowledge Dr. H. Zhu of the University of Texas, Austin, for generously supplying plasmid pRB241c/+, Dr. J. Guillemette of the University of British Columbia for plasmid pGYM, and Dr. N. Sandal of the University of Aarhus, Denmark, for the *lba* gene.

A.7 References

Bailey, J. E. Toward a science of metabolic engineering. *Science* **1991**, *252*, 1668-1675.

Becana, M.; Salin, M. L.; Ji, L.; Klucas, R. V. Flavin-mediated reduction of ferric leghemoglobin from soybean nodules. *Plants* **1991**, *183*, 575-583.

Brennand, J.; Margison, G. P. Reduction of the toxicity and mutagenicity of alkylating agents in mammalian cells harboring the *Escherichia coli* alkylatransferase gene. *Proc. Natl. Acad. Sci. USA.* **1986**, *83*, 6292-6296.

Chen, R.; Bailey, J. E. Energetic effect of *Vitreoscilla* hemoglobin expression in *Escherichia coli*: An on-line ^{31}P NMR and saturation transfer study. *Biotechnol. Prog.* **1994**, *10*, 360-364.

Chen, W.; Hughes, D. E.; Bailey, J. E. Intracellular expression of *Vitreoscilla* hemoglobin alters the aerobic metabolism of *Saccharomyces cerevisiae*. *Biotechnol. Prog.* **1994**, *10*, 308-313.

DeBaere, I.; Perutz, M. F.; Kiger, L.; Marden, M. C.; Poyart, C. Formation of two hydrogen bonds from the globin to the heme-linked oxygen molecule in *Ascaris* hemoglobin. *Proc. Natl. Acad. Sci. USA* **1994**, *91*, 1594-1597.

DeModena, J. A.; Gutierrez, S.; Velasco, J.; Fernandez, F. J.; Fachini, R. A.; Galazzo, J. L.; Hughes, D. E.; Martin, J. F. The production of cephalosporin C by *Acremonium chrysogenum* is improved by the intracellular expression of a bacterial hemoglobin. *Bio/Technol.* **1993**, *11*, 926-929.

Guillemette, J. G.; Matsushima-Hibiya, Y.; Atkinson, T.; Smith, M. Expression in *Escherichia coli* of a synthetic gene coding for horse heart myoglobin. *Protein Engineering* **1991**, *4*, 585-592.

Hart, R. A.; Bailey, J. E. Purification and aqueous 2-phase partitioning properties of recombinant *Vitreoscilla* hemoglobin. *Enz. Microb. Technol.* **1991**, *13*, 788-795.

Hart, R. A.; Rinas, U.; Bailey, J. E. Protein composition of *Vitreoscilla* hemoglobin inclusion bodies produced in *Escherichia coli. J. Biol. Chem.* **1990**, *265*, 12728-12733.

Ioannidis, N.; Copper, C. E.; Poole, R. K. Spectroscopic studies on an oxygen-binding haemoglobin-like flavohaemoprotein from *Escherichia coli*. *Biochem. J.* **1992**, *288*, 649-655.

Iwaasa, H.; Takagi, T.; Shikama, K. Amino acid sequence of yeast hemoglobin. *J. Mol. Biol.* **1992**, *227*, 948-954.

Kallio, P. T.; Kim, D. J.; Tsai, P. S.; Bailey, J. E. Intracellular expression of *Vitreoscilla* hemoglobin alters *Escherichia coli* energy metabolism under oxygen-limited conditions. *Eur. J. Biochem.* **1994**, *219*, 201-208.

Khosla, C.; Bailey, J. E. Evidence of partial export of *Vitreoscilla* hemoglobin into the periplasmic space in *Escherichia coli*. Implication for protein function. *J. Mol. Biol.* **1989**, *210*, 79-89.

Khosla, C.; Bailey, J. E. Heterologous expression of a bacterial haemoglobin improves the growth properties of recombinant *Escherichia coli*. *Nature* **1988a**, *331*, 633-635.

Khosla, C.; Bailey, J. E. The *Vitreoscilla* hemoglobin gene: Molecular cloning, nucleotide sequence and genetic expression in *Escherichia coli*. *Mol. Gen. Genet.* **1988b**, *214*, 158-161.

Khosla, C.; Curtis, J. E.; DeModena, J.; Rinas, U.; Bailey, J. E. Expression of intracellular hemoglobin improves protein synthesis in oxygen-limited *Escherichia coli*. *Bio/Technol.* **1990b**, *8*, 849-853.

Khosravi, M.; Webster, D. A.; Stark, B. C. Presence of bacterial hemoglobin gene improves α-amylase production of a recombinant *Escherichia coli* strain. *Plasmid* **1990**, *24*, 190-194.

Kunkel, T. A. Rapid and efficient site-specific mutagenesis without phenotypic selection. *Proc. Natl. Acad. Sci. USA*. **1985**, *82*, 488-492.

Laemmli, U. K. Cleavage of structural proteins during the assembly of the head of bacteriophage T4. *Nature* **1970**, *227*, 680-685.

Magnolo, S. K.; Leenutaphong, D. L.; DeModena, J. A.; Curtis, J. E.; Bailey, J. E.; Galazzo, J. L.; Hughes, D. E. Actinorhodin production by *Streptomyces coelicolor* and growth of *Streptomyces lividans* are improved by the expression of a bacterial hemoglobin. *Bio/Technol.* **1991**, *9*, 473-476.

Orii, Y.; Webster, D. A. Photodissociation of oxygenated cytochrome *o*(s) (*Vitreoscilla*) and kinetic studies of reassociation. *J. Biol. Chem.* **1986**, *261*, 3544-3547.

Oshino, R.; Asakura, T.; Takio, K.; Oshino, N.; Chance, B. Purification and molecular properties of yeast hemoglobin. *Eur. J. Biochem.* **1973**, *39*, 581-590.

Oshino, R.; Oshino, N.; Chance, B.; Hagihara B. The properties of yeast hemoglobin and its physiological function in the cell. *Eur. J. Biochem.* **1973**, *35*, 23-33.

Pendse, G. J.; Bailey, J. E. Effect of *Vitreoscilla* hemoglobin expression on growth and specific tissue plasminogen activator productivity in recombinant Chinese hamster ovary cells. *Biotechnol. Bioeng.* **1994**, *44*, 1367-1370.

Saiki, R. K.; Gelfand, D. H.; Stoffel, S.; Scharf, S. J.; Higuchi, R.; Horn, G. T.; Mullis, K. B.; Erlich, H. A. Primer–directed enzymatic amplification of DNA with a thermostable DNA polymerase. *Science* **1988**, *239*, 487-491.

Sambrook, J.; Frisch, E. F.; Maniatis, F. E. In *Molecular Cloning: a laboratory manual*; Cold Spring Harbor Laboratory, Cold Spring Harbor, N.Y.; 1989.

Sander, F. C.; Fachini, R. A.; Hughes, D. E.; Galazzo, J. L.; Bailey, J. E. Expression of *Vitreoscilla* hemoglobin in *Corynebacterium glutamicum* increases final concentration and yield of L-lysine. *ECB6: Proceedings of the 6th European Congress on Biotechnology* **1993**; pp. 607-610.

Sanger, F.; Nicklen, S.; Caulson, A. R. DNA sequencing with chain–termination inhibitors. *Proc. Natl. Acad. Sci. USA.* **1977**, *74*, 5463-5467.

Stanzak, R.; Matsushima, P.; Baltz, D. H.; Roa, R. N. Cloning and expression in *Streptomyces lividans* of clustered erythromycin biosynthesis genes from *Streptomyces erythreus*. *Bio/Technol.* **1986**, *4*, 229-232.

Strauch, M. A.; Spiegelman, G. B.; Perego, M.; Johnson, W. C.; Burbulys, D.; Hoch, J. A. The transition state transcription regulator *abrB* of *Bacillus subtilis* is a DNA binding protein. *EMBO* **1989**, *8*, 1615-1621.

Tsai, P. S.; Rao, G.; Bailey, J. E. Improvement of *Escherichia coli* microaerobic oxygen metabolism by *Vitreoscilla* hemoglobin: New insights from NAD(P)H fluorescence and culture redox potential. *Biotechnol. Bioeng.* **1995**, in press.

Vasudevan, S. G.; Armarego, W. L. F.; Shaw, D. C.; Lilley, P. E.; Dixon, N. E.; Poole, R. K. Isolation and nucleotide sequence of the *hmp* gene that encodes a haemoglobin-like protein in *Escherichia coli* K-12. *Mol. Gen. Genet.* **1991**, *226*, 49-58.

Wakabayashi, S.; Matsubara, H.; Webster, D. A. Primary sequence of a dimeric bacterial haemoglobin from *Vitreoscilla*. *Nature* **1986**, *322*, 481-483.

Webster, D. A. Structure and function of bacterial hemoglobin and related proteins. In *Advances in inorganic biochemistry*; 1988; vol. 7, pp. 245-265.

Winston, S. E.; Fuller, S. A.; Hurrell, J. G. R. Western blotting. In *Current Protocols in Molecular Biology*; F. M. Ausubel, R. Brent, R. E. Kingston, D. D. Moore, J. G. Seidman, J. A. Smith, and K. Struhl (ed.), John Wiley & Sons, Inc., N.Y.; 1987; pp. 10.8.1-10.8.6.

Wittenberg, J. B.; Wittenberg, B. A.; Trinick, M.; Gibson, Q. H.; Fleming, A. I.; Bogusz, D.; Appleby, C. A. In *Nitrogen fixation research progress*, H. J. Evans, P. J. Bottomley, and W. E. Newton, Eds., Martinus Nijhoff Publishers, Dordrecht; 1985, p.354.

Zhu, H.; Riggs, A. F. Yeast flavohemoglobin is an ancient protein related to globins and a reductase family. *Proc. Natl. Acad. Sci. USA*. **1992**, *89*, 5015-5019.

A.8 Table

Table 1. Plasmids

Plasmids	Relevant properties	Source
pKQV4	pKK223, Amp^r, $lacI^q$	Strauch et al., 1989
pPPC1	pKQV4, *vhb*$^+$	From this study
pPPC2	pKQV4, *hmb*$^+$	From this study
pKLA	pKQV4, *yfb*$^+$	From this study
pBluescript SK II$^+$		Stratagene, Inc.
pBluV	pBluescript SK II$^+$, *vhb*$^+$	From this study
pBluV1	pBluV, ^{85}His –> Tyr	From this study
pBluV3	pBluV, ^{85}His –> Ala	From this study
pBluV4	pBluV, ^{85}His –> Arg	From this study

A.9 Figures

Figure 1 A). CO–reduced minus reduced absorbance spectra of VHb, HMb, and YFb. Soluble fraction of DH5α:pKQV4 (control), DH5α:pPPC1 (VHb), DH5α:pPPC2 (HMb), and DH5α:pKLA (YFb) cultures were used to determine the activity of the respective globins. Wavelengths at which the maximal and the minimal absorbencies occur are marked.

B). 15% SDS-PAGE (Coomassie blue stained) of DH5α:pKQV4 (lane 1), DH5α:pPPC1 (lane 2), DH5α:pPPC2 (lane 3), and DH5α:pKLA (lane 4). The presence of yeast flavohemoglobin (~44 kD) in DH5α:pKLA is indicated by the arrow.

Figure 2 Effect of different globins on cell growth. Fed–batch cultivation of DH5α:pKQV4 (Δ), DH5α:pPPC1 (O), DH5α:pPPC2 (X), and DH5α:pKLA (•) are shown. Optical density (*A600*) profiles of cells are indicated by solid lines (—) and dissolved oxygen (DO%) profiles are shown with dashed lines (– – –). Growth conditions in a Sixfors bioreactor are described in Materials and Methods.

Figure 3 A). CO–reduced minus reduced absorbance spectra of VHb mutants: DH5α:pBluV1 (A), DH5α:pBluV (B), DH5α:pBluV3 (C), DH5α:pBluV4 (D). Wavelengths at which the maximal and the minimal absorbencies occur are marked. Concentrations of the globins were estimated using the reported extinction coefficient of VHb, $\varepsilon = 1.067 \times 10^5$ $(M\ cm)^{-1}$ (Hart and Bailey, 1991): DH5α:pBluV, 15 μM; DH5α:pBluV1, 1.7 μM; DH5α:pBluV3, 1.5 μM; DH5α:pBluV4, 1.7 μM. B). Western blotting of VHb mutants. Lane 1: VHb standard

prepared from JM101:pRED2 cell extract (Khosla and Bailey, 1989). Lane 2: DH5α:pBluescript II SK^+. Lane 3: DH5α:pBluV. Lane 4: DH5α:pBluV1. Lane 5: DH5α:pBluV3. Lane 6: DH5α:pBluV4. Sample preparations and the subsequent Western blotting are described in Materials and Methods.

Figure 4 Effect of VHb mutations on cell growth. Fed–batch cultivation of DH5α:pBluescript II SK^+ (Δ), DH5α:pBluV (O), DH5α:pBluV1 (X), DH5α:pBluV3 (●), and DH5α:pBluV4 (◊) are shown. Optical density (*A600*) profiles of cells are indicated by solid lines (——) and dissolved oxygen (DO%) profiles are shown with dash lines (– – –). Growth conditions in the Sixfors bioreactor are described in Materials and Methods.

Figure 1A

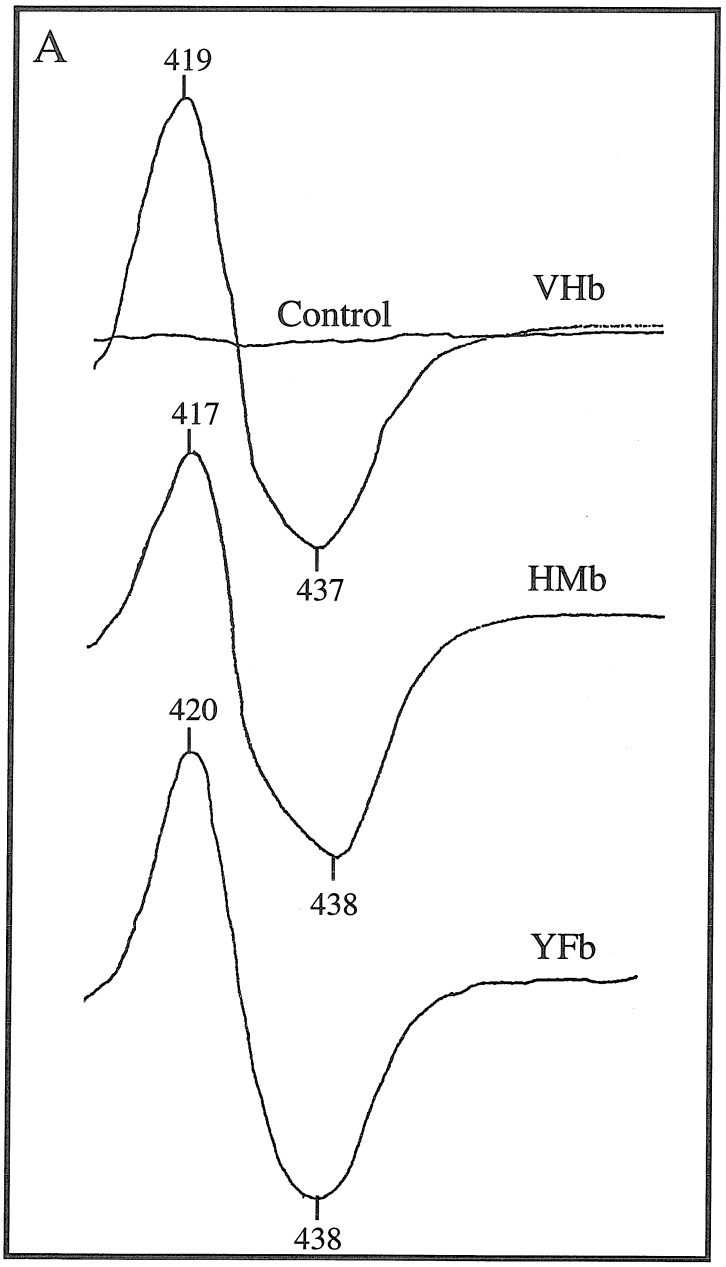

Figure 1B

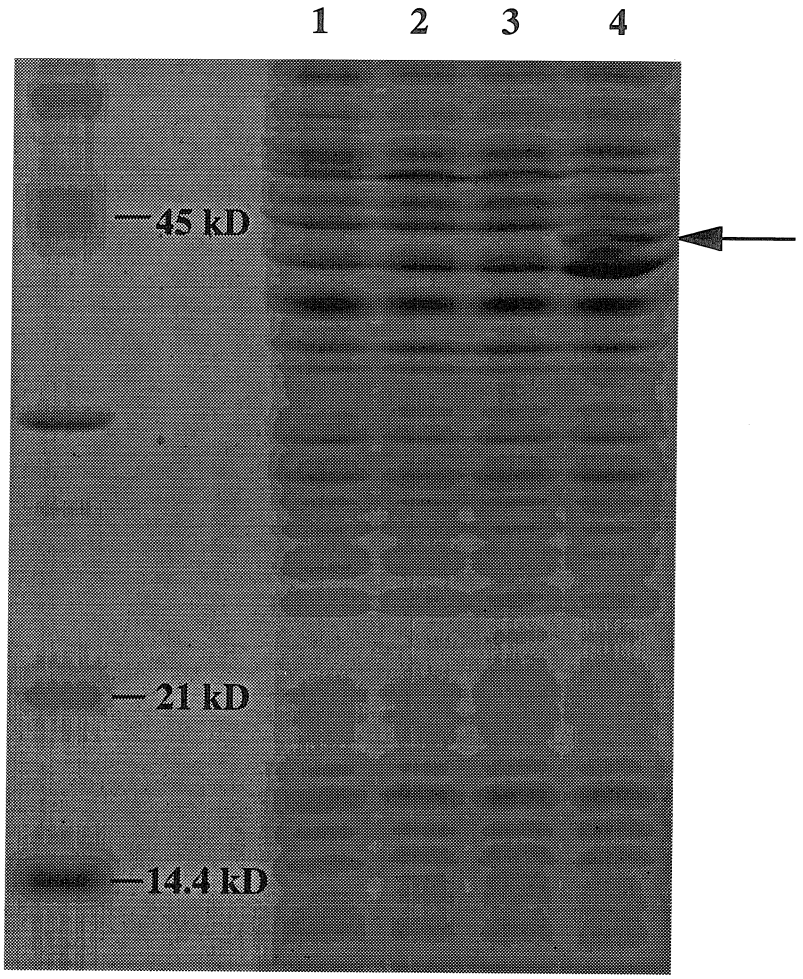

Figure 2

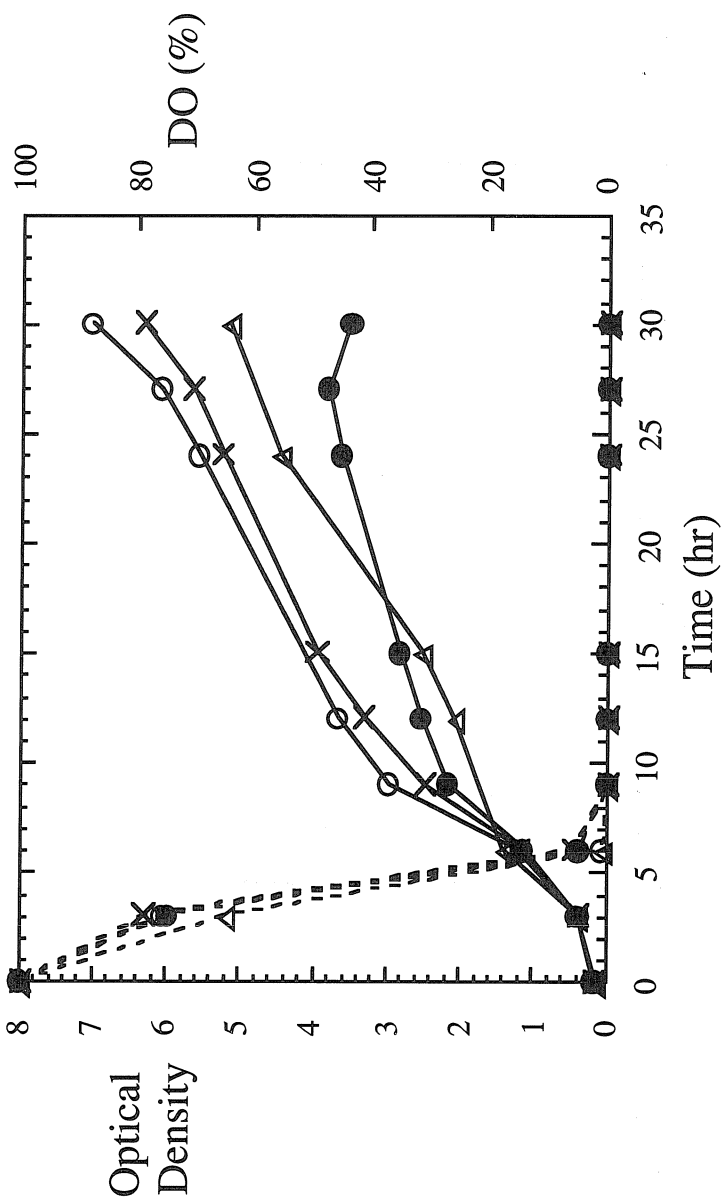
DO (%)
100
80
60
40
20
0
Optical Density
8
7
6
5
4
3
2
1
0
0
5
10
15
20
25
30
35
Time (hr)

Figure 3A

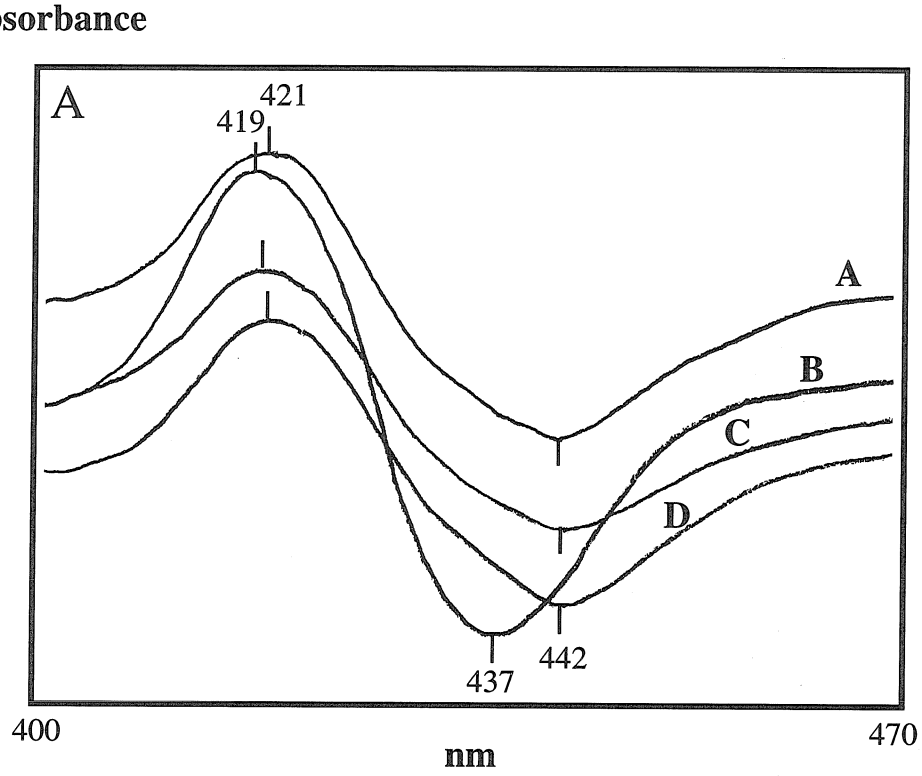

Figure 3B

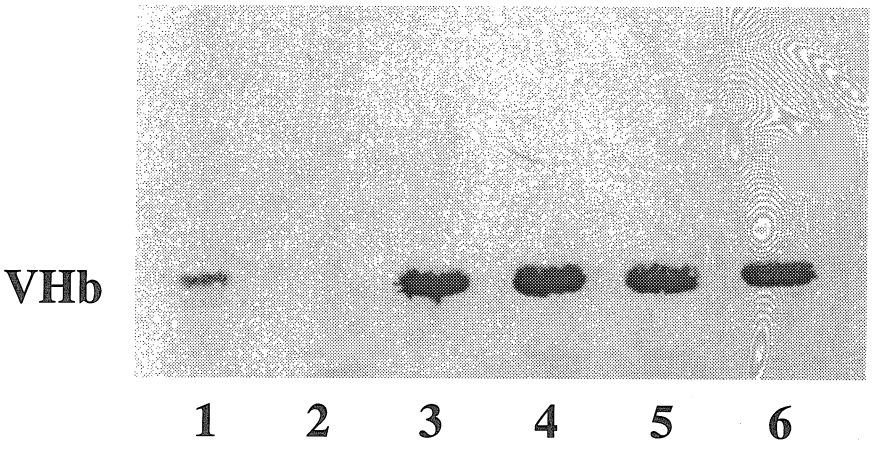

Figure 4

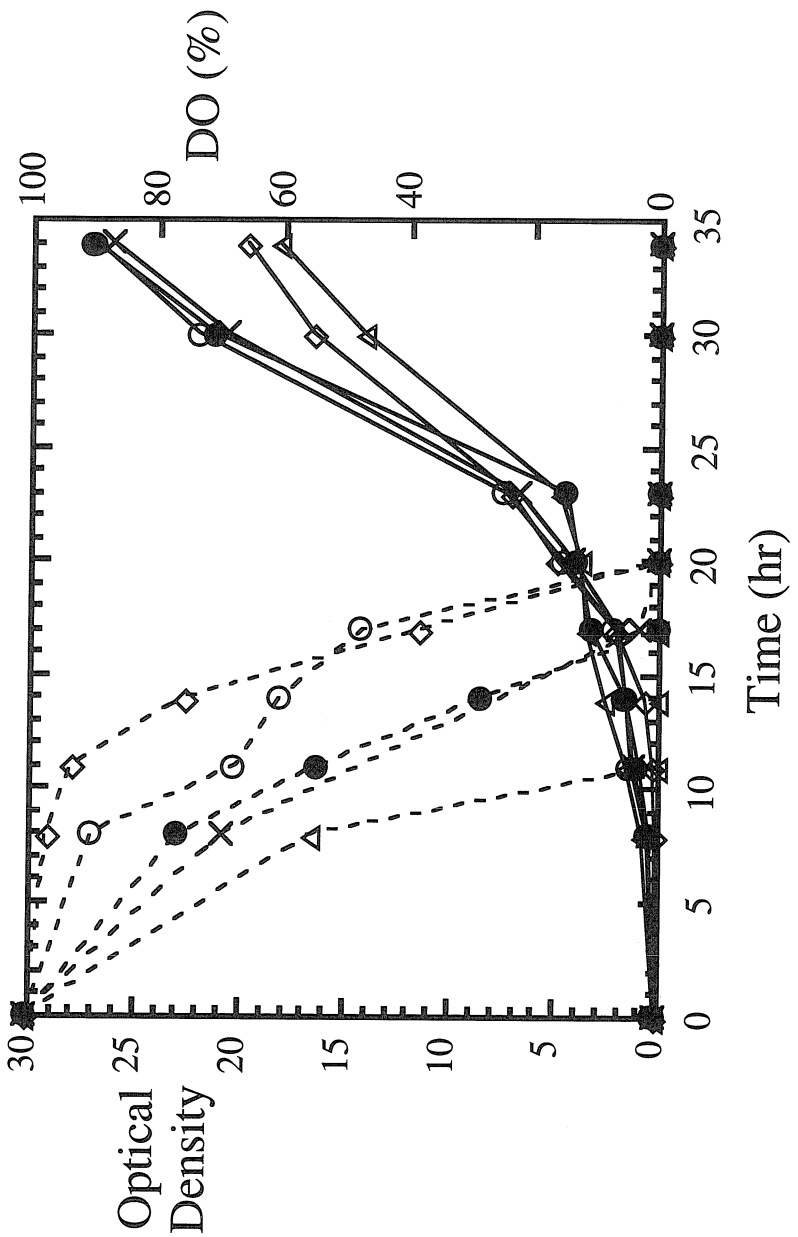
DO (%)
100
80
60
40
0
Optical Density
30
25
20
15
10
5
0
Time (hr)
0
5
10
15
20
25
30
35